NOTICE

The quality of this microform is heavily dependent upon the quality of the original thesis submitted for microfilming. Every effort has been made to ensure the highest quality of reproduction possible.

If pages are missing, contact the university which granted the degree.

Some pages may have indistinct print especially if the original pages were typed with a poor typewriter ribbon or if the university sent us an inferior photocopy

Reproduction in full or in part of this microform is governed by the Canadian Copyright Act, R.S.C. 1970, c. C-30, and subsequent amendments.

AVIS

La qualité de cette microforme dépend grandement de la qualité de la thèse soumise au microfilmage. Nous avons tout fait pour assurer une qualité supérieure de reproduction.

S'il manque des pages, veuillez communiquer avec l'université qui a conféré le grade.

La qualité d'impression de certaines pages peut laisser à désirer, surtout si les pages originales ont été dactylographiées à l'aide d'un ruban usé ou si l'université nous a fait parvenir une photocopie de qualité inférieure.

La reproduction, même partielle, de cette microforme est soumise à la Loi canadienne sur le droit d'auteur, SRC 1970, c. C-30, et ses amendements subséquents.

Assessment of Harmonics in Three-Phase ac-dc Converters Operating Under Unbalanced Supply Conditions

Ali I. Maswood

A Thesis

in

The Department

Of

Electrical Engineering

Presented in Partial Fulfillment of the Requirements
for the Degree of Doctor of Philosophy at
Concordia University
Montréal, Québec, Canada

March 1989

ISBN 0-315-51340-3

ABSTRACT

Assessment of Harmonics in Three-Phase ac-dc Converters Operating Under Unbalanced Supply Conditions

Ali I. Maswood, Ph.D.
Concordia University, 1989.

Most electrical systems are designed on the basis of a balanced three-phase supply operating at a given fundamental frequency. However, in a three-phase system, the supply voltage can be unbalanced for a variety of reasons, and this unbalance can degrade the performance of equipment dependant on the 3-phase supply bus. Three phase ac-dc converters which are used extensively in industry for various high power applications are a good example of a class of equipment in this category. Moreover,the inherent non-linearity of these converters and the harmonics they produce is only aggravated when they are supplied by an unbalanced source. A major problem associated with them is their inherent non-linearity and the harmonics they generate into the supply. This work, therefore, concentrates on the analysis of the operation of these converters under unbalanced supply conditions. Specifically, a 3-phase 6 pulse fully controlled bridge is analyzed. In this work, the non-linearity of these converters and calculation of harmonics are based upon the three-phase fully controlled

six-pulse bridge, assuming both balanced and unbalanced supply voltages. Primary importance is given to the fact that under unbalanced supply conditions, the switching functions of switches are no longer similar to one another as is true in the case of a balanced supply. Moreover, the switching patterns are found to be functions of the magnitudes of the supply phase voltages, and the transfer functions for the individual phases are different. This principle is the essence of the research conducted in this thesis.

To show the differences between converter operations and to achieve the correct harmonic spectrum of input and output currents, a three-phase converter is fully analyzed using the transfer function approach. The performance of the converter is evaluated under both balanced and unbalanced supply conditions. The evaluation of performance parameters is carried out for converters using both natural and forced commutation. Finally, the simulated converter harmonic spectra are verified experimentally.

Converters are analyzed at different load factor conditions for the gurantee of load current continuity, and performance parameters. It is found that the harmonic generation characteristics are degraded as the supply becomes unbalanced. This situation gets worse at the lower converter output voltage levels. Thus, the harmonic characteristics are evaluated in terms of the input power

factor of the converter, the harmonic and distortion factor of the input current, the distortion factor of the output current, and the total harmonic distortion of the converter output voltage.

As a guide to finding a solution to the problem of undesirable harmonics, input and output filters are designed. Also, a computer aided analysis of the proposed converter input and output filters is carried out to ensure that they meet the desired specifications for input current and load voltage. This design procedure can very well be utilized to choose optimum filter LC components.

Finally, converters using forced commutation are analyzed and their harmonic generation characteristics are established. It is noted that for converters using certain types of forced commutation under unbalanced supply, the input current harmonic content remains practically unchanged.

TABLE OF CONTENTS

LIST OF TABLES

LIST OF FIGURES

LIST OF ACRONYMS

PF - Input Power factor.

HF - Harmonic factor of the input line current.

DF - Distortion factor of the input line current.

THD - Total harmonic distortion.

LF - Load factor.

PU - Per unit.

TPF - True input Power factor

RF - Ripple factor.

TKVA - Total KVA rating.

LKVA - kVA rating of the inductor.

CKVA - kVA rating of the capacitor.

CAD - Computer aided design.

PWM - Pulse width modulation.

MSPWM - Modified sinusoidal PWM.

PWMOCD - PWM for optimum current distortion.

PWMSHE - PWM for specific harmonic elimination.

LIST OF ABBREVIATIONS AND PRINCIPAL SYMBOLS

A_c	Amplitudes of carrier waveforms
A_r	Amplitudes of reference waveforms
CkVA	kVA rating of the capacitor
E_1, E_2, E_3	Peak value of the line to line voltage in Volt
E_c	Counter emf of the load circuit, in Volt
f	Source frequency, in Hz
f_c	Carrier wave frequency
f_r	Reference wave frequency
H_n	nth harmonic component of switching function
I_{ci}	rms value of the current through the input filter capacitor, in Ampere
i_i	Instantaneous input current, in Ampere
i_o	Instantaneous output current, in Ampere
I_i	rms value of input current, in Ampere
$I_{i,1}$	rms value of the fundamental component of input current, in Ampere
I_r	rms value of rectifier input current (with filter), in Ampere
I_{dc}	Average output current, in Ampere
I_n	Peak value of the nth harmonic output current, in Ampere
L	Load inductance, in Henry
LKVA	kVA rating of the input filter inductor
MI	Modulation index

R	Load resistance, in Ohm
$S(\theta)$	Switching function
T_n	nth switching angle, in electrical degrees
V_{dc}	Average output voltage, in Volt
V_1, V_2, V_3	Supply rms line to line voltages, in volt
V_{an}, V_{bn}, V_{cn}	Supply rms line to neutral voltages, in volt
v_{om}	mth harmonic component of instantaneous output voltage, in Volt
V_n	Normalized average output voltage, in Volt
α	Delay angle, in radian or in Electrical degrees
β_n	Phase of the nth output current harmonic component
δ_k	Phase angle of the load impedance, in radian
ω	General symbol for angular frequencies in radian ($\omega = 2\pi f$, $\theta = \omega t$)
ψ_n	Phase of nth harmonic component of switching function, in radian
ϕ_1, ϕ_2, ϕ_3	Phase angles of line to line voltages in radian
$X_{L,i}$	Filter inductor impedance at fundamental frequency
$X_{C,i}$	Filter capacitor impedance at fundamental frequency
Z_k	kth component of load impedance, in Ohm

ACKNOWLEDGMENTS

My sincere thanks and gratitude to Dr. M. H. Rashid, my supervisor for his guidance and support during my graduate studies and in the development of this thesis work. I certainly am humbly proud to be a member of his research team. I would also like to thank Dr. P. D. Ziogas for sharing his knowledge with me in times of need.

My friends and research colleagues Joseph Wood, Prasad Enjetti and others, for their support and friendship.

And finally, to all my family members for their support and love.

DEDICATION

This work is dedicated to my parents and other family members whose sacrifices and example have put us where we are today.

CHAPTER 1

INTRODUCTION

1.1 General

In mechanics, the term harmonic means the vibration of a string at a frequency which is a multiple of the fundamental frequency. In electricity, by harmonics we understand any electrical signal whose frequency is an integer multiple of the actual supply frequency. The presence of unwanted harmonics in power systems is a problem for both the producers and the consumers of electrical energy.

Today harmonics are generated by a variety of sources; among them, non-linear loads such as silicon controlled rectifiers (SCRs) and the power transistors used in power converters and microprocessor controls. These power converters generate harmonics throughout a given system. In the past, any number of harmonic producing loads could be tolerated by a power system. Today, however, utilities can no longer afford to degrade their product with high levels of system harmonics. Moreover, sophisticated loads such as computers, control elements, and distant relays demand a non-polluted power supply for their proper operation, and the utilities have seriously started looking for the sources of harmonics and the means for their elimination.

There are six major sources of harmonics:

1. Network non-linearities from the loads using solid state power converters such as rectifiers, inverters, voltage controllers, frequency controllers, and static VAR compensators.

2. Transformer magnetizing currents.

3. Tooth ripple or the ripple in the voltage waveforms of rotating machines.

4. Recent power conservation measures to ensure improved motor efficiency and load matching employing semiconductor devices for switching, produce voltage and current waveforms rich in harmonics.

5. Modern motor control devices used in traction, HVDC power conversion, and transmission.

6. Conventional non-linear loads such as arc furnaces, and welders.

The effects of these harmonics on the power system are to be avoided. The more widespread effects could be summarized as follows:

1. Inductive interference with the telecommunication system.

2. Di-electric breakdown of insulated cables, and capacitor bank failures.

3. Mechanical oscillations and overheating of electrical machines, and malfunctions of motor controllers.

4. Over-voltages and excessive currents in the system.

5. Signal interference causing relay malfunction especially in microprocessor based and solid-state control systems.

Any concern for electrical waveform distortion should be shared by all those involved in control of the problem. Networks containing non-linear circuit parameters such as rectifiers carry non-sinusoidal currents even when the applied voltage has a pure sinusoidal waveform.

The derivation of the harmonic current produced by solid-state power converters requires accurate information about the ac voltage waveforms at the converter input, the converter configuration, the type of control, the ac system impedance, and the dc circuit parameters [19]. This information is used to build circuit models which are used

to simulate the actual power system. In the system simulation, the relationship between the input and the output of the converter is derived using a transfer function approach [1]. According to this method, the switches are replaced by switching functions that act like a transfer function between the input and the output and determine the input and the output quantities in terms of Fourier series components. This is symbolically represented in Fig 1-1. For convenience, it is assumed that:

(1) The switches are loss-less and ideal.

(2) The switches derive gating signals from their respective phases.

(3) The switching functions are symmetrical about the origin of their respective phases and have quarter wave symmetry.

(4) The effect of the output voltage drop due to commutation reactance has been ignored since it is expected to be less than 5% of the output voltage.

1.2 Review of Previous Work

A great deal of work has been done on the harmonic generation problem ever since the introduction of solid state power conversion techniques. Most of the previous

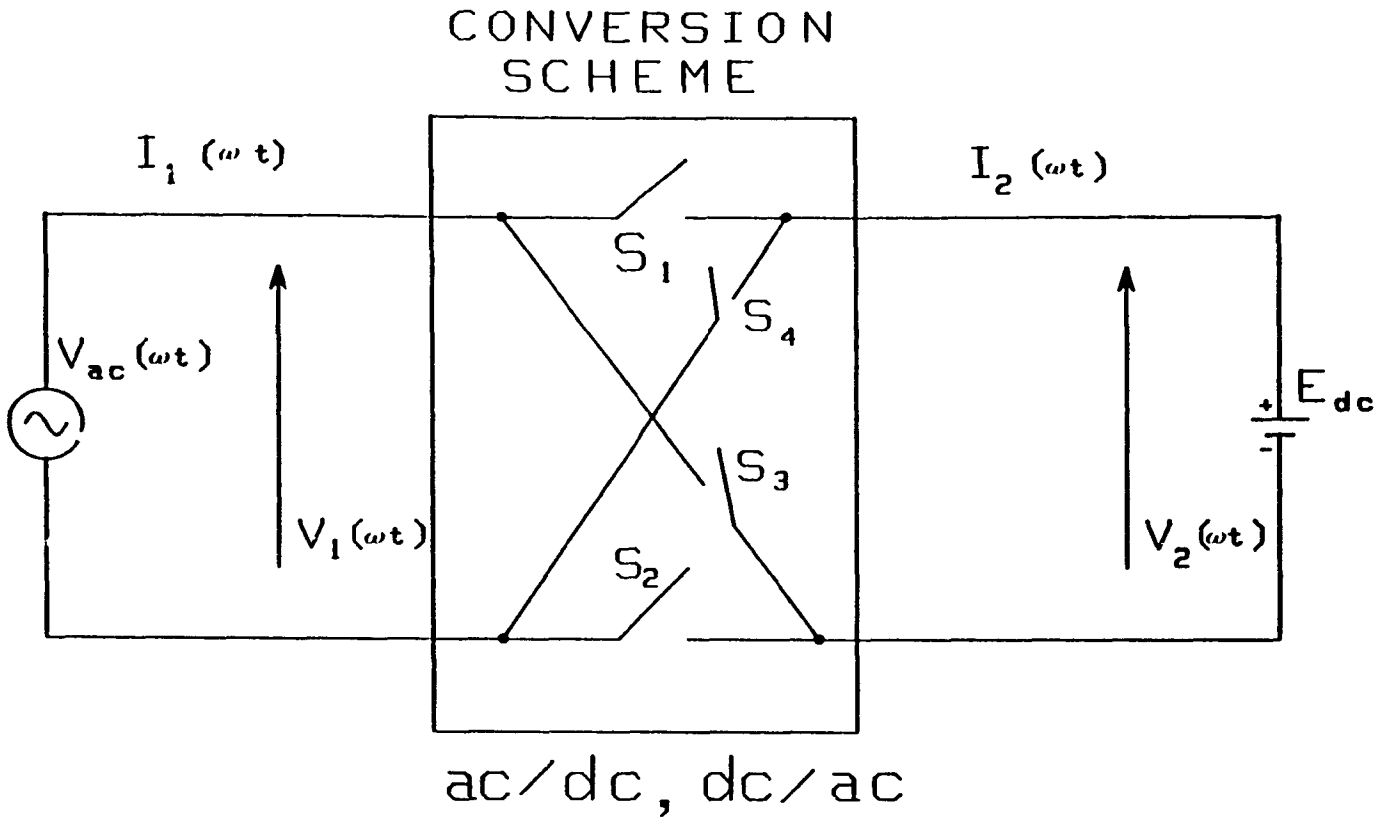

Fig. 1-1: ac/dc, dc/ac conversion scheme.

analyses focused on the converter performance under normal operating conditions, i.e. balanced supply conditions. Perhaps the first investigation on converter generated harmonics was done by John Reeve and P.C.S. Krishnayya [10]. They investigated certain harmonic disturbances with respect to variations in unbalanced commutating and supply voltages and with unequal firing angles. The investigation was done for two transformer connections, - wye/wye and wye/delta [10]. Also, John Baron and John Reeve calculated the proper commutation angle under unbalanced supply conditions or timing errors of the firing pulses [11]. A decade later, John Reeve and T. Subbarao analyzed the converter generated harmonics due to unbalanced transformer impedances in HVDC conversion schemes. It was shown that unwanted harmonics, especially triplen harmonics could be minimized by balancing the transformer phase impedances as closely as practical for 6 pulse bridge operation. They recommended using a 12-pulse system consisting of two 6-pulse bridges with the advantage that the two dominant ac harmonics, i.e. the 5th and the 7th were filtered. They also proposed the use of synchronized-control between the firing control of each bridge and suggested that logic circuits should be designed for accurate phase matching [12].

Further work by Arun G. Phadke and James Harlow [13] investigated the problem of non-characteristic harmonics generation from errors in firing angles in an automatic control system. They concluded that non-characteristic harmonics due to random errors in firing angle control can

be restricted to a very small value if individual firing control is avoided whenever possible. Ainsworth [14] showed that certain types of instabilities in converter operation can be avoided through the use of an equally-spaced firing-pulse method instead of using voltage cross-over point control. The equally spaced method will eliminate non-characteristic harmonics thereby allowing the converter to be safely operated even with relatively weak ac system conditions [14]. However, this is true only when the dc side impedance is infinite, which is rare in practice. Yacamini [15] proved that under non-infinite dc side impedance converter operation, stability cannot be guaranteed even with the equal pulse-space firing method. He further proved that if a resonance at a particular integer frequency exists on the dc side, even with infinite dc side impedance, high harmonic-current levels can exist on the dc side. These high harmonic non-characteristic currents can cause non-characteristic currents to flow on ac side of the converter. If these non-characteristic harmonics in the ac side add to the characteristic harmonics, the classical conditions for instability exists. This problem is found quite frequently in high voltage dc systems and is most likely to occur at the second harmonic on the ac side and at a large amount of fundamental current on the dc side.

1.3 Scope of this Thesis

Previous investigations of the problems of harmonic

generation by static power converters lack the following:

1) The transfer function approach was not used to calculate the switching functions of the switches, e.g. diodes or thyristors. This approach is widely accepted and is considered an accurate method of finding relationships between the input and the output variables of converters.

2) In practice a converter is usually operated at different output voltage levels (from maximum to minimum). Consequently, it is necessary to investigate the converter operation and converter generated harmonics at various output voltages. Most of the previous studies neglected this fact.

3) In recent years, the performance of a converter and the quality of input current is expressed in terms of input power factor (PF) of the converter, and harmonic factor (HF) of the input current. Moreover, frequently used terms such as distortion factor (DF) of currents and voltages, and total harmonic distortion (THD) of the output voltage give an overall idea of the harmonic pollution of a particular waveform.

4) A converter might be required to operate at a

certain output voltage level. In angle-controlled thyristor converters, this is controlled by the delay angle (α). It is essential that we know input PF, HF, DF and THD at any particular delay angle (α).

The conduction periods of diodes or thyristors in the same arm of a 3-phase bridge converter are found from the voltage cross-over points. The procedure is to find the value of the switching function of a particular switch and subtract the value of the switching function of the other switch in the same arm of the converter bridge. This gives the transfer function of that particular phase. The transfer functions of the other two phases are identical except that they are phase shifted by 120 and 240 electrical degrees.

The objective of this thesis is to find the correct harmonic spectra of the input currents and the output voltage of ac-dc converters under balanced and unbalanced supply conditions. The harmonic spectra are to be derived for the full range of the converter operation, something that had not been taken into account by previous researchers. Furthermore, a new concept has been proposed by which transfer functions of different phases are calculated separately when the supply becomes unbalanced. The details of the research work are presented in the following 5 chapters.

A 3-phase converter is simulated in Chapter 2. The relationships between the input and the output are derived using a transfer function approach. Performance parameters

are calculated for the entire converter operating range, and for different operating conditions, (e.g.) supply unbalances. Additionally, input pf, HF, and DF of the output current are also calculated at different load PF conditions.

Chapter 3 focuses on the importance of calculating separate transfer functions for unbalanced supply conditions to find 'more accurate' harmonic spectra. The causes for the increase in the input PF at the lower converter output range are also analyzed. Performance parameters have been found using separate transfer functions.

In Chapter 4 input and output filters have been designed to provide some solutions to the problems caused by the unbalanced supply mentioned in chapter 3. The filter components are selected to meet certain specifications. At the same time, emphasis has been placed on the optimization of the filter L/C ratio. Chapter 4 also verifies the simulated results. In the laboratory, an experimental circuit for a 3-phase angle controlled converter was developed and was used to measure the harmonic spectra of the input and output currents at unbalanced supply voltages.

In Chapter 5 converters with forced commutation techniques are analyzed under both balanced and unbalanced supply conditions. Performance parameters are found and harmonic spectra of the input and output currents are calculated.

Chapter 6 discusses the various types of converter control strategies and compares their degrees of harmonic generation. Depending on the need of the user, it also

suggests the types of control strategies and ranges of converter operations to meet desirable specifications.

CHAPTER 2

MATHEMATICAL MODELING AND ANALYSIS OF NATURALLY COMMUTATED CONVERTERS

2.1 Switching Function

Considering a general configuration of an ac-dc converter as shown in Fig. 2-1, the relationship between the input and output can be obtained through the transfer function of the converter.

The transfer function of a converter can be written in Fourier series as:

$$S(\theta) = \sum_{n=1}^{\infty} H_n \, \mathrm{Sin} \, (n\theta + \psi_n) \qquad (2.1)$$

where: H_n- Magnitude of the nth harmonic component of the switching function.

ψ_n- Phase of the nth harmonic component of the switching function.

Considering the thyristors as static switches, if the switches are closed and opened according to some pre-determined sequence, the realization of the transfer function can be obtained. The mathematical expression in Eqn. (2.1) describing the switching pattern of a switch assumes a value of logic 1 when the switch is closed, and

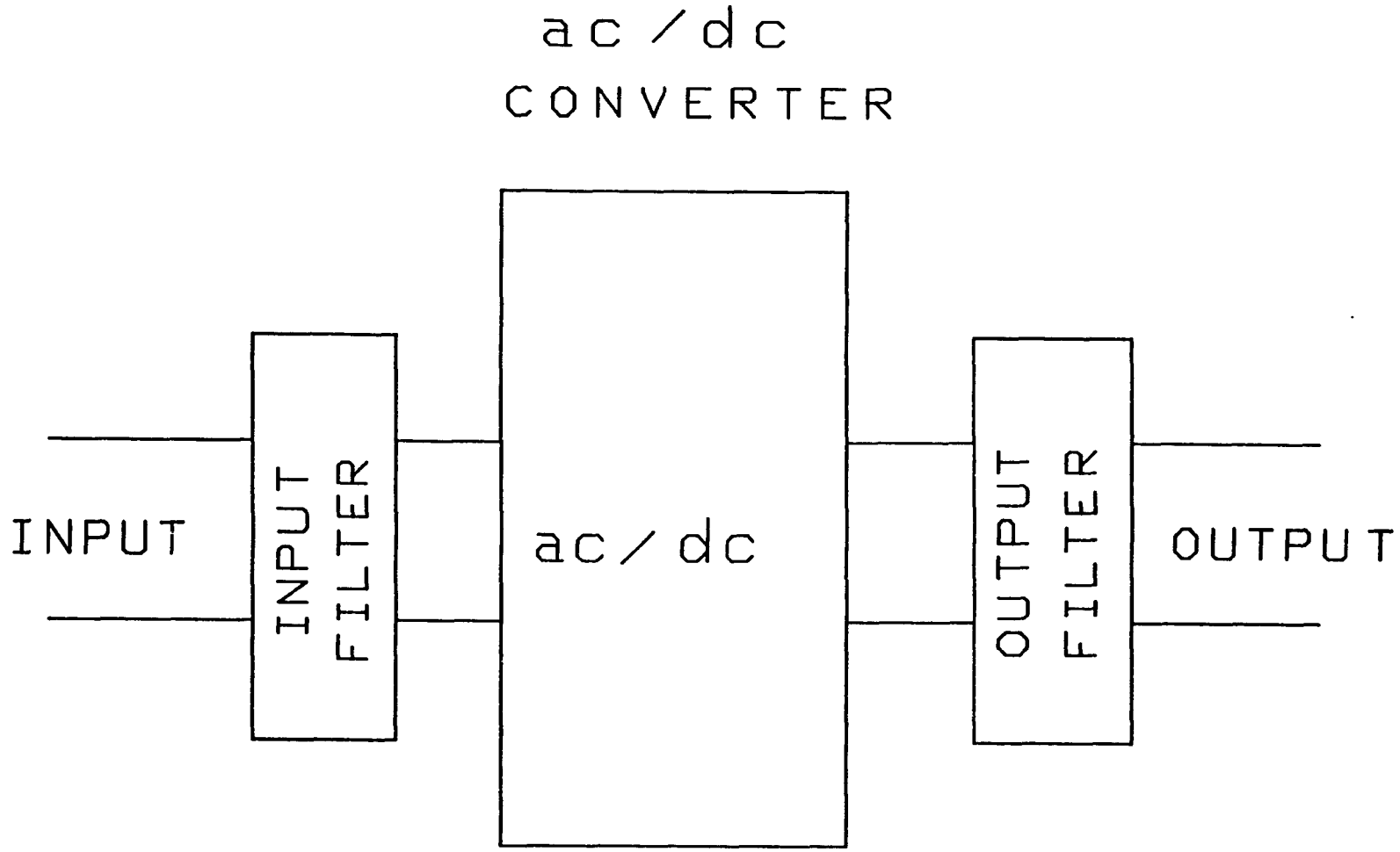

Fig. 2-1: Symbolic representation of a static power converter.

logic zero when the switch is open. As the switches are opened and closed according to some predetermined repetitive pattern, a train of pulses with amplitude equal to 1 can be obtained. The mathematical expression which is generally known as 'switching function' is the function that describes the switching pattern of a phase having amplitude levels of 1,0, and -1.

Let us consider a phase angle controlled converter as shown in Fig.s 2-2. Figure 2.3 shows the input voltage and input current with zero phase shift. The timing reference for the occurrence of the switching function is derived from the zero crossing of the respective phase voltages (Fig. 2-3a). Under balanced supply, phase voltage v_1 crosses phase voltage v_2 at 30° (assuming v_1 is the reference phase). The switching function of phase 1 consists of positive and negative halves. The positive half is implemented by switch 1 when phase voltage v_1 is higher than others. The negative half portion is implemented by switch 4. Under balanced supply, the switching functions of the switches are shown as in Fig. 2-3(b). The resulting switching function which is called transfer function, is the switching function 1 minus switching function 4. This is shown in Fig. 2-4(a). Once the transfer function for phase 1 is determined, the input current essentially follows the same pattern (under a very high load inductance). The input currents for the other two phases are determined in the same manner, only they are phase shifted from each other by 120 and 240 electrical

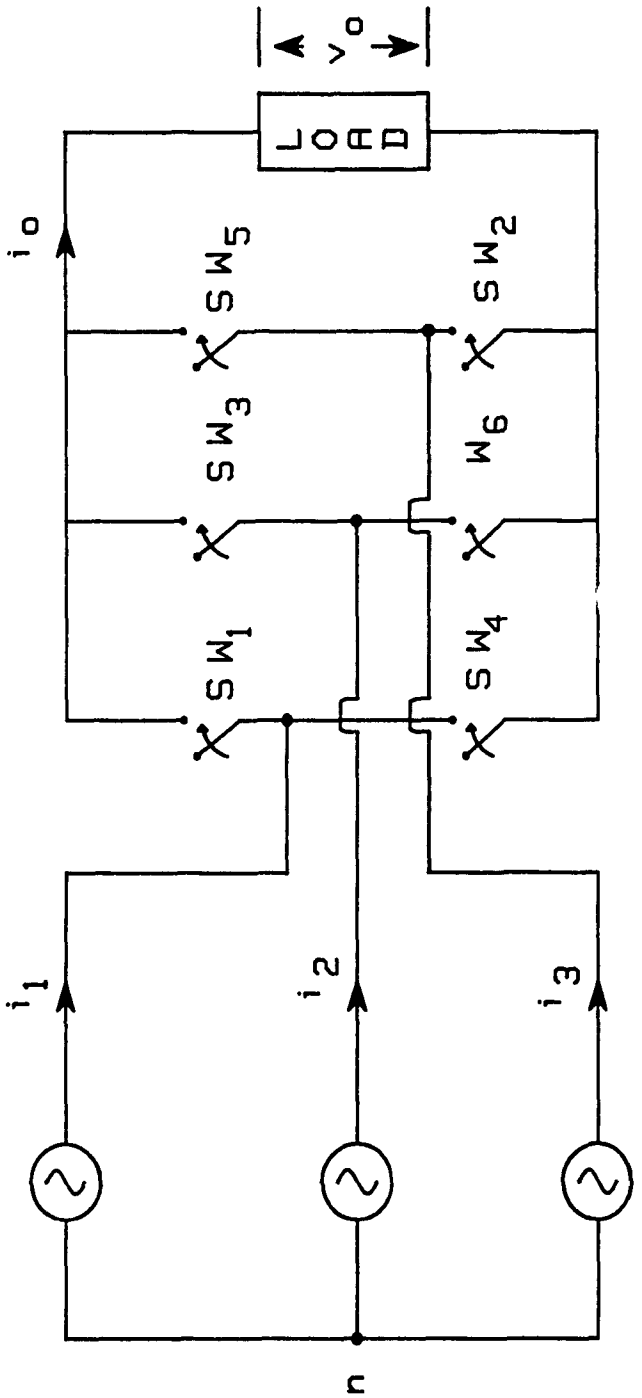

Fig. 2-2: Typical three-phase phase-controlled bridge rectifier.

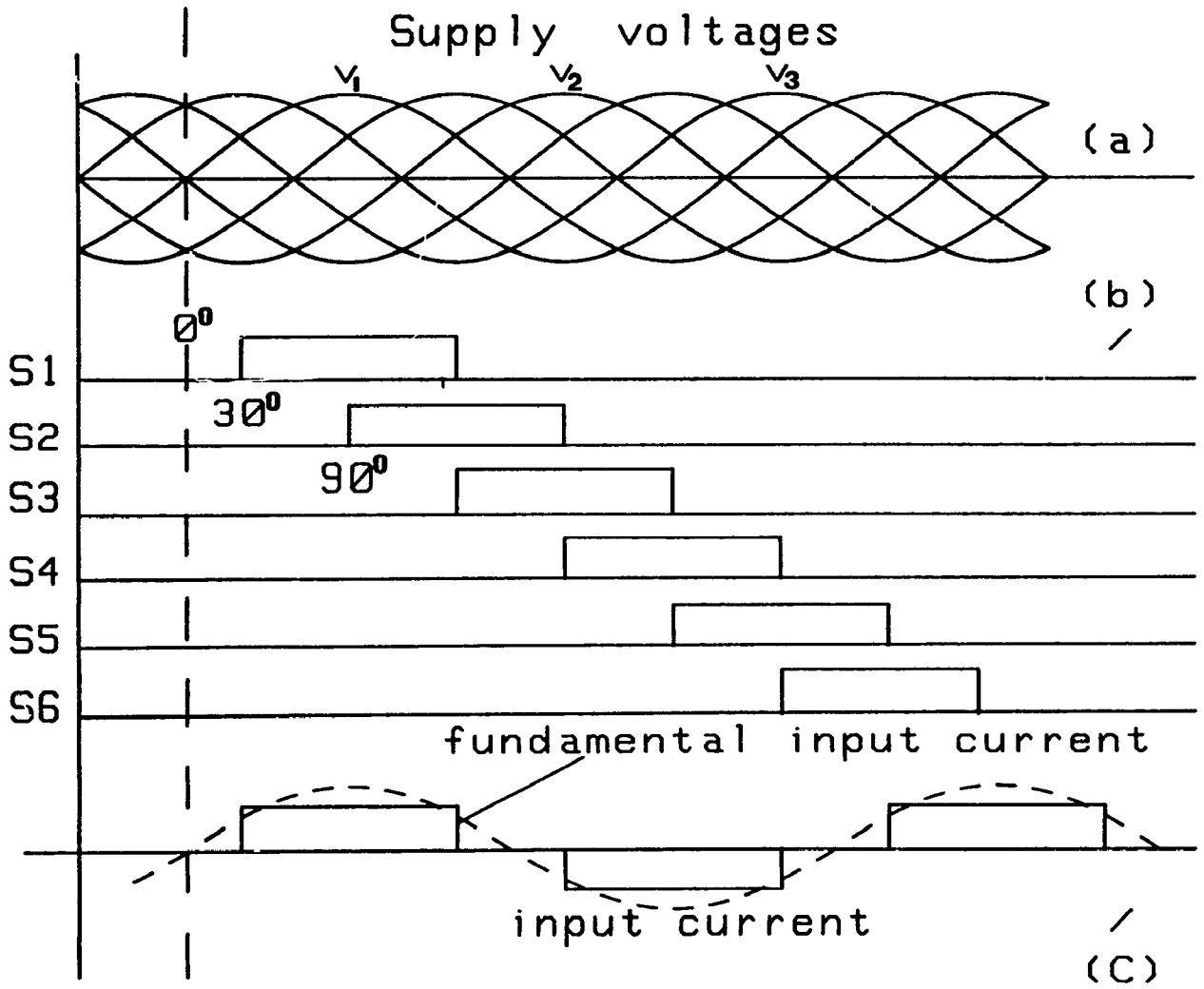

Fig. 2-3: Three-phase phase controlled bridge rectifier and associated waveforms.

(a) Supply line to line voltages.
(b) Switching functions.
(c) Input line current.

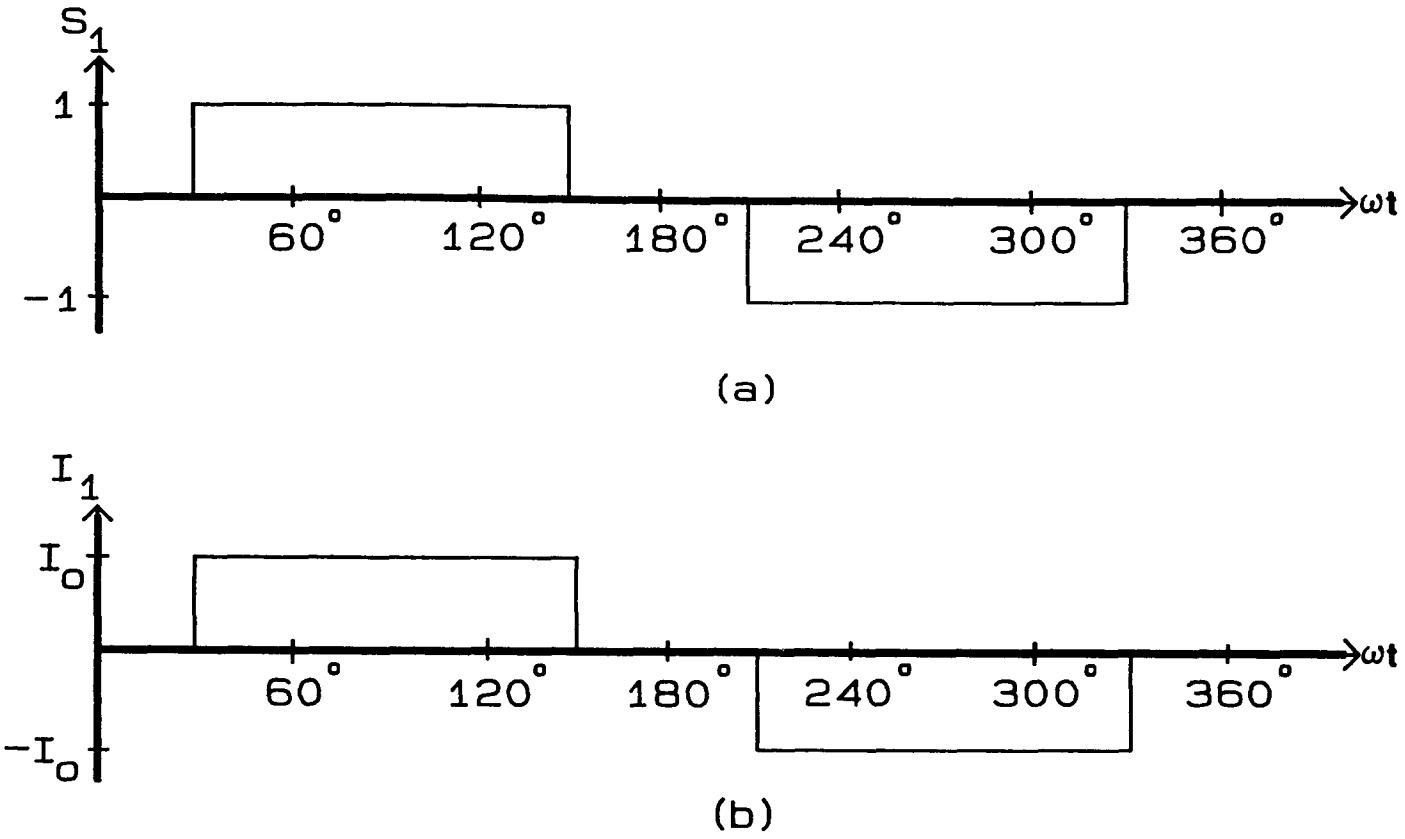

Fig. 2-4: (a) The transfer function of the rectifier for phase 1.
(b) Input line current for phase 1.

input current and the resulting fundamental component of input line current are shown in Fig. 2-3(c).

2.2 Analysis of The Converter

The transfer function of a converter can be expressed in Fourier series as:

$$S(\theta) = \sum_{n=1}^{\infty} H_n \, Sin(n\theta + \psi_n) \qquad (2.2)$$

If the supply line to line voltages are:

$$v_1 = E_1 \, Sin \, (\, \theta - \varphi_1) \qquad (2.3)$$

$$v_2 = E_2 \, Sin \, (\, \theta - \varphi_2) \qquad (2.4)$$

$$v_3 = E_3 \, Sin \, (\, \theta - \varphi_3) \qquad (2.5)$$

then the output voltage of the converter can be expressed as:

$$v_O = \{V_i(\theta)\} \, \{ \, S \, (\theta) \, \} = \{ \, S_1(\theta) - S_4(\theta)\} \, E_1 \, Sin(\theta - \phi_1) + \{S_3 - S_6(\theta)\}E_2Sin(\theta - \phi_2) + \{S_5(\theta) - S_2(\theta)\} \, E_3Sin(\theta - \phi_3) \qquad (2.6)$$

Where $\{S_1(\theta)-S_4(\theta)\}$, $\{S_3(\theta)-S_6(\theta)\}$, $\{S_5(\theta)-S_2(\theta)\}$ are the transfer functions with respect to the input port of the converter, and ϕ_1, ϕ_2, ϕ_3 are the phase shifts.

Substituting $S(\theta)$ from Eqn. (2.2) in Eqn. (2.6) and after trigonometric transformation to find the kth component of the output voltage, Eqn.(2.6) can be written as :

$$v_{o_k} = \frac{E_1 H_{k+1}}{2} \cos(k\theta - k\phi_1 - (k+1)\alpha) - \frac{E_1 H_{k-1}}{2} \cos(k\theta - k\phi_1 - (k-1)\alpha) + \frac{E_2 H_{k+1}}{2} \cos(k\theta - k\phi_2 - (k+1)\alpha) - \frac{E_2 H_{k-1}}{2} \cos(k\theta - k\phi_2 - (k-1)\alpha) + \frac{E_3 H_{k+1}}{2} \cos(k\theta - k\phi_3 - (K+1)\alpha) - \frac{E_3 H_{k-1}}{2} \cos(k\theta - k\phi_3 - (k-1)\alpha) \quad (2.7)$$

where: α - delay angle in radian.

The output average voltage can be obtained from Eqn.(2.7) by selecting proper terms and putting n=1, as:

$$V_{dc} = \frac{1}{2} (E_1 + E_2 + E_3) H_1 \cos \alpha \quad (2.8)$$

The rms ripple content of the output voltage (i.e. V_{01}, V_{02}, etc.) can be obtained from Eqn. (2.7) by substituting k=1,2,3 etc., and by selecting the proper terms.

2.2.1 Output Current

For a R-L load and at kth supply frequency, the load impedance can be expressed as:

$$Z_k \angle \sigma_k = \{ R^2 + (2k\pi fL)^2 \}^{1/2} \angle \tan^{-1} \left(\frac{2k\pi fL}{R} \right) \quad (2.9)$$

where σ_k - phase angle of the load impedance.

If the load has a fixed dc voltage (e.g. battery or

back emf of a dc machine), the average output current is expressed as:

$$I_{dc} = \frac{V_{dc}}{R} - \frac{E_c}{R} \qquad (2.10)$$

Where: E_c is the fixed dc voltage.

The output current of the converter can be expressed as:

$$i_o(\theta) = I_{dc} + \sum_{n=2}^{\infty} I_n \sin(n\theta + \beta_n) \qquad (2.11)$$

Where:

I_n = Peak value of the nth harmonic output current.

β_n = Phase of the nth harmonic output current component.

2.2.2. Input Line Current

Considering the converter to be loss-less, the instantaneous input power to the converter must be equal to the instantaneous output power from the converter. Thus:

$$\{v_i(\theta)\}\{i_i(\theta)\} = \{v_o(\theta)\}\{i_o(\theta)\}$$

$$\text{or } \{v_i(\theta)\}\{i_i(\theta)\} = \{v_i(\theta)\}\{S(\theta)\}\{i_o(\theta)\}$$

$$\text{or } i_i(\theta) = \{S(\theta)\}\{i_o(\theta) \qquad (2.12)$$

Rewriting Eqn. (2.10) in terms of Fourier series and substituting the value of $i_o(\theta)$, the instantaneous input line current can be expressed as:

$$i_i(\theta) = \left(\sum_{k=1}^{\infty} H_k \sin(k\theta + \psi_k) \right) \left(I_{DC} + \sum_{n=1}^{\infty} I_n \sin(n\theta + \beta_n) \right)$$

$$= I_{DC} \sum_{k=2}^{\infty} H_k \sin(k\theta+\psi_k) + \left(\sum_{k=1}^{\infty} \sum_{n=1}^{\infty} \frac{H_k I_n}{2} \left[\cos(n-k)\theta + \beta_n - \psi_k \right) \right.$$

$$\left. - \cos\{(n+k)\theta + \beta_n - \psi_k\} \right] \qquad (2.13)$$

The details of the derivations are given in Appendix A.

2.3 Converter Performances under Discontinuous Load Current Mode.

In many analytic and converter simulation work, the load current is assumed to be continuous [12]. In practice, the continuity of the load current depends on two key factors; (a) the type of the load circuit, (b) the range of delay angle (α). Depending on the load circuit and large delay angle, it is possible for discontinuous conduction to occur either in the rectifier or in the inverter mode of operation. If the load at the dc terminal (converter output) is capable of absorbing mean power, the current waveform inevitably becomes discontinuous as the delay angle approaches towards 90^{o}. It is found that if the delay angle lies between 0^{o} and 60^{o}, the instantaneous voltage at the dc terminals is positive at all times. Hence, beyond these delay angles, the current in a R-L passive load must be continuous. However, as the delay angle is increased, the

output dc voltage changes to negative polarity. At this instant, it is only up to the time constant (R-L ratio) of the load circuit to decide whether or not this negative voltage excursion can be adsorbed. If so, a net positive current flow can be maintained.

In practice there are loads which have the capability of storing voltage (i.e. capacitor or the dc machine armature with back emf). They may lead to discontinuous load current mode at any converter operating range, if the average load current demand is small.

It is essential that, in the study of converter performance, the load current discontinuity is taken into consideration, since it is 'reflected' into the input current spectrum through the switching functions of the converter. The magnitude of the ac ripple in the output load current is comparable with the direct component. As long as the peak instantaneous value of the ac ripple current is less than the direct component, and the net current is always greater than zero, the converter can be kept in continuous conduction mode [22].

2.4 Input Harmonic Current Spectrum

Under ideal conditions,(i.e. ripple free load current), the switching function harmonic spectrum represents the input current harmonic spectrum.A very high load inductance causes the load current to be ripple free. But in practice this is hardly achievable and the load current contains some

ripples. This will cause some deviation of the frequency spectrum of the input current from the frequency spectrum of the switching function.

Each supply line conducts 120^{o} in the positive half cycle and 120^{o} in the negative half cycle, so that the effective value of the switching function is fixed. This dictates the increase of the amplitude of higher order harmonics for a decrease of lower order harmonics.

Fig.2-5 shows the input current harmonic spectrum of the simulated converter under balanced supply and high load inductance.

2.5 Performance Parameters with balanced Supply

A computer program was developed simulating the converter. The harmonic factor (HF), level of lower order harmonics (LOH) in the input line current, and the input power factor (PF) were calculated under balanced supply conditions. The results are presented in graphical form against the variations of normalized output voltage. The output voltage is normalized with respect to the maximum output voltage of the converter. It is to be noted that all the performance parameters are derived at $E_c = 0$.

2.5.1 Input Power Factor

Converters normally operate at a satisfactory power factor at a full load, but the power factor decreases with

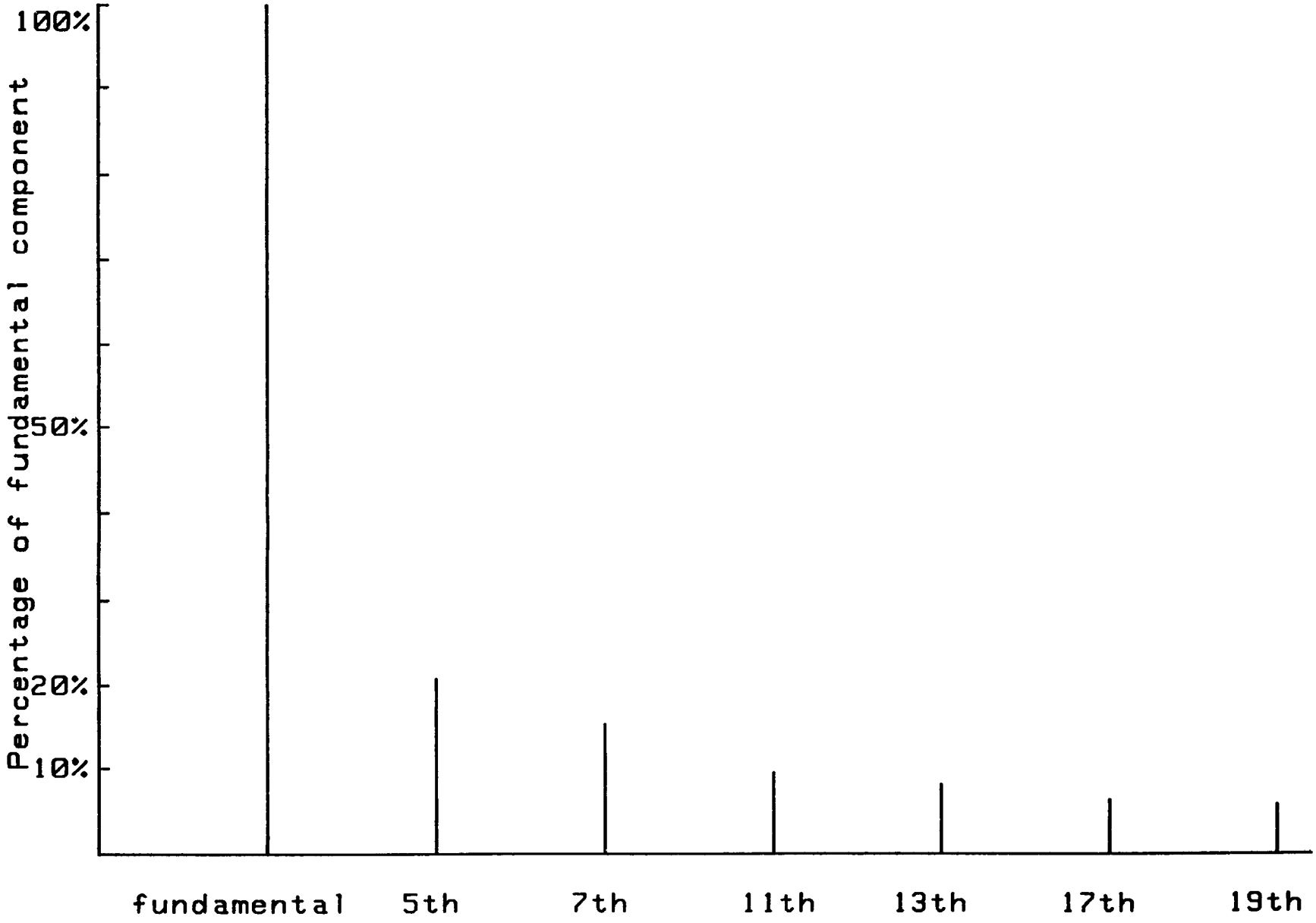

Fig. 2-5: Input line current harmonic spectrum.

2.5.1 Input Power Factor

Converters normally operate at a satisfactory power factor at a full load, but the power factor decreases with the reduction of dc output voltage. With a series load, the input power factor of a converter is expressed as [4]:

$$PF = \left(\frac{I_1}{I_i}\right) \cos(\varphi) \tag{2.28}$$

Where:

$$\cos \varphi = \cos \left(\tan^{-1} \left(I_{iQ}/I_{ip}\right)\right) \tag{2.29}$$

I_1= rms value of the fundamental input current,

I_i= rms input current.

I_{iQ} and I_{ip}= reactive and active components of the fundamental input current.

Eqn. (29) is called the displacement factor or fundamental power factor. This equation can be used for any rectifier except where the number of diode is 1. From figure 2-6, it can be concluded that power factor at the high output region of the converter is quite satisfactory and is approximately equal to 0.96 pu. This corresponds to a delay angle (α) of 0^{o}. As the delay angle is increased, the output voltage decreases, so does the power factor. It is evident from Fig. 2-5 that the power factor decreases in a linear fashion. For a very large value of delay angle (α), the PF becomes very poor, and this should be avoided from the harmonic generation point of view.

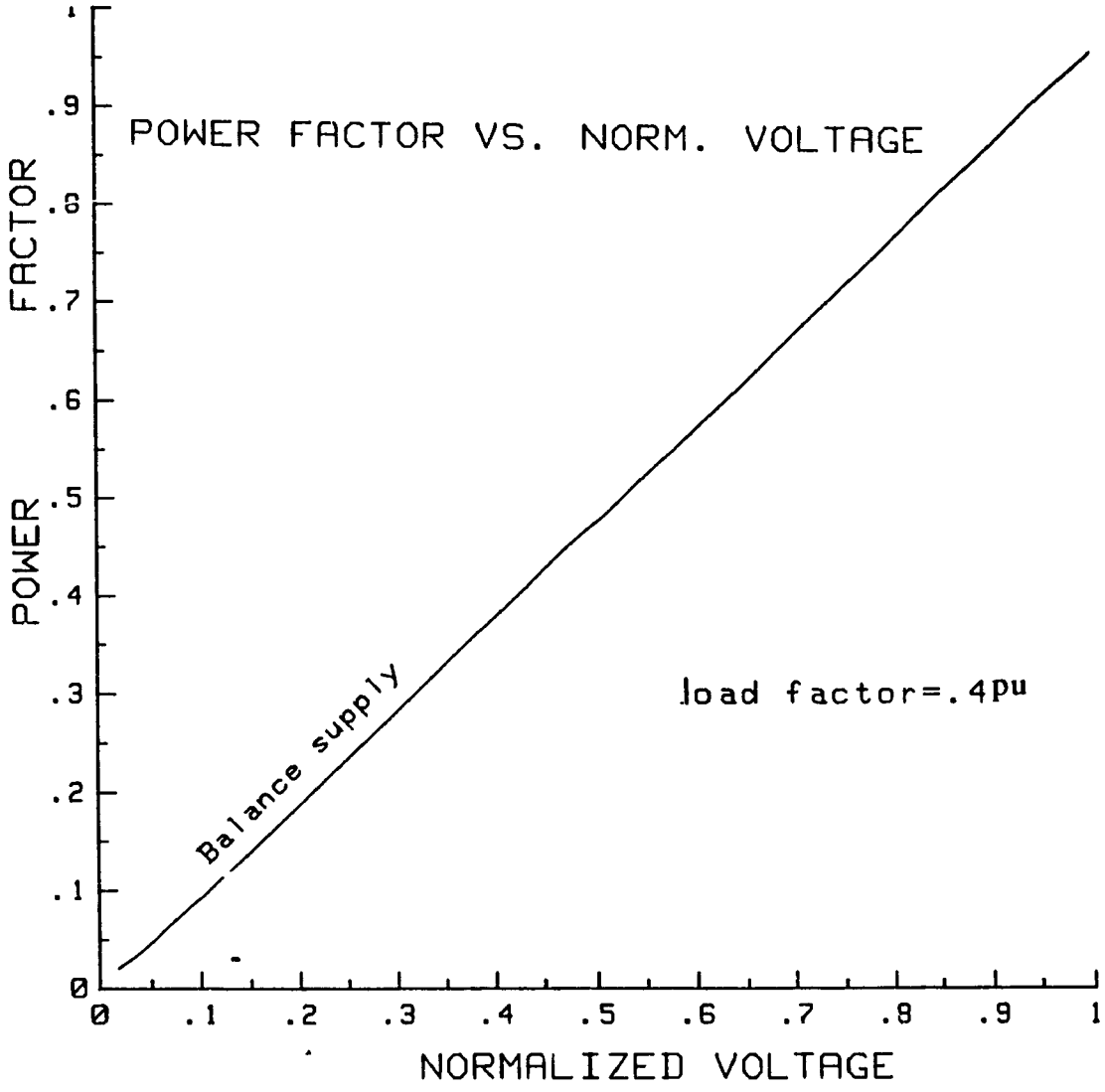

Fig. 2-6: Converter input power factor.

2.5.2 Harmonic factor

The input current is not pure sinusoidal and contains currents of harmonic frequencies. The harmonic factor of the input line current is defined as [4]:

$$HF = \frac{((I_i^2 - I_1^2)^{1/2})}{I_1} = \frac{(\sum_{n=2}^{\infty} I_{in}^2)^{1/2}}{I_1} \qquad (2.30)$$

Where; I_{in} - is the rms value of the nth harmonic input current.

It can be noticed from Fig. 2-7, that the harmonic factor at higher output voltage of the converter is comparatively low. At a very low output voltage, the HF rises sharply and assumes a value of 1.7 pu at approximately 119^{o} of delay angle.

2.5.3 Distortion factor

The size of a filter is determined by the order and the magnitude of the harmonic components in the waveform. The distortion factor reflects the presence of lower order harmonics at the converter input. Considering a general second order filter, distortion factor is calculated from [4]:

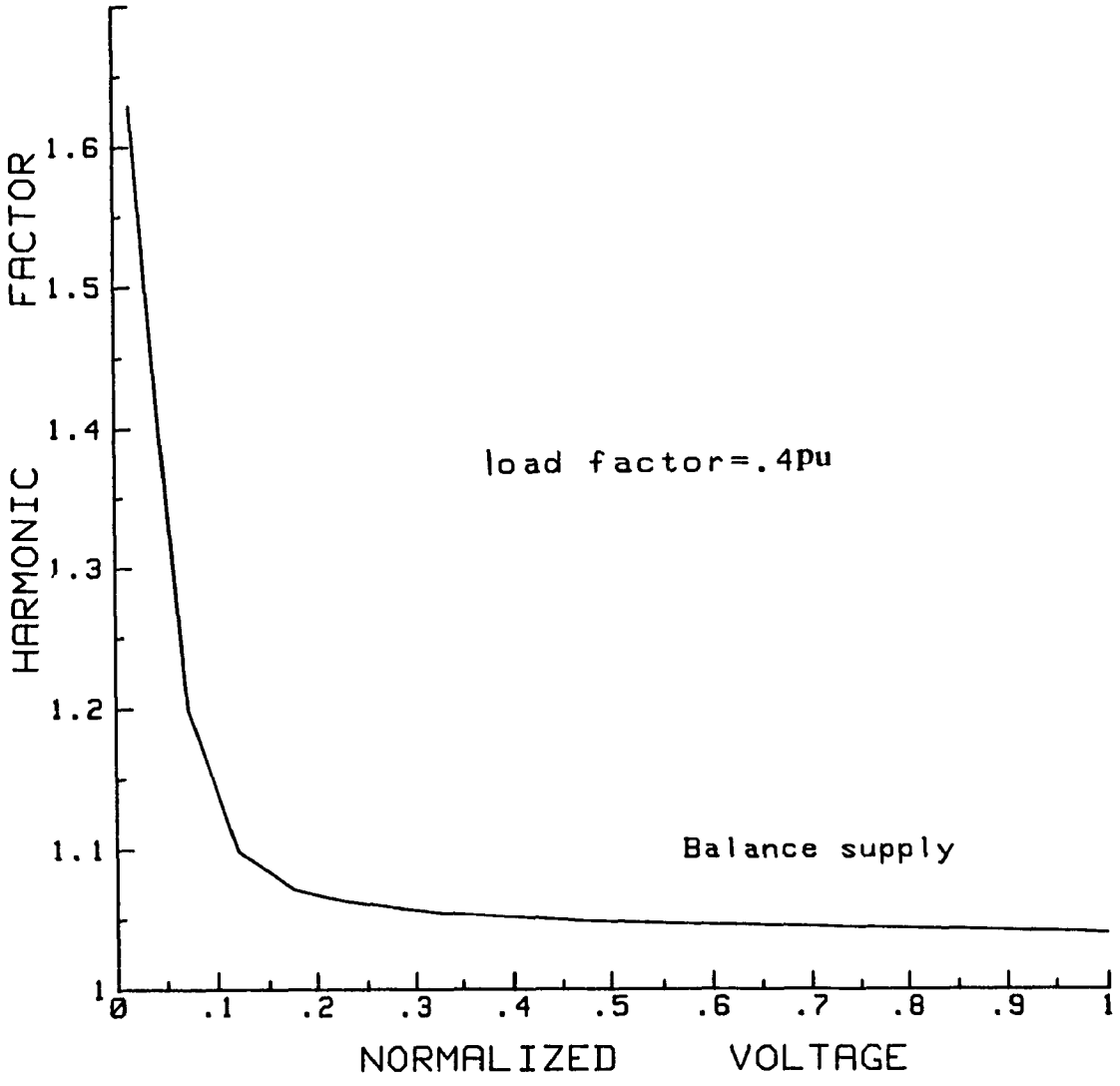

Fig. 2-7: Harmonic factor of the input line current.

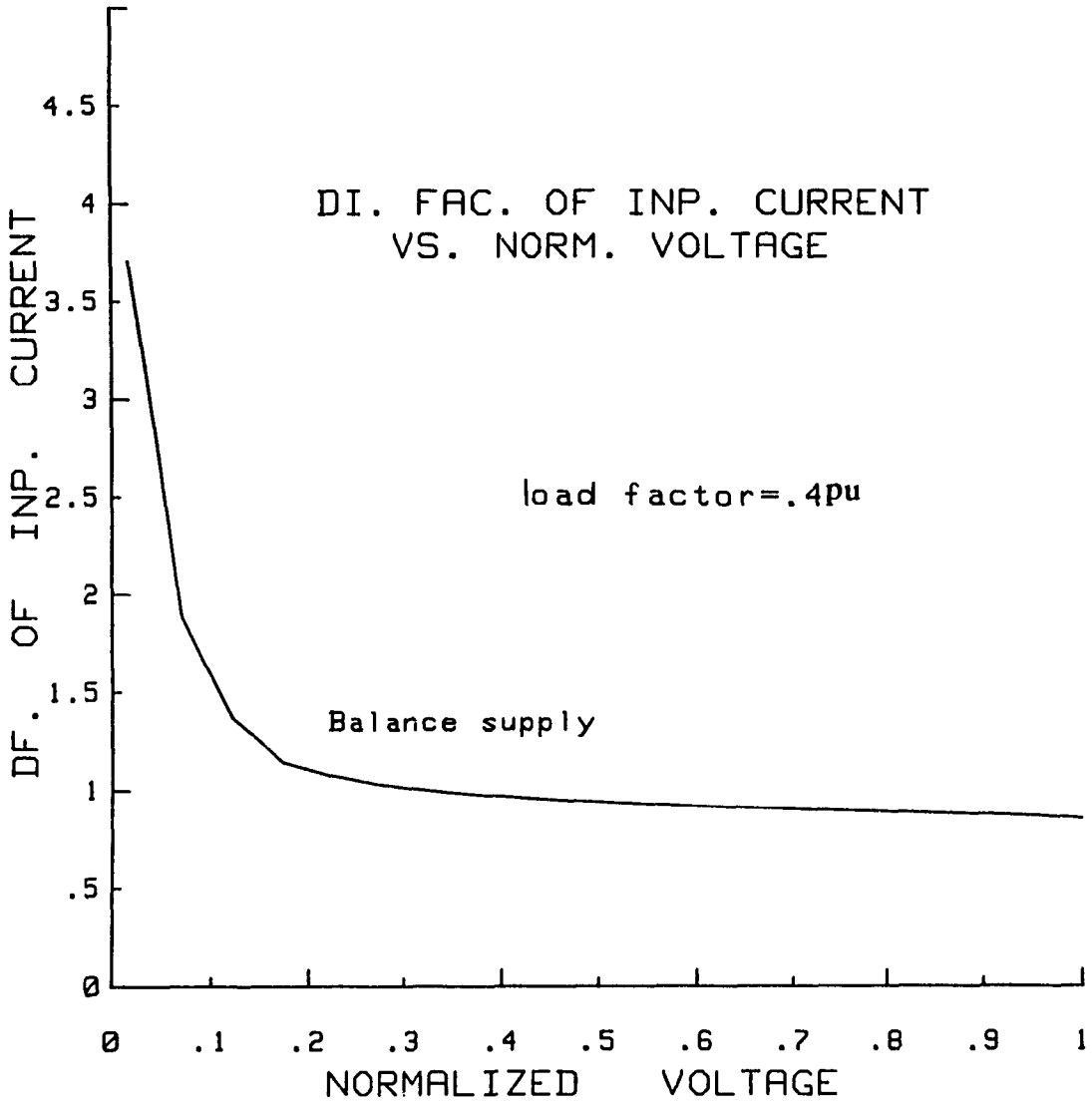

Fig. 2.8: Distortion factor of input line current.

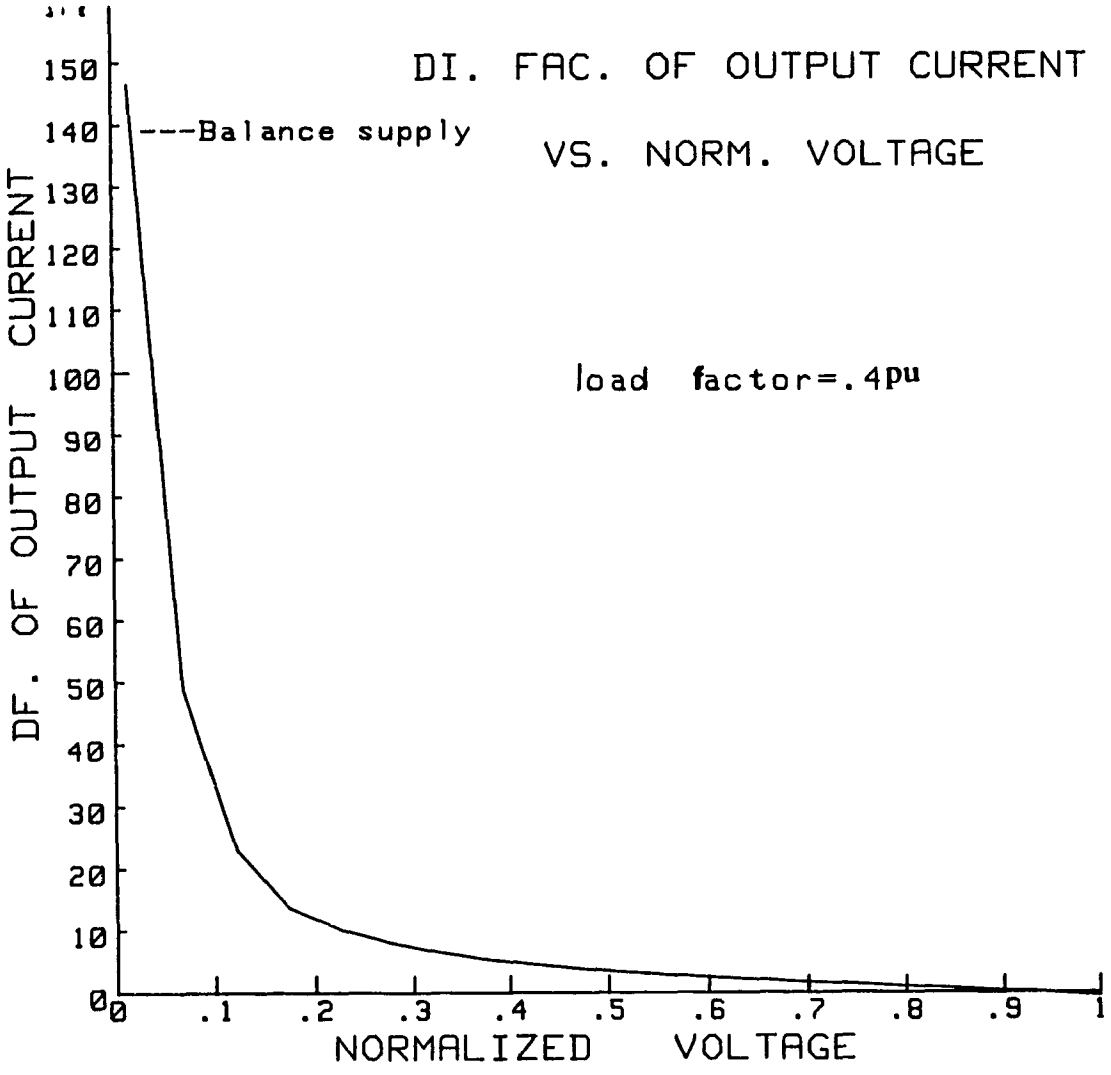

Fig. 2-9: Distortion factor of output current.

$$DF(\%) = \frac{[\sum_{n=2}^{\infty}(I_n/n^2)^2]^{1/2}}{I_1} \times 100 \qquad (2.31)$$

Where: I_1- rms value of the fundamental component of input current, and;

I_n- rms value of the nth harmonic current.

Figures 2-8 and 2-9 show the distortion factors of the input and output currents, against the normalized output voltage of the converter. As it is evident from the Fig.s, the input and output currents are less distorted at the higher converter output range and stay approximately the same throughout the normal converter operation. But the distortion increases sharply at the very low converter output region.

2.5.4 Total harmonic distortion (THD) of the output voltage

The total harmonic distortion of the output voltage indicates the presence of harmonics in the waveform. In practice it is used as a measure of the closeness between the waveform and its fundamental component. It also sets an overall idea about the wave shape. A higher ripple content makes the THD higher. The THD is defined as [4]:

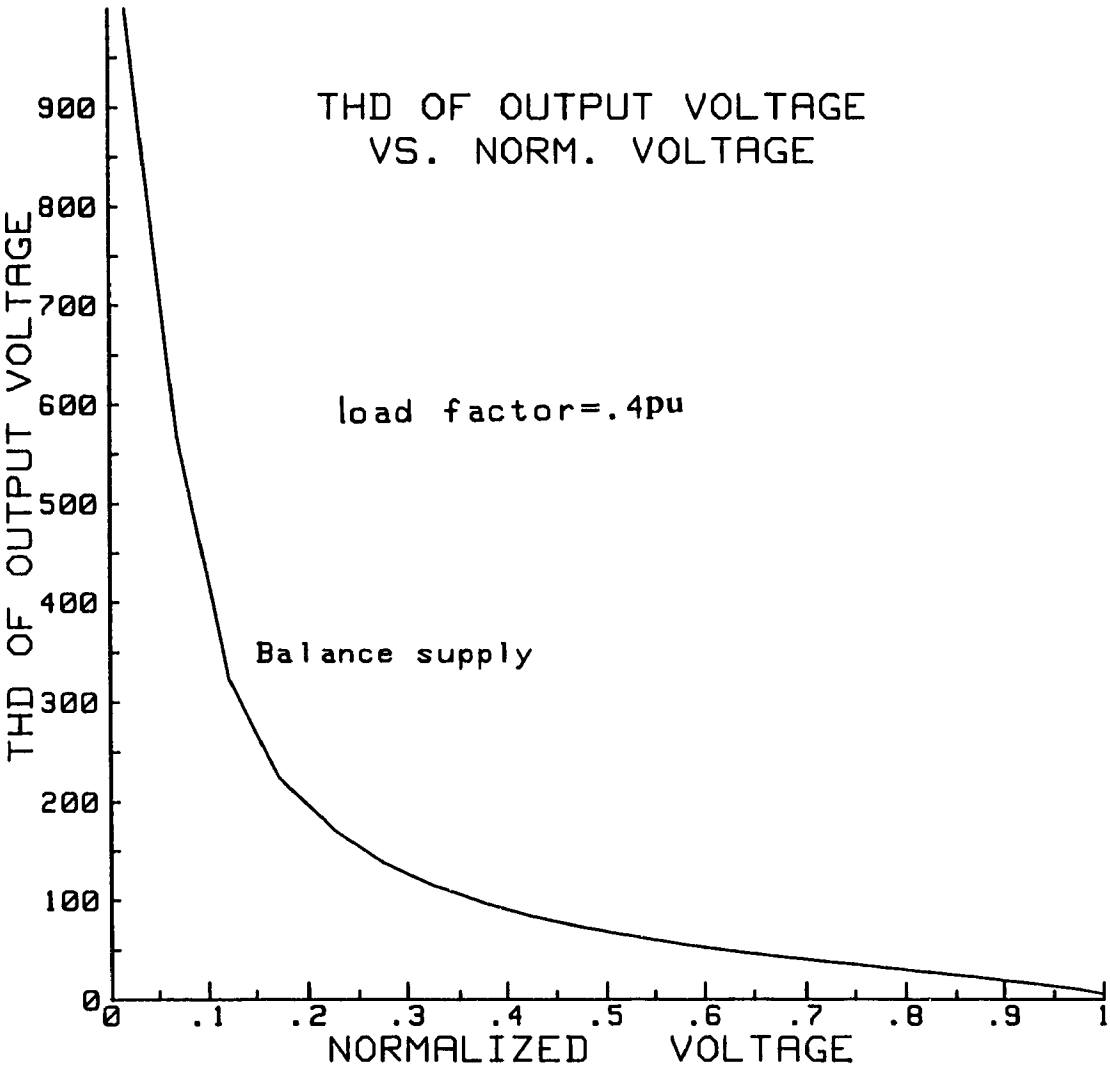

Fig. 2-10: Total harmonic distortion of the output voltage.

$$THD\ (\%) = \left[\sum_{n=2}^{\infty} (V_n/V_1)^2 \right]^{1/2} \times 100 \qquad (2.32)$$

Where:

V_n and V_1 bear the same significance as in the case of DF.

From Fig. 2-10, it can be seen that the THD of the output voltage varies throughout the whole operating range of the converter, but it is considerably low at the higher converter output range.

2.5.5 Lower order harmonics

From the input filtering point of view, it is essential to have a specific knowledge about the order and relative amplitude of the lower harmonic components. It is found that under balanced supply, only characteristic (i.e. 5th, 7th etc.) harmonics are present at the converter input. Triplen harmonics are totally absent.

Figure 2-11 shows the lower order harmonics as a function of normalized output voltage. As expected the amplitudes of the lower order harmonics (i.e. 5th, 7th) are substantially higher than those of the relatively higher order harmonics (i.e. 11th,13th) over the whole operating range of the converter.

2.6 Converter Under Varying Load Factor

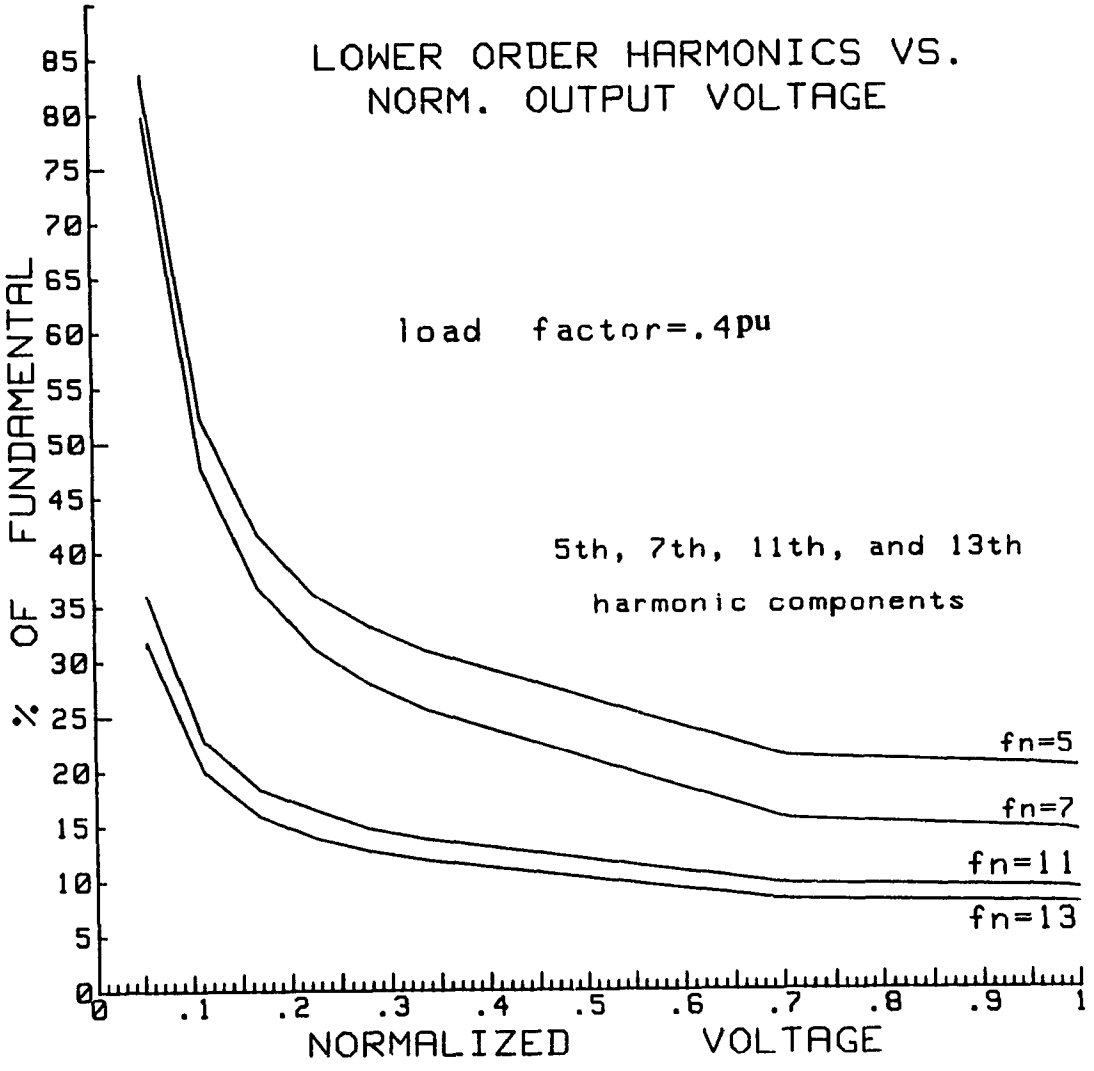

Fig. 2-11: Lower order harmonics of input line current.

The load factor of a converter can be defined as:

$$LF = R / 2\pi f_i L \qquad (2.33)$$

Where:

R = resistance of the load circuit,

f_i = input current frequency,

L = inductance of the load circuit.

Under the condition of ideal converter operation, the load inductance is assumed to be very high compared to the load resistance. In this situation the output current is a constant dc value with no ripples and is usually continuous. According to the transfer function approach for input current calculation, the output current is 'reflected' also into the input current, hence the input current pulses become ripple free.

In practice, the load is usually of R-L type, where the inductance may not be very high compared to the resistance. This will lead to a situation where the output current is not a constant dc, but also contains ripples. The input current will also be changed, and the pulses will no longer be ripple-free rectangles. At a sufficiently low value of inductance (R=XL), the input current will assume unpredictable shape and will contain very high ripples. This will eventually increase the harmonic content of the input current. Another situation associated with it is that the

output current may become discontinuous depending on the delay angle (α).

2.7 Performance Parameters under Varying Load Factor (LF) Conditions

Performance parameters such as input power factor (PF) of the converter, harmonic factor (HF) of input current, and distortion factor of output current (DFOC) have been calculated for varying load factor conditions and at balanced supply. The LF has been varied from a value of 0.99 pu,when the load is mostly resistive, to a value of 0.05, when the load is mostly inductive.

Figure 2-12 shows the input PF of the converter against the normalized converter output voltage. The PF has been calculated for 4 different values of LF, i.e. LF = 0.05, 0.4, 0.6 and 0.99. It can be seen that at the higher converter output region the input PF does not change appreciably. However at the lower output region, input PF increases slightly for higher values of LF.

The HF characteristics of Fig. 2-13 show that when the load is mostly resistive, i.e. LF = 0.99, the HF is comparatively higher than that under mostly inductive load. This holds true at the higher output region. As the output decreases at higher delay angle (α), the HF sharply increases and assumes a very high value at the lowest converter output region and at mostly resistive load. This

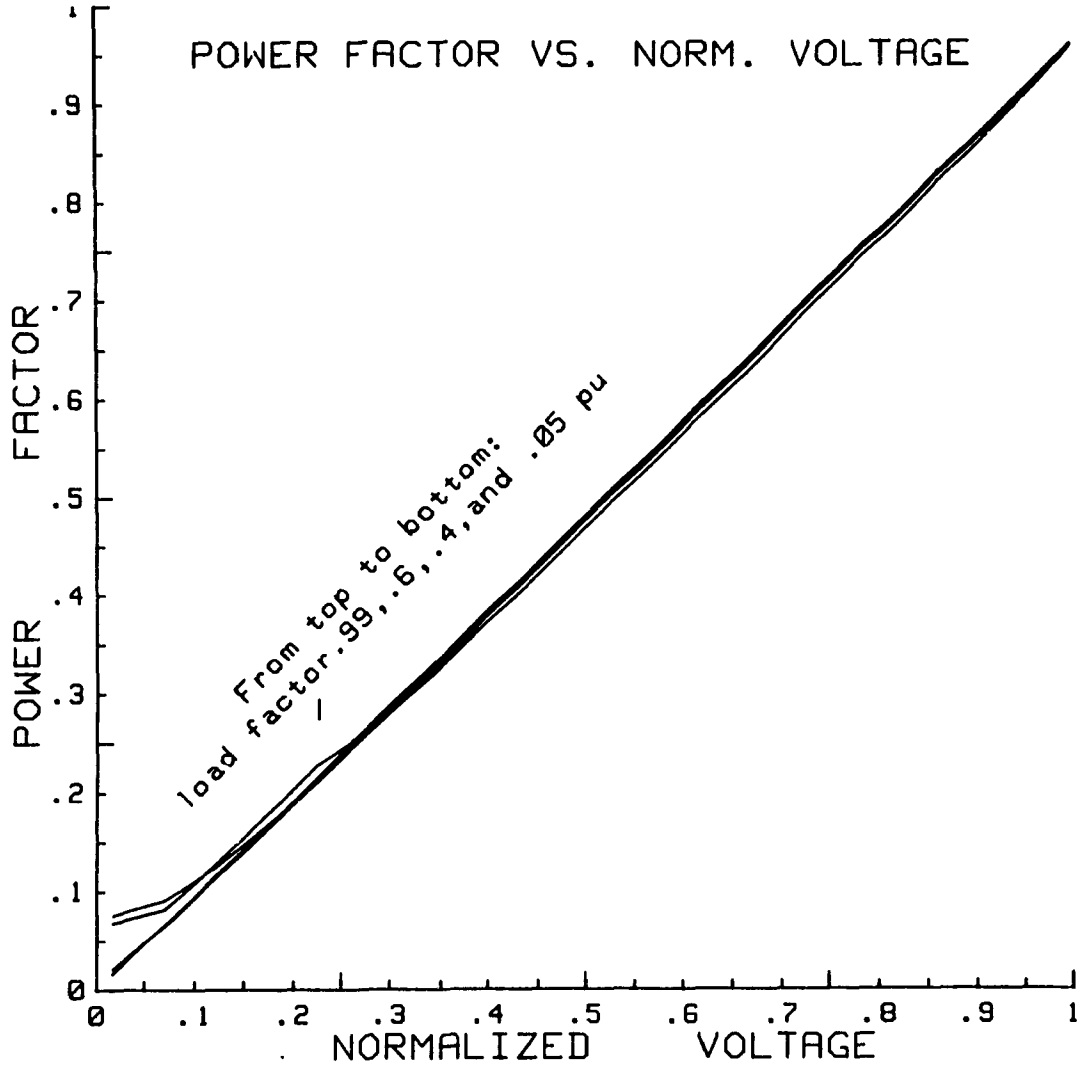

Fig. 2-12: Converter input power-factor at different load factors.

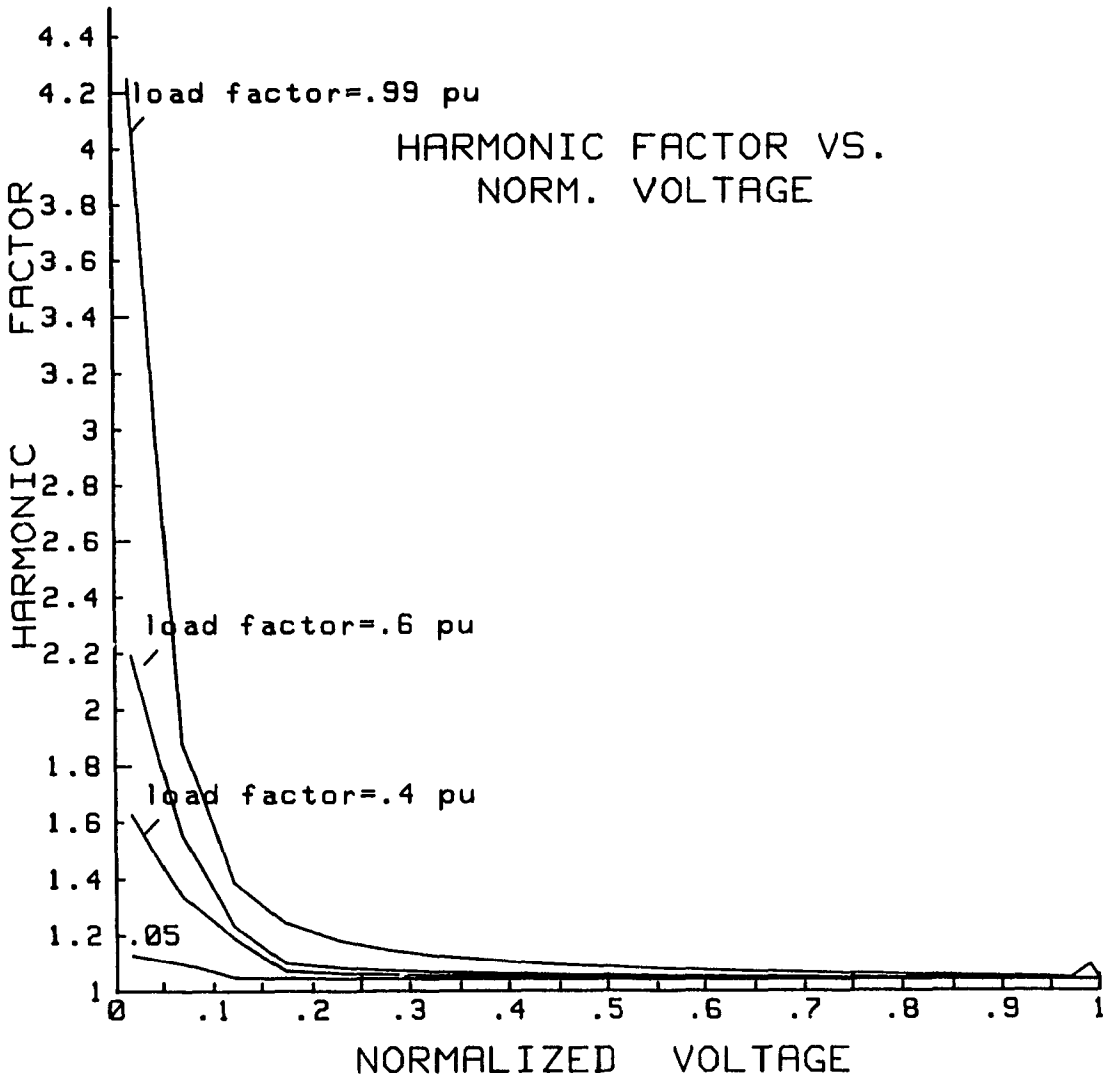

Fig. 2-13: Harmonic factor of input current at different load factors.

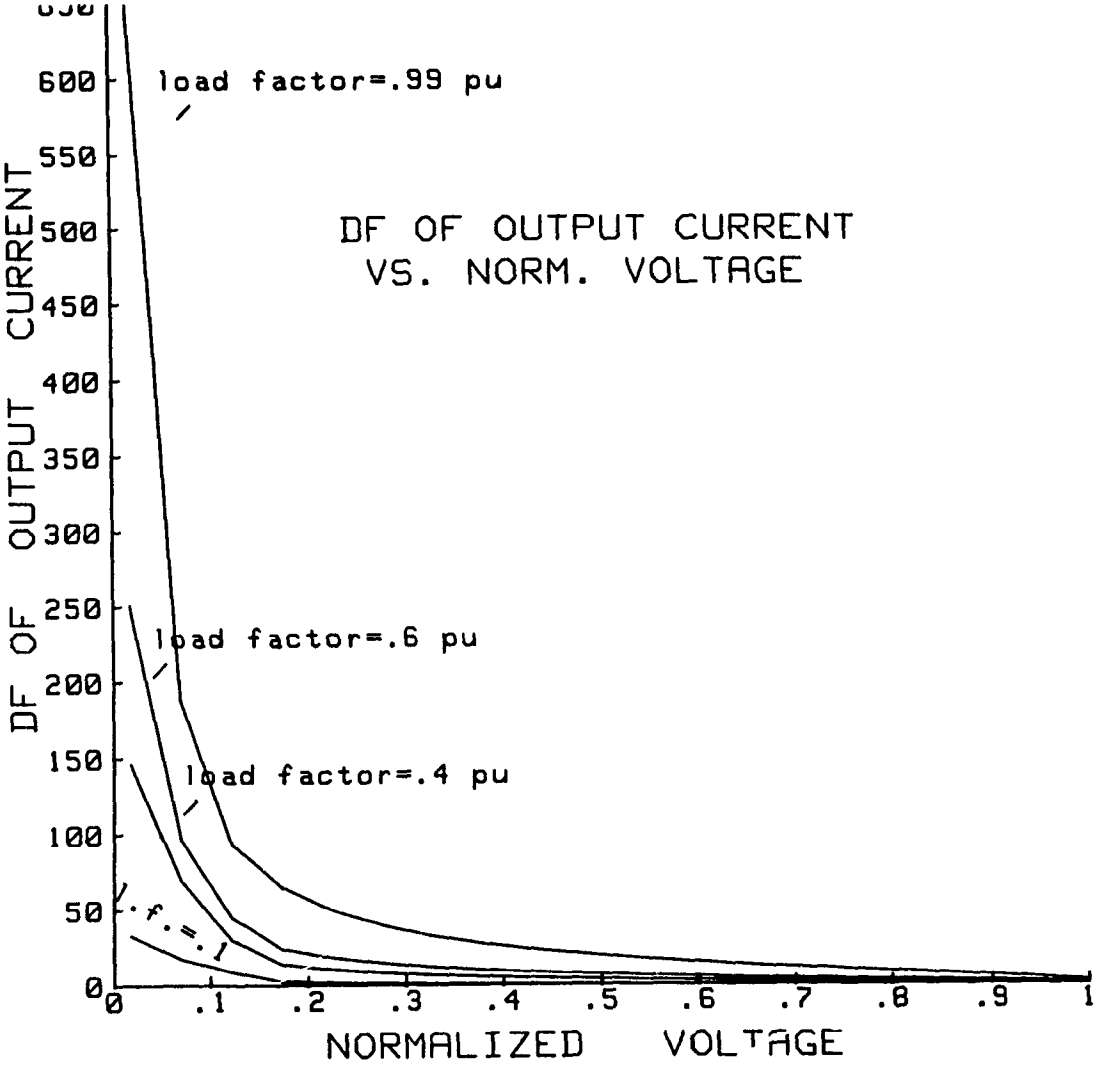

Fig. 2-14: Distortion factor of output current at different load factors.

is a situation that is likely to be avoided to reduce a very high harmonic pollution of the input current and discontinuity of the load current.

The output current is most likely to be affected when the load factor is changed. Fig. 2-14 shows the output current distortion against the change of delay angle(α) for various degrees of LF. For higher values of delay angle, and for a mostly resistive load the output current is highly distorted and assumes a value of about 650 % for a highly inductive load, the 'current quality' is comparatively good and stays about 35 percent even at the lowest converter output voltage. At the higher converter output, the output current distortion factor however, does not differ substantially from each other.

2.8 The Effect of Fixed dc Voltage (E_c) on the Performance Parameters

In all the performance parameters discussed so far, it was assumed that the load was purely of R-L type. However in practice, the load may include a fixed dc voltage in the form of a battery or the back emf of a dc machine. The performance parameters of a converter working under such a condition is a matter of interest.

Figures 2-15, 2-16, and 2-17 show the average output current, input PF, and DF of converter output current at different values of E_c varying against the normalized output

voltage. Three different values of E_c have been chosen to see the differences in performance parameters. The parameters have been evaluated at a constant LF = 0.4 pu.

It can be seen from Fig. 2-15 that for E_c = 1 pu, at normalized output voltage (V_n) $\simeq$ 0.61 pu, and delay angle (α) = 85^o, the average output current becomes zero. Further increase of delay angle tends to change the polarity of the output voltage. It is evident that at V_n smaller than 0.6 pu, the load current becomes discontinuous. For E_c = 0.5 pu and E_c = 0.25 pu, the load currents become discontinuous at relatively higher values of delay angles (V_n = 0.3 pu and V_n = 0.15 pu respectively). It can generally be said that for a converter, the higher the value of E_c, the smaller the range of converter operation.

The PF characteristics of Fig. 2-16 show that at the high converter output regions, the input PF does not change significantly along with the change of E_c. However, at points where the converter is about to enter discontinuous load current mode, the PF drops to a significant low value. This is especially evident for E_c = 1 pu. This sudden decrease of PF can be found from the fact that at points where the average output currents become zero, the fundamental input current suddenly assumes a very low value. It is known that the output current always 'reflects' itself to the input current, hence this sudden decrease of PF characteristics.

In general, the output current becomes distorted as the delay angle increases as shown in Fig. 2-17. At E_c = 0.25 pu, the output current has the highest DF, and is about 114.

This is comparatively higher than the DFs at E_c = 0.5 pu and E_c = 1 pu. However, this high value of DF occurs only at very low converter output region (V_n = 0.15 pu). A converter is hardly expected to work in this low range of output voltage.

From figures 2-15 and 2-17, it is evident that the peak values of the DF at V_n = 0.61 pu, V_n = 0.3 pu and V_n = 0.15 pu are due to the fact that the average output currents of the converter becomes very low. As the delay angle increases, the average output current decreases significantly and leads towards zero. On the other hand, the ripple output current decreases slightly. Just before zero average output current, the output current consists of only ripple contents and consequently has the highest DF. It can be concluded that a converter should not be operated with a large fixed dc voltage. This is because the range of operation is narrow, PF drops suddenly, and the converter enters into discontinuous load current mode at a low delay angle.

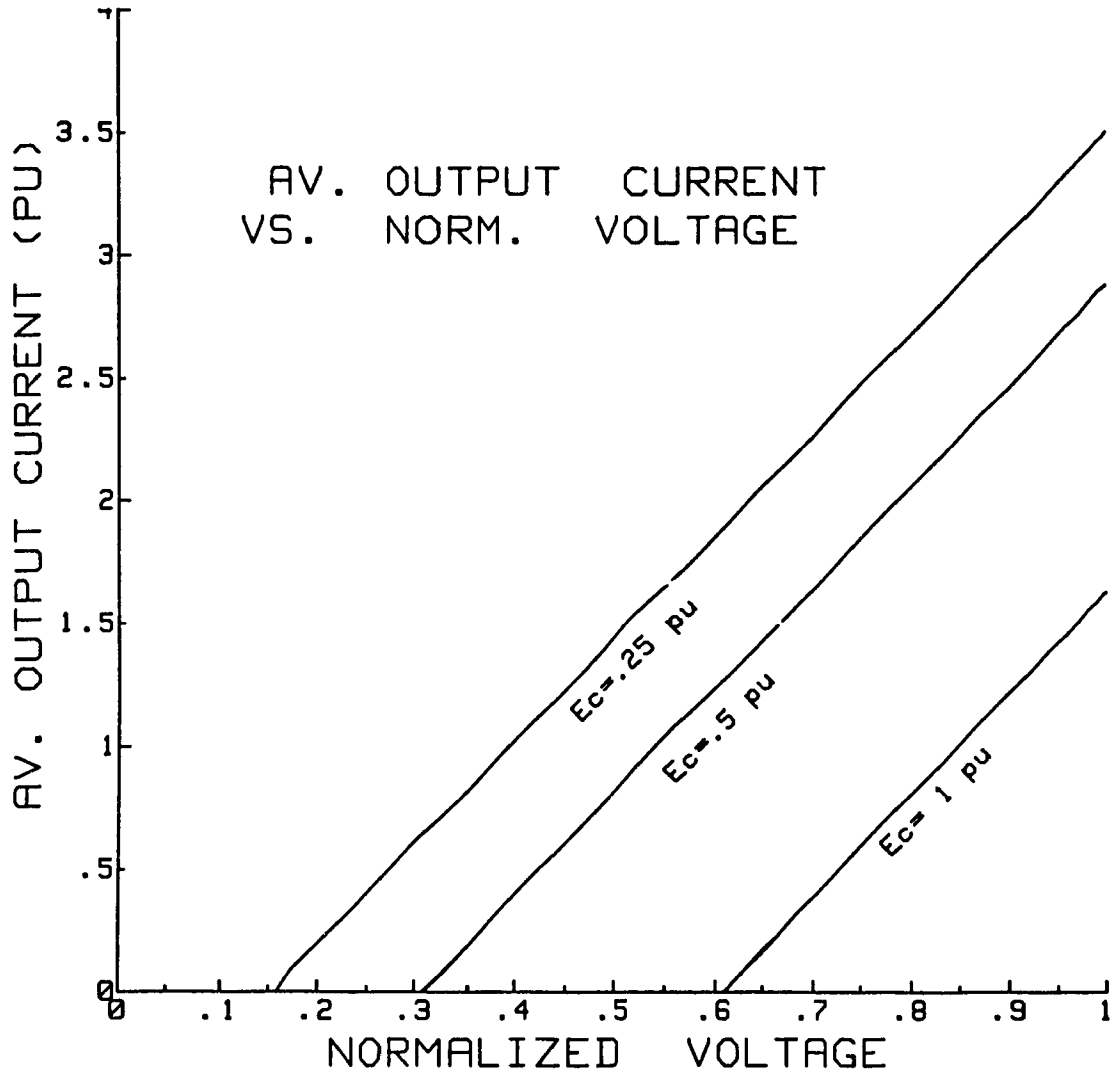

Fig. 2-15: Converter average output current at various fixed dc voltages.

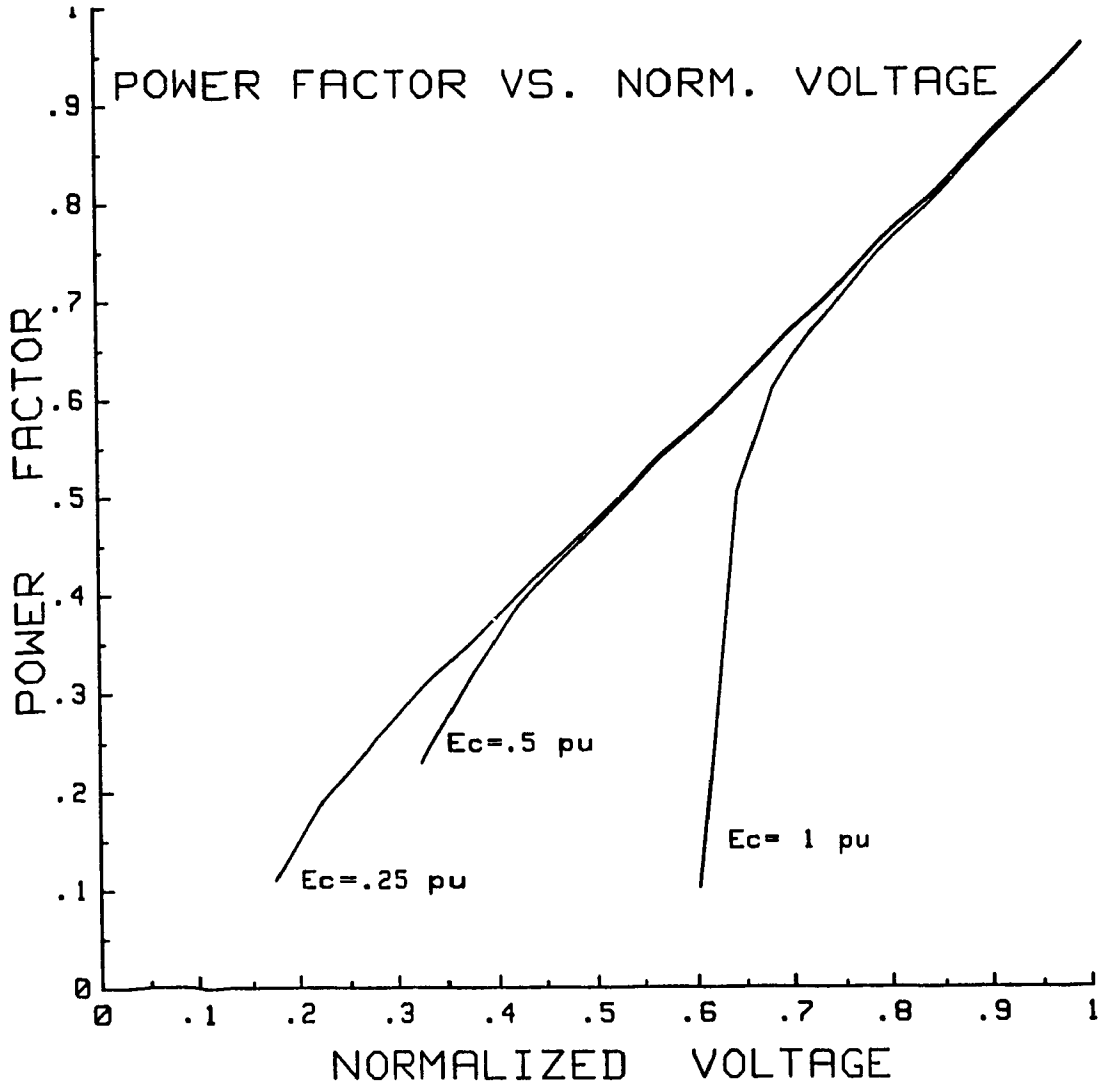

Fig. 2-16: Converter input Pf at various fixed dc voltages.

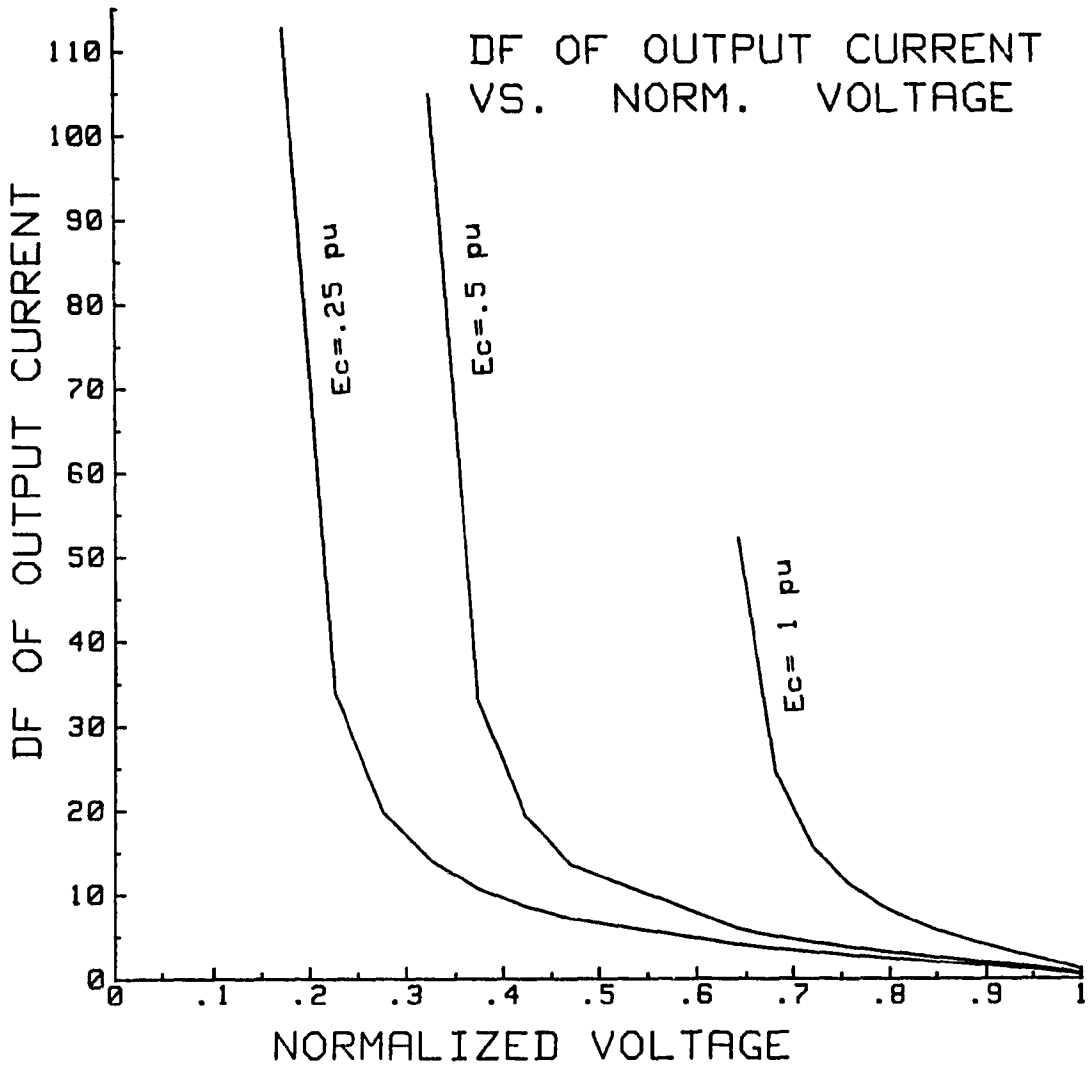

Fig. 2-17: Converter output current distortion at various fixed dc voltages.

CHAPTER 3

THE CONCEPT OF UNBALANCE AND THE CONSEQUENT CONVERTER PERFORMANCE

3.1 The concept

In an electrical system supply voltages can be unbalanced due to various reasons. In an ideal balanced 3-phase system, the magnitudes of the supply voltages for the 3 different phases should be equal and the phase angles should be 120 and 240 electrical degrees apart from a reference phase with zero phase shift. Among several reasons of supply voltage unbalances, unbalanced load or unbalanced phase impedances are considered common. In addition, line to line or line to ground faults are also present in power system, resulting in serious supply voltage unbalances. There are some limitations up to which unbalances can be tolerated in power system. In practice it is rather impractical to put any limitations on the degree of supply unbalances. The severe consequences of voltage unbalances are clearly recognized in the current National Electrical Manufacturers Association (NEMA) motor standard MG-1(40). It points out that a $3\frac{1}{2}$ % voltage unbalance can result in a 25% increase in motor temperature rise and shortening of motor insulation life by one-half. The NEMA motor standard specifies only one percent unbalance [20].

Unbalance in the supply causes the system impedance to go up. If it is assumed that the system impedance up to the service bus is around six to eight percent on the service transformer kVA, then the observed voltage drop when fully loaded will be from two to four percent depending on the load power factor. The voltage drop in the system (including phase shifts) will be seven percent [20]. If the transformer is 100% loaded with thyristors, then each harmonic will cause a seven percent distortion because system impedance increases with harmonic order and required load current decreases with harmonic order in the same proportion [20]. If ten lower-order harmonics are necessary to provide the required DC smoothness, the total harmonic voltage distortion will be $\sqrt{10*7^2} = 7*3.2 = 22\%$.

It is not always possible or practical to use input filters to trap harmonics for resonance and other associated problems. For example, if resonance occurs at one of the lower harmonics, one can expect considerably more than five percent wave distortion [20]. Resonances above the fourteenth harmonic generally do not cause trouble because of the small amount of energy associated with them. However, loads such as computers, electronic devices and gas discharge lamps are sensitive even to the slightest harmonics. Although tuned input filters seem to be a practical solution to trap the harmonic of a particular frequency, this suffers from the change of system impedance caused by the change in utility system. This again results

in resonance.

It is evident that monitoring the exact harmonics under different converter operation ranges is essential from a filtering point of view. Unbalances between the supply voltages in a 3-phase system cause substantial changes in the converter performance. An unbalance may be caused by changes in the magnitudes or phases of the supply voltage. In many situations both might be responsible.

The effects of supply unbalances are explained with Fig. 3-1. The switching functions for different switches corresponding to particular phases are found from the voltage crossover points. Under balanced supply conditions, the switching functions are all similar. So if the transfer function for phase 1 is known, the transfer functions for other two phases can be derived. However, this concept can not be applied when the supply becomes unbalanced as seen from Fig. 3-1. Fig. 3-1 corresponds to unbalance due to only change in magnitude. These changes the voltage crossover points, and consequently the switching functions. It is found that though the switching functions of positive and negative pulses for a particular phase remain essentially the same, but the transfer functions for the other two phases are different ($D_1 = D_2 = D_3$, where D_1, D_2, and D_3 are the widths of the corresponding switching functions). This leads to the fact that the transfer function derived in section 2.2 can not be directly applied to calculate input and the output parameters of the converters. Instead, three

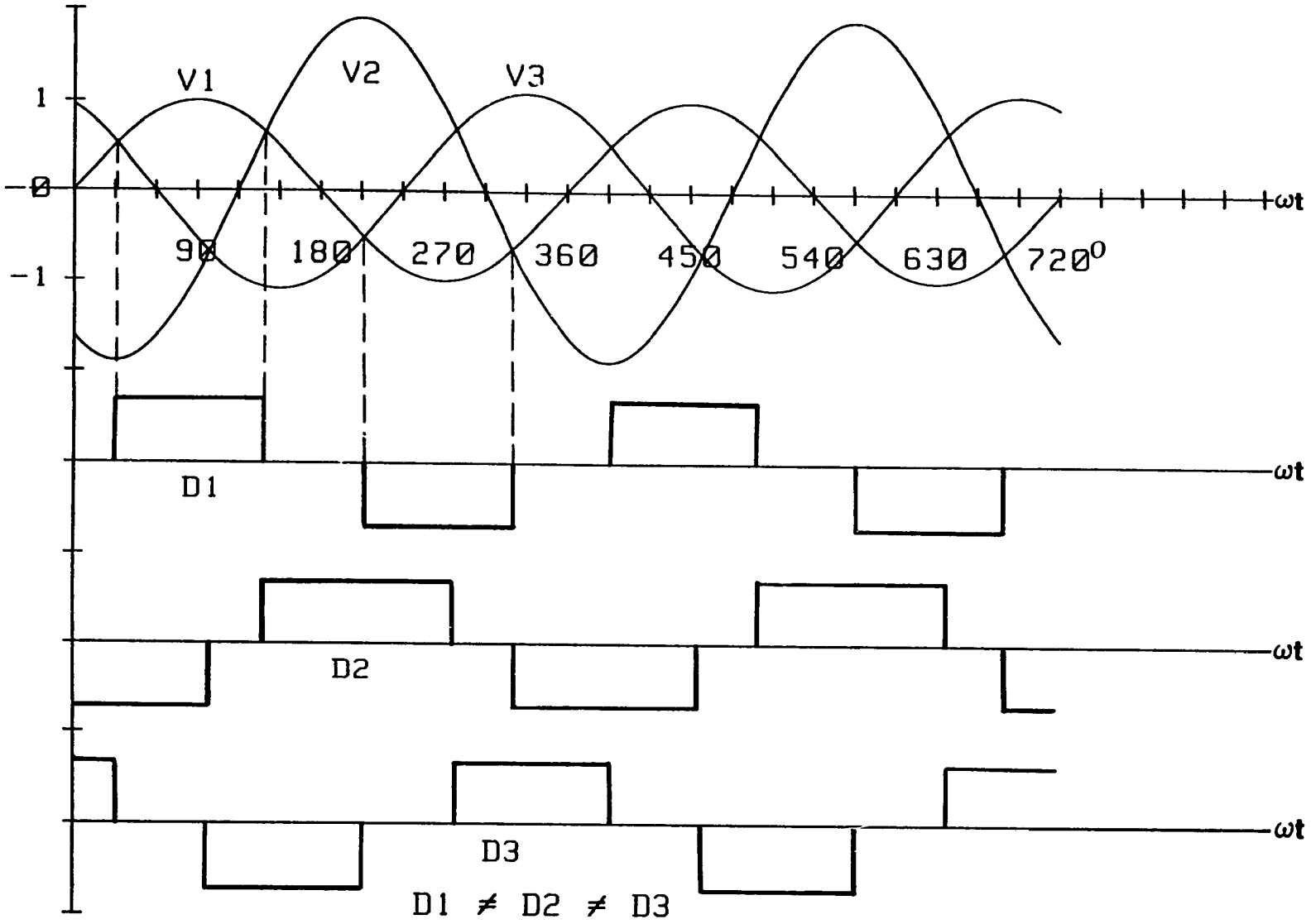

Fig. 3-1: Variation of switching functions under unbalanced supply.

different transfer functions for three different phases need to be calculated. The transfer function with respect to the input port of the converter is expressed as $[S_1(\theta)-S_4(\theta)]$ for phase 1, $[S_3(\theta)-S_6(\theta)]$ for phase 2 and $[S_5(\theta)-S_2(\theta)]$ for phase 3, where $[S_1(\theta),\ldots S_6(\theta)]$ are the corresponding switching functions of the thyristor switches. In the transfer function approach, the Fourier series is employed to calculate the switching functions where the limits of integrations are found from voltage cross-over points. For phase 1, the switching functions start at a point where $|v_3| = |v_1|$ and terminate at a point where $|v_1| = |v_2|$, to give the positive pulse of the switching function of phase 1 as shown in Fig. 3-1. v_1, v_2, and v_3 are the corresponding instantaneous line to line voltages and are given by :

$$v_1 = E_1 \text{ Sin } (\theta - \phi_1) \qquad (3.1)$$

$$v_2 = E_2 \text{ Sin } (\theta - \phi_2) \qquad (3.2)$$

$$v_3 = E_3 \text{ Sin } (\theta - \phi_3) \qquad (3.3)$$

Where: E_1, E_2, E_3 = Peak values of the supply voltages.

ϕ_1, ϕ_2, ϕ_3= Phase angles of the supply voltages.

Equating $v_1 = v_3$, and assuming that $\phi_1 = 0^o$, we have:

$$E_3\text{Sin}(\theta - \varphi_3) = E_1\text{sin}(\theta)$$

$$\text{or} \quad E_1 \sin(\omega t) = E_3 \sin(\omega t - 120^{\circ})$$

$$\text{or} \quad E_1 \sin(\omega t) = E_3 \left((-\sin(\omega t)(1/2) - (\cos(\omega t)) \left(\frac{\sqrt{3}}{2}\right) \right)$$

$$\text{or} \quad \tan(\omega t) = - \frac{\frac{\sqrt{3}}{2} E_3}{E_1 + \frac{E_3}{2}}$$

the point of intersection of the two voltages is:

$$\omega t = \tan^{-1} \left(\frac{\frac{\sqrt{3}}{2} E_3}{\frac{2E_1 + E_3}{2}} \right) \tag{3.4}$$

And the termination point for the positive pulse of the switching function of phase 1 can be found to be:

$$\omega t = \tan^{-1} \left[\left(\frac{(E_1 + E_2)\sqrt{3}}{E_1 - E_2} \right) \right] + \frac{\Pi}{3} \tag{3.5}$$

The transfer functions of the other two phases are found similarly.

From the above expressions, it can be seen that the transfer functions are functions of magnitudes of input voltages E_1, E_2, E_3. The transfer function in section 2-2 has to be calculated using E_1, E_2, E_3 as variables. As a result there would be three different transfer functions for three different phases. Considering these, the converter has been simulated using the transfer function approach

developed in section 2-2.

3.2 Input Current Harmonic Spectrum

Under unbalanced supply, due to the non-symmetries of the switching functions, the input line currents for the three different phases are evaluated separately.

The input line current spectrum for line 1, 2, and 3 are shown in Figs. 3-2(a), (b), (c) respectively. It is evident from the Figs. that in addition to the characteristic harmonics, non-characteristic harmonics (i.e. harmonics of orders 3, 9, 15) are also generated. But their magnitudes are comparatively small compared to the fundamental, for example, the 3rd component is only 12% of the fundamental. The 9th and 15th harmonic magnitudes are even smaller. All these Fig.s represent the changes due to unbalance in the magnitude of the supply voltage (5% unbalance), and a delay angle of 107^{o} only.

In practice, the supply could be unbalanced due to a change in the phase angles, and also due to changes in both magnitudes and phase angles of the supply voltages. Under both situations, the input line currents contain non-characteristics harmonics.

3.3 Output Current Harmonic Spectrum

The rectifier dc output harmonics are significantly

phase 1.

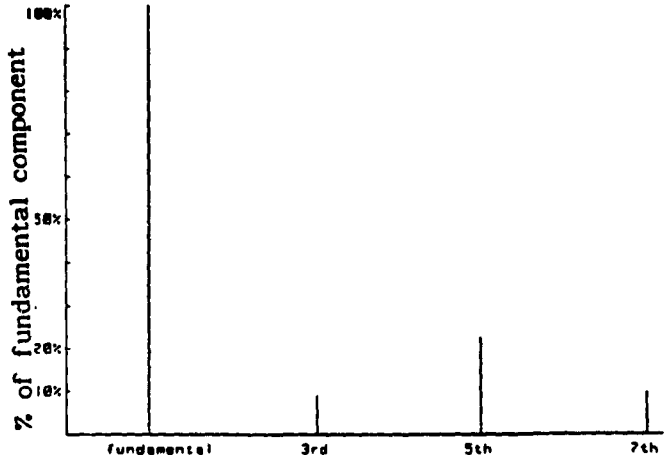

phase 2.

phase 3.

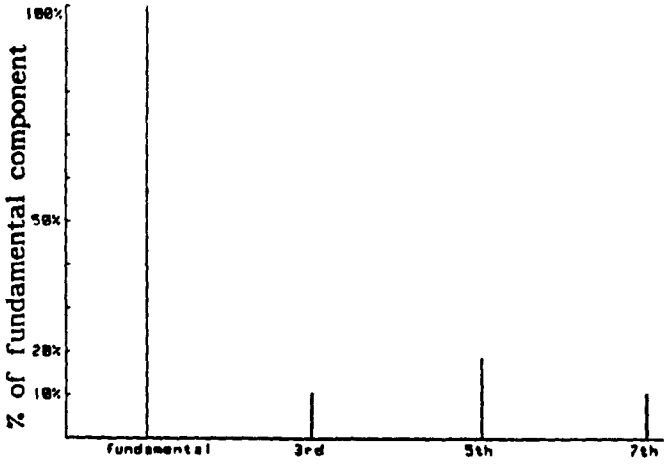

Fig. 3-2(a), (b), and (c): Input current harmonic spectra for phases 1, 2, and 3.

different from the ac harmonics. In the input current harmonics, the dc wave form contains only even harmonics. These harmonics are adversely affected by phase delay (α). Moreover, the load type, i.e. resistive, inductive, back emf plays a significant role on them. Under balanced supply conditions, the orders of harmonic present are $m = nq$, where q is the number of pulses, and n is an integer. For a 6 pulse rectifier, the lowest harmonic is 6th. When the supply becomes unbalanced, the harmonic orders are however shifted. Though the harmonics present are of even orders, and the lowest order is 2nd, and has a high magnitude and is found to be dependent on only on the degrees of unbalances and load factor, and is independent of delay angle.

This 2nd harmonic magnitude is of alarming value and may cause a significant problem for a load (for example: an inverter) that may be connected to the dc side of a rectifier. The other two lower harmonics (i.e. 4th, and 6th) are however comparatively small and are not expected to cause major problem.

It has been found that, in general, harmonics that are not multiples of 6 are independent of phase delay, and are constant throughout the whole converter operating range. Harmonics that are multiples of 6 are however affected by phase delay.

3.4 Supply Voltage Unbalances

If we assume that the line to neutral rms supply voltages are V_{an}, V_{bn}, V_{cn}(a, b, c correspond to phases 1, 2, and 3), then their corresponding zero, positive, and negative sequence voltages can be expressed respectively as:

$$\bar{V}_Z = 1/3 \ (\bar{V}_{an} + \bar{V}_{bn} + \bar{V}_{cn}) \qquad (3\ 6)$$

$$\bar{V}_P = 1/3 \ (\bar{V}_{an} + a^* \bar{V}_{bn} + a^{2*} \bar{V}_{cn}) \qquad (3.7)$$

$$\bar{V}_N = 1/3 \ (\bar{V}_{an} + a^{2*} \bar{V}_{bn} + a^* \bar{V}_{cn}) \qquad (3.8)$$

where 'a' is an operator, and its value is $1\angle 120^0$. We can define a variable 'u' such that:

$$u = \left| \frac{V_N}{V_P} \right| \qquad (3.9)$$

and 'u' is the normalized value of the negative sequence with respect to the positive sequences (It is to be noted that 'u' is known as voltage unbalance factor (VUF) in some European standards).

The following table shows the values of the line to neutral voltages which would result in a certain amount of unbalance. The results are presented for unbalances up to 20 %. However, in practice, unbalances are only tolerated up to 5%.

Table 3.1 Line to neutral voltages

u	V_{an}	V_{bn}	V_{cn}
balanced	$1\angle 0^{o}$	$\angle -120^{o}$	$\angle -240^{o}$
unbalanced			
2%	$1\angle 0^{o}$	$.95\angle 120^{o}$	$1.01\angle 240^{o}$
4%	$1\angle 0^{o}$	$.9\ \angle 120^{o}$	$1\ \angle 240^{o}$
5%	$1\angle 0^{o}$	$.861\angle 120^{o}$	$.863\angle 240^{o}$
6%	$1\angle 0^{o}$	$1.2\ \angle\ 120^{o}$	$1.06\angle 240^{o}$
10%	$1\angle 0^{o}$	$1.4\ \angle\ 120^{o}$	$1.1\ \angle 240^{o}$
14%	$1\angle 0^{o}$	$1.55\angle\ 120^{o}$	$1.13\angle 240^{o}$
20%	$1\angle 0^{o}$	$1.90\angle\ 120^{o}$	$1.1\ \angle 240^{o}$

3.5 Performance Parameters under Unbalanced Supply Voltages

The computer program simulating the converter developed in section 2.4 cannot be directly used to find the performance parameters when the supply is unbalanced. The program simulating the converter has to be modified, where the transfer functions for three different phases have to be calculated separately. All the performance parameters such as PF, HF, DF, and THD evaluated in section 2.4 are re-calculated for various levels of unbalances in terms of both magnitude and phase angles of the supply voltages. The results are presented in graphical forms against the normalized output voltage of the converter.

3.5.1 Input power factor

The expression for power factor (PF) used in section 2.4.1 cannot be used when the supply becomes unbalanced. Instead, the expression should include all the three input currents separately, since they are different. Hence by PF we understand the 'total' PF of the converter. The following expression fulfills that criterion.

$$TPF = \frac{V_{an}\, I_{a1}\cos(\varphi_{a1}) + V_{bn}\, I_{b1}\cos(\varphi_{b1}) + V_{cn}\, I_{c1}\cos(\varphi_{c1})}{V_{an}I_a + V_{bn}I_b + V_{cn}I_c} \qquad (3.10)$$

Where:

V_{an}- Line to neutral input rms voltage.

I_{a1}- Fundamental component of rms input current.

φ_{a1}- Phase shift between V_{an} and I_{a1}.

When the supply becomes balanced, $V_{an} = V_{bn} = V_{cn} = V$. Substituting in Eq. (3.10), we have:

$$TPF = \frac{V\,(I_1\cos(\varphi) + I_1\cos(\varphi) + I_1\cos(\varphi))}{V(I + I + I)} =$$

$$= \frac{3\, I_1\cos(\varphi)}{3\, I} = \left(\frac{I_1}{I}\right)\cos(\varphi) \qquad (3.11)$$

This is what is theoretically expected when the supply is balanced. The TPF of the converter under unbalanced

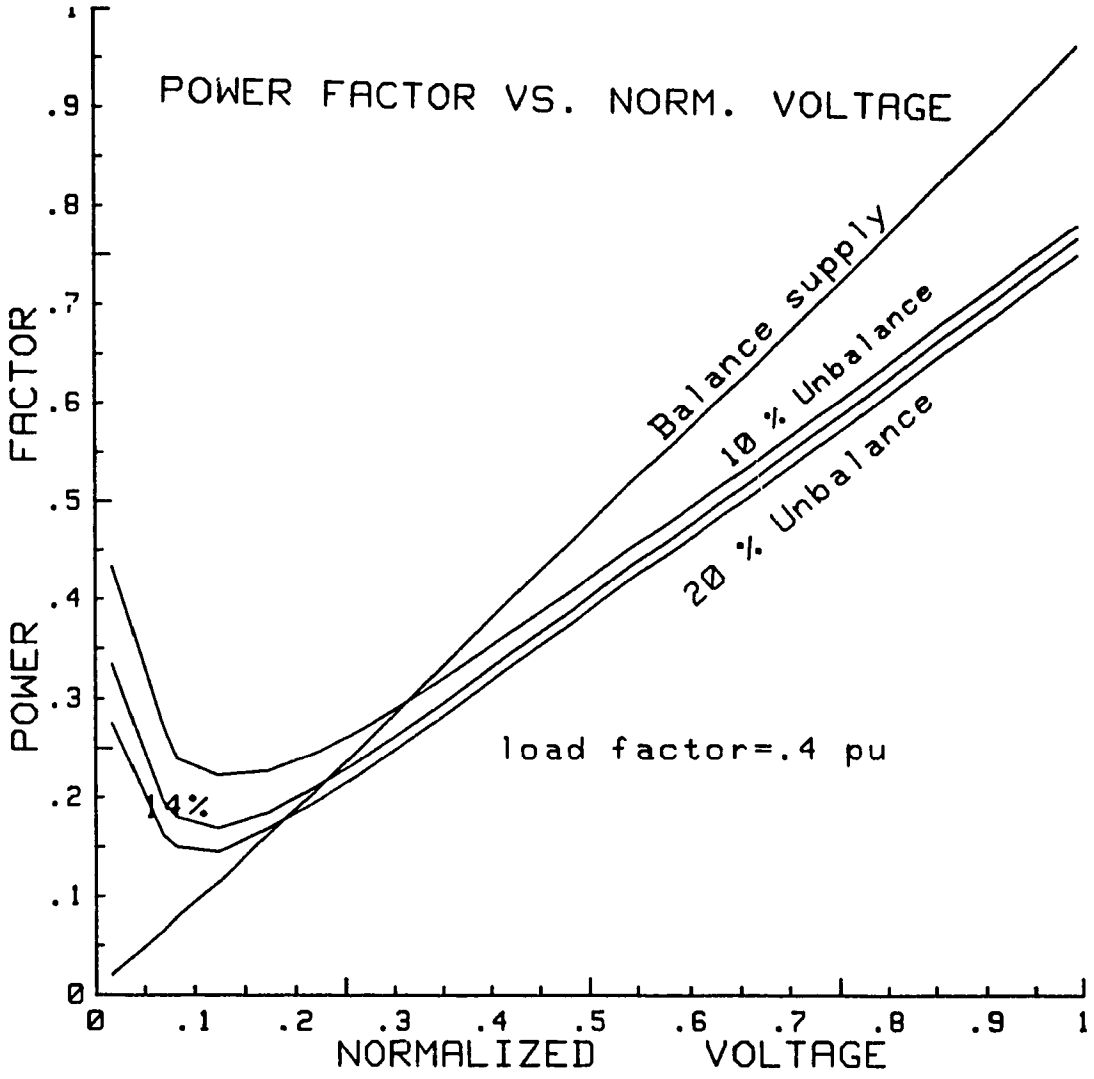

Fig. 3-3: Converter input power factor at unbalanced supply.

supply condition is presented in graphical form in Fig. 3-3 against the normalized output voltage. As the supply becomes more and more unbalanced, the TPF decreases. It further decreases rapidly as the delay angle increases, i.e. converter output voltage decreases. It can be seen from Fig. 3-3 that under unbalanced supply and at the lower output region of the converter ($\alpha > 110^{o}$), the TPF tends to increase. This is a very interesting phenomenon and has been investigated further. It occures due to following reasons.

Looking at Fig. 3-4, it can be noticed that under unbalanced supply conditions, the reactive part of the fundamental input current is substantially higher than that under balanced supply conditions. The value of the expression, $\cos(\varphi) = \cos(\tan^{-1}(I_{1p}/I_{1q}))$ in Eqn.(2.29) depends on the ratio of the magnitude of I_{1p} and I_{1q}.

If we define, $I_{1p}/I_{1q} = A$, and if $A = 1$, then $I_{1q} = I_{1p}$ and $\cos(\varphi) = 0.707$. if $A<1$, PF increases. When $A>1$, displacement factor and consequently TPF decrease further from 0.707, and $I_{1p} > I_{1q}$. Beyond $\alpha = 77^{o}$, $I_{1p} > I_{1q}$ until $\alpha = 116^{o}$. At this point and beyond, $I_{1p} < I_{1q}$, this increases displacement factor, and the overall TPF of the converter. Under balanced supply as we increase α, the active component of the fundamental input current I_{1p} always stays bigger than the reactive component of the fundamental input current I_{1q}. This keeps the TPF decreasing as we increase the delay angle α. The difference of the type of the rate of change of the active and reactive components of

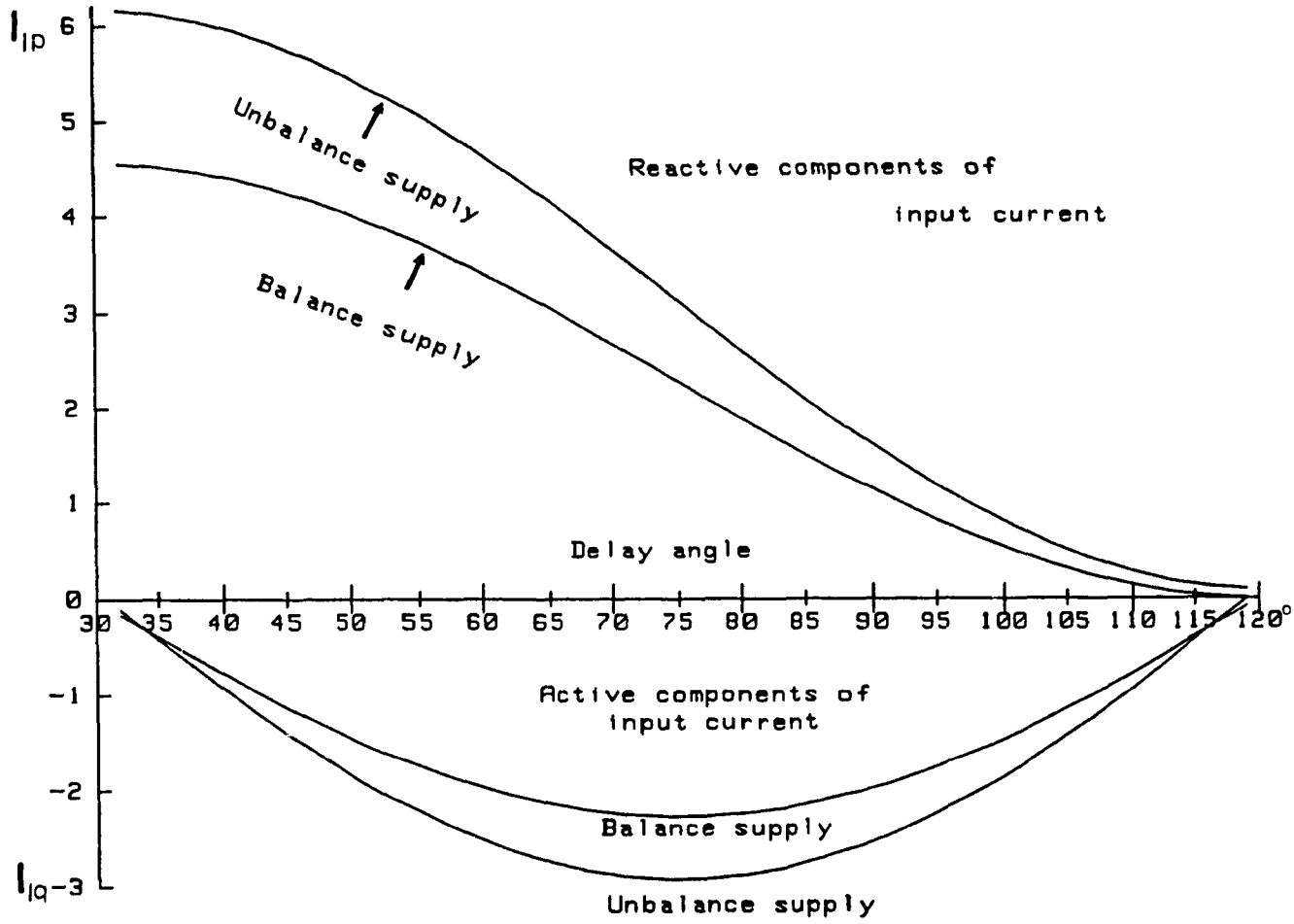

Fig. 3-4: Variation of active and reactive components of fundamental input current vs. delay angle (α).

the fundamental input current under unbalanced supply conditions is responsible for this sudden increase of PF at the lower output range.

3.5.2 Harmonic factor

The harmonic factor of the input current under unbalanced supply is defined in the same way as in the case of balanced supply. Since theoretically there are three input currents, there should also be three different harmonic factors. The HF is defined as the ratio of the rms nth harmonic component to the fundamental rms component. It has been found that no matter how the input currents differ from each other, this ratio remains the same, for any of the three input currents and for a particular delay angle (α). This gives rise to a situation that, though the input line currents may have different harmonic spectra, the HFs are the same for different phases.

From Fig. 3-5 it can be noticed that the HF increases along with the increase of the degree of unbalance, and increases slightly with the delay angle. However, it increases sharply at the very low converter output voltage.

3.5.3 Distortion factor

The distortion factor of input and output currents under unbalanced supply have been calculated in the same way

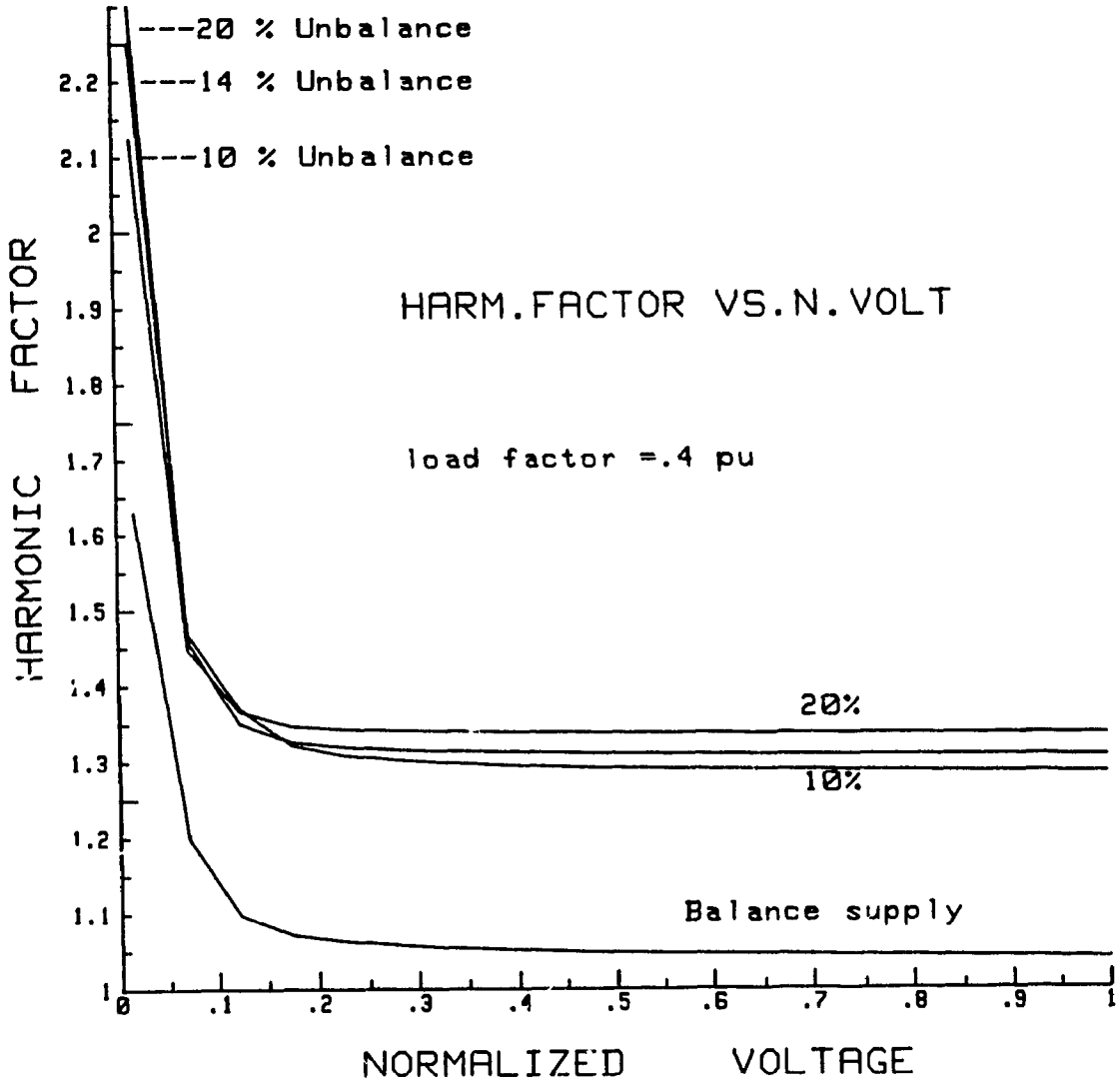

Fig. 3-5: Harmonic factor of input current at unbalanced supply.

as they had been in section 2.5.3. Under unbalanced supply conditions we have three different input currents, the expression of DF for input currents implies the same logic used in HF, to be used again. Consequently all the input currents are distorted by equal degrees at a particular delay angle.

Figure 3-6 shows the distortion factor of one of the three line currents. It essentially follows the same pattern of change as that of HF.

The output current is not pure dc and has ripple content. The DF of output current is shown in Fig. 3-7. As it is evident, that the distortion factor of the output current does not differ appreciably at the higher output range of the converter. However, at a very high value of delay angle, and at a relatively high degree of unbalanced supply (i.e. 20%) the distortion factor attains a substantial high value.

3.5.4 THD of output voltage

The total harmonic distortion of the output voltage is evaluated in a similar way as was done under balanced supply in section 2.5.4. The THD is presented in Fig. 3-8 varying with the normalized output voltage. Under unbalanced supply, output voltage contains high value of 2nd and other even harmonics in addition to the usual 6n (n = 1, 2, 3,...) order of harmonics. The relative high value of overall THD

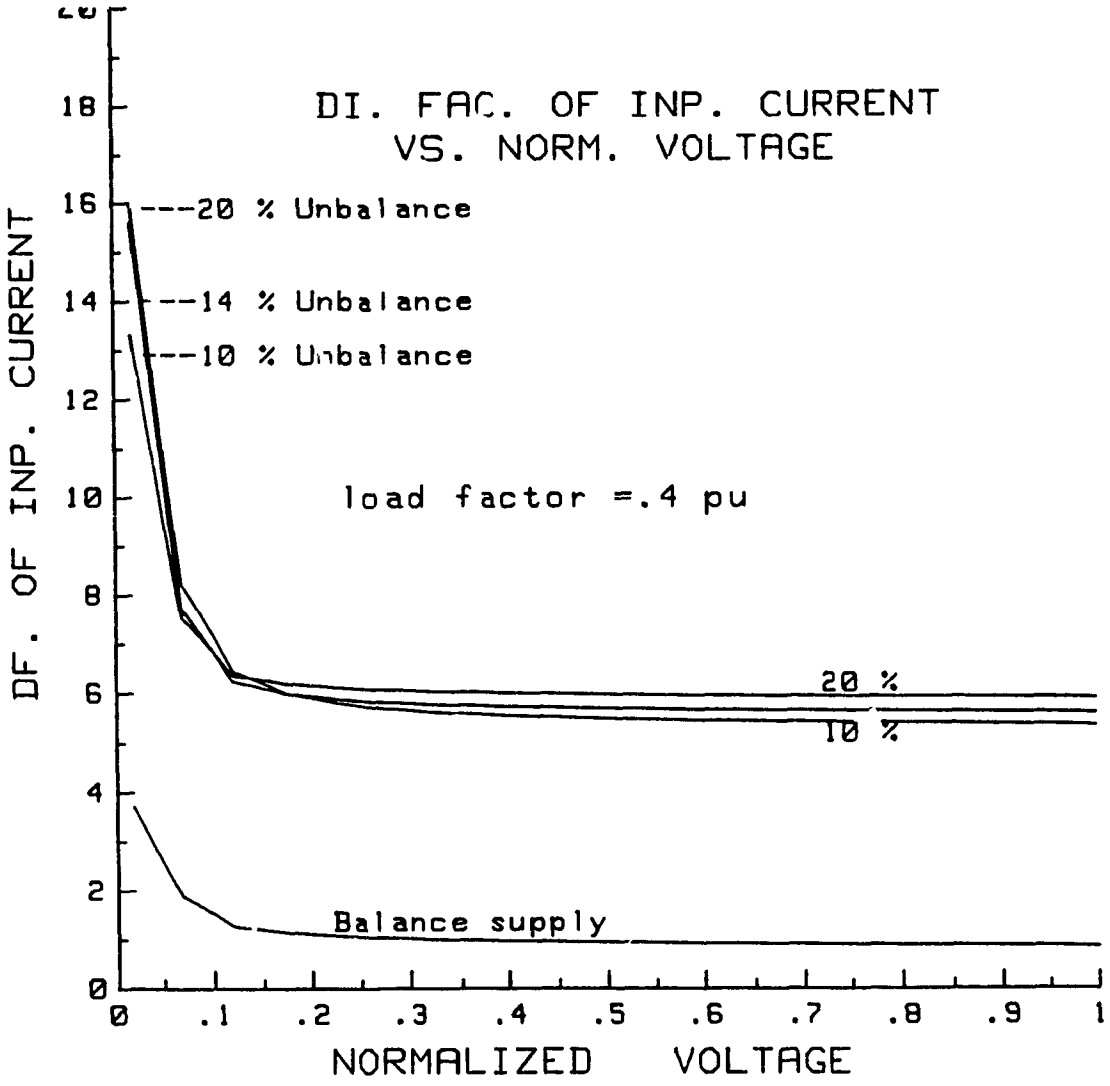

Fig. 3-6: Distortion factor of input current at unbalanced supply.

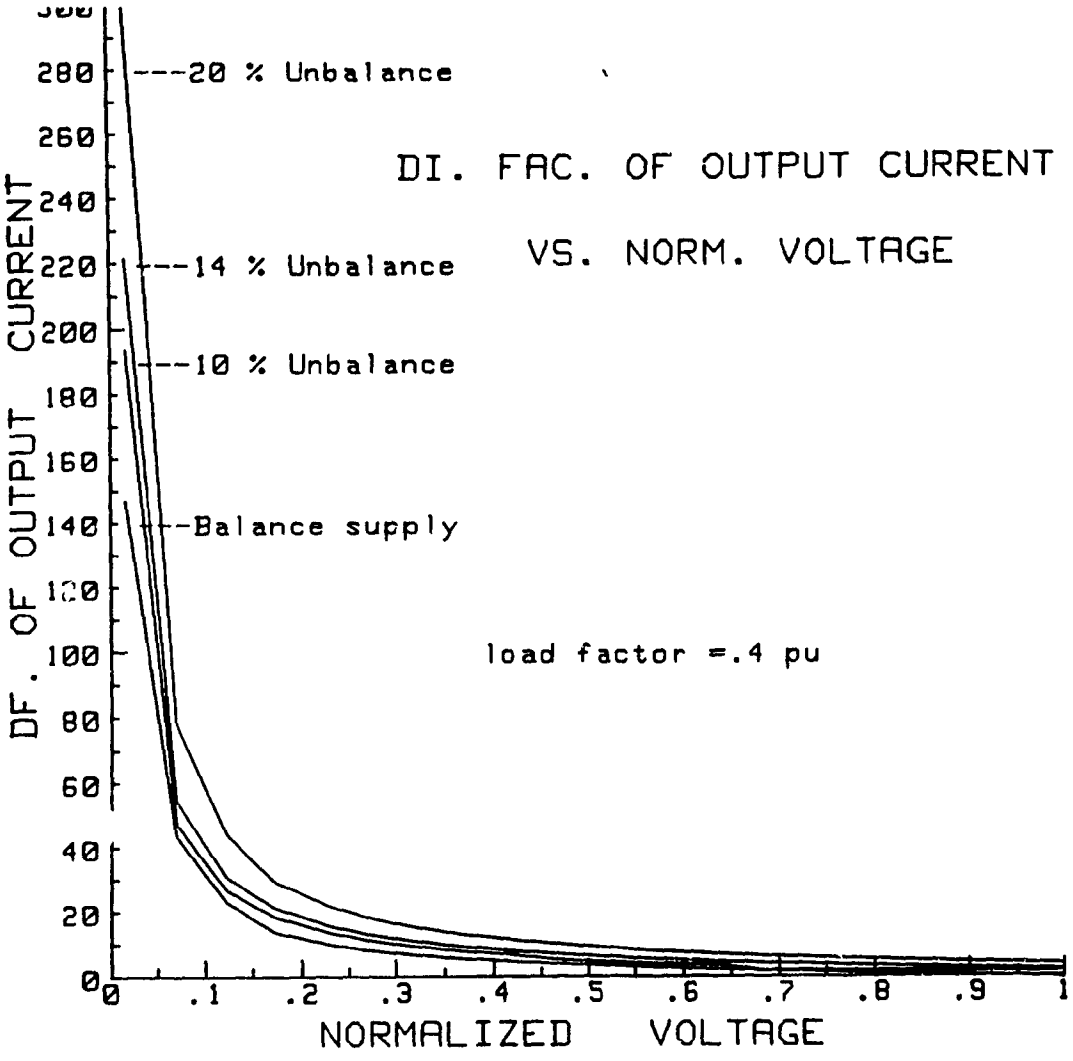

Fig. 3-7: Distortion factor of output current at unbalanced supply.

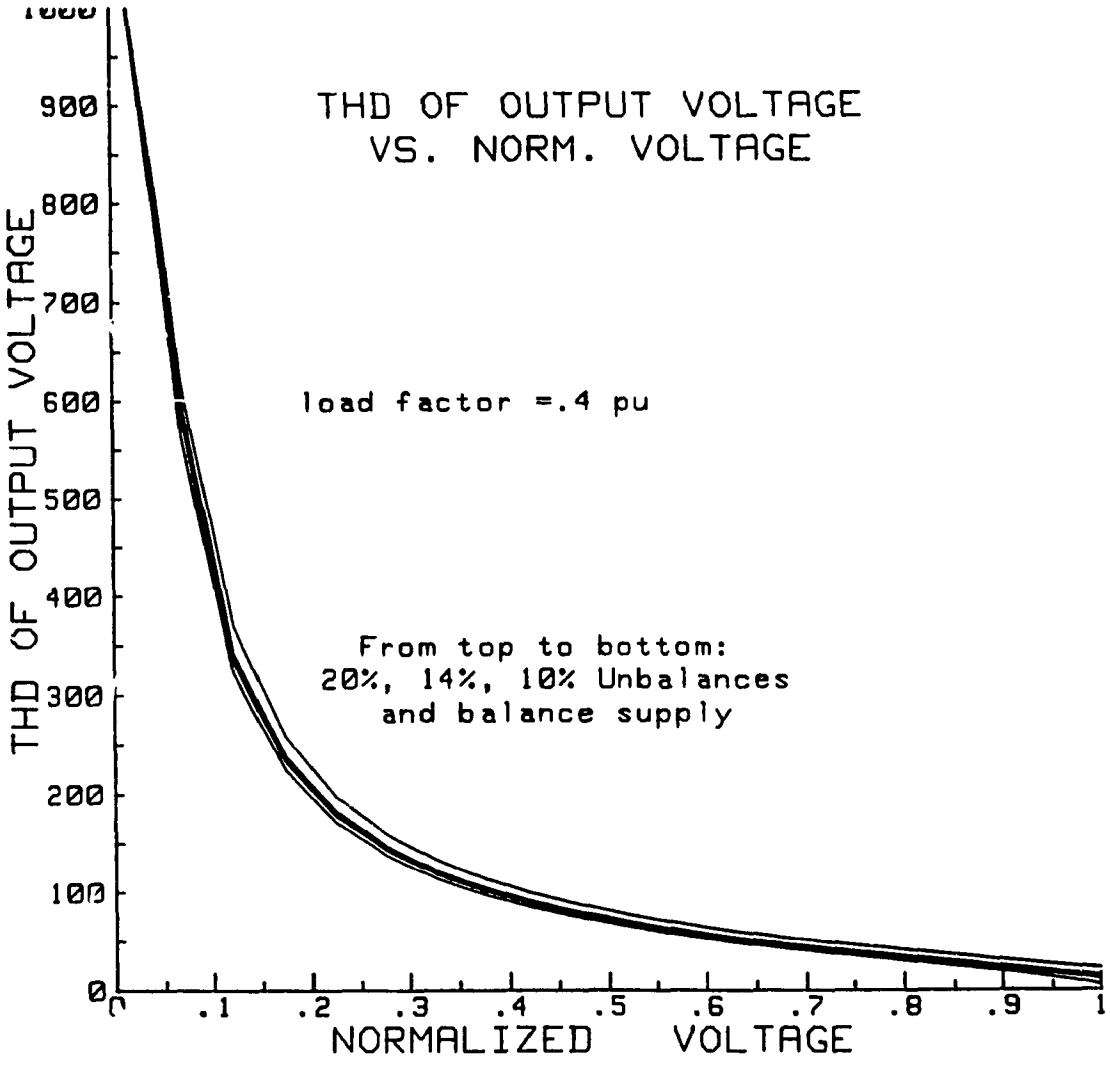

Fig. 3-8: Total harmonic distortion of output voltage at unbalanced supply.

compared to the THD under balanced supply can be attributed to these non characteristic harmonics.

3.5.5 Lower order harmonics

Figure 3-9 shows the lower order harmonics for 20% unbalanced supply varying with the change of converter output voltage. Comparing this with the one under balanced supply (section 2.5.4) we can see a major increase in terms of harmonic content, especially in the lower output region of the converter.

3.6 Performance Parameters under Small Unbalances of Supply Voltages

Under lower values of supply unbalance, performance parameters such as PF, HF, DFIC etc. are presented in tabular form, since in graphical form, they overlap each other and become hardly distinguishable. Tables 3.2 and 3.3 show the performance parameters for 2 and 4 percent unbalances and for the lower output region of the converter, i.e. from 0.017 to 0.485 pu of normalized output voltage of the converter output.

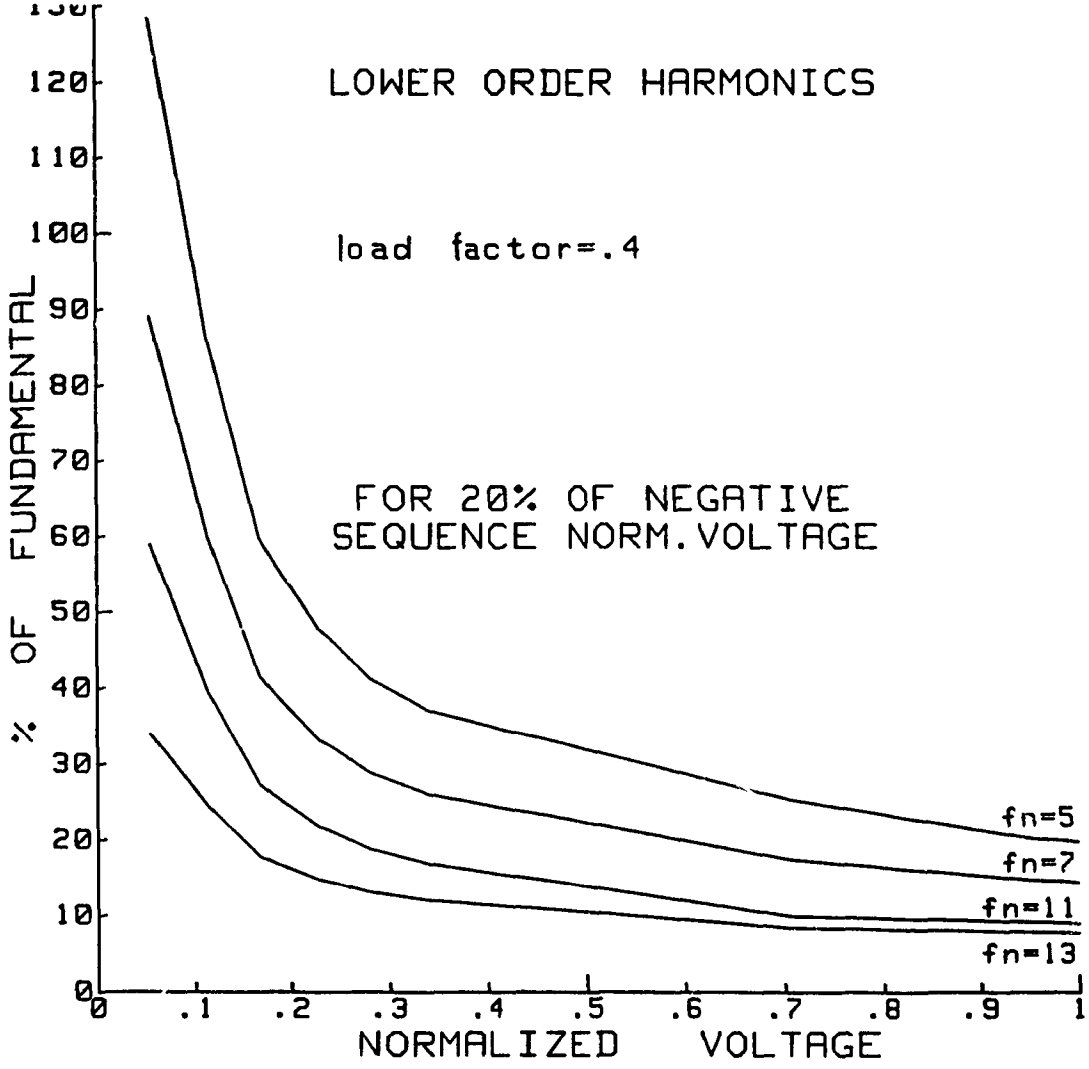

Fig. 3-9: Lower order harmonics of input current at 20% unbalanced supply.

Table 3.2 Two-percent supply unbalance

Normalized voltage	PF	HF	DFIC	DFOC	THDOV
0.017	0.033	1.578	3.680	149.338	1240.00
0.035	0.002	1.265	2.323	74.648	1049.12
0.105	0.082	1.097	1.349	24.808	378.86
0.174	0.154	1.072	1.150	14.795	204.92
0.259	0.238	1.060	1.049	9.746	148.72
0.342	0.320	1.054	.999	7.185	109.58
0.439	0.414	1.050	.963	5.376	81.87
0.454	0.429	1.050	.958	5.149	78.38
0.470	0.444	1.049	.954	4.937	75.14
0.485	0.459	1.049	.950	4.739	72.09

Table 3.3 Four-percent supply unbalance

Normalized voltage	PF	HF	DFIC	DFOC	THDOV
0.017	0.064	1.527	3.832	153.504	1260.14
0.035	0.023	1.253	2.421	76.732	1009.86
0.105	0.073	1.096	1.371	25.507	379.95
0.174	0.147	1.071	1.157	15.219	226.55
0.259	0.234	1.059	1.052	10.036	149.57
0.342	0.316	1.052	1.000	7.410	109.92
0.439	0.411	1.050	0.964	5.559	82.15
0.454	0.426	1.050	0.959	5.327	78.66
0.470	0.441	1.049	0.955	5.111	75.41
0.485	0.456	1.049	0.951	4.908	72.36

CHAPTER 4

INPUT AND OUTPUT FILTER DESIGN UNDER UNBALANCED SUPPLY CONDITIONS

4.1 Input Current Analysis

The input line current of a converter is expressed as:

$$I_r(\theta) = \sum_{n=1}^{\infty} I_{r(n)} \text{Sin } (n\theta + \varphi_{r(n)}) \qquad (4.1)$$

where:

$I_{r(n)}$- amplitude of the nth component of the rectifier input current.

$\varphi_{r(n)}$- phase shift of the nth component with reference to the line to neutral voltage.

Figure 4-1(a) shows the analytical model of a second order input filter. Under unbalanced supply conditions there are three different input currents, and theoretically three different input filters need to be designed. However, for practicality and convenience, if a filter is designed for that particular phase where one expects the maximum distortion of the current, that filter can be used for other two phases. Moreover, the same filter design technique can be used to design the two other filters. The filter design example in this chapter is done for phase 2 only, and for a supply unbalance of 5%.

The input current to the filter can be expressed as :

$$I_i(\theta) = \sum_{n=1}^{\infty} I_{i(n)} \text{Sin } (n\theta + \varphi_{i(n)}) \qquad (4.2)$$

where:

$I_{i(n)}$- amplitude of the nth component of the input line current.

$\varphi_{i(n)}$- phase shift of nth component of the $I_i(\theta)$ with reference to the fundamental component of voltage across the capacitor ($V_{r(1)}$).

The harmonic component of the input filter line current $I_{i(n)}$ can be found as:

$$I_{i(n)} = - \frac{X_{Ci}}{n^2 X_{L(i)} - X_{c(i)}} I_{r(n)} \qquad (4.3)$$

n = 5,7,11,13,... under balanced supply.

n = 3,5,7,9,..... under unbalanced supply.

where:

$X_{L(i)}$- Filter inductor reactance at fundamental frequency.

$X_{c(i)}$- Filter capacitor reactance at fundamental frequency.

From Fig. 4-1(b), the fundamental component of the ac source current $I_{i(1)}$ can be found by the vector addition of

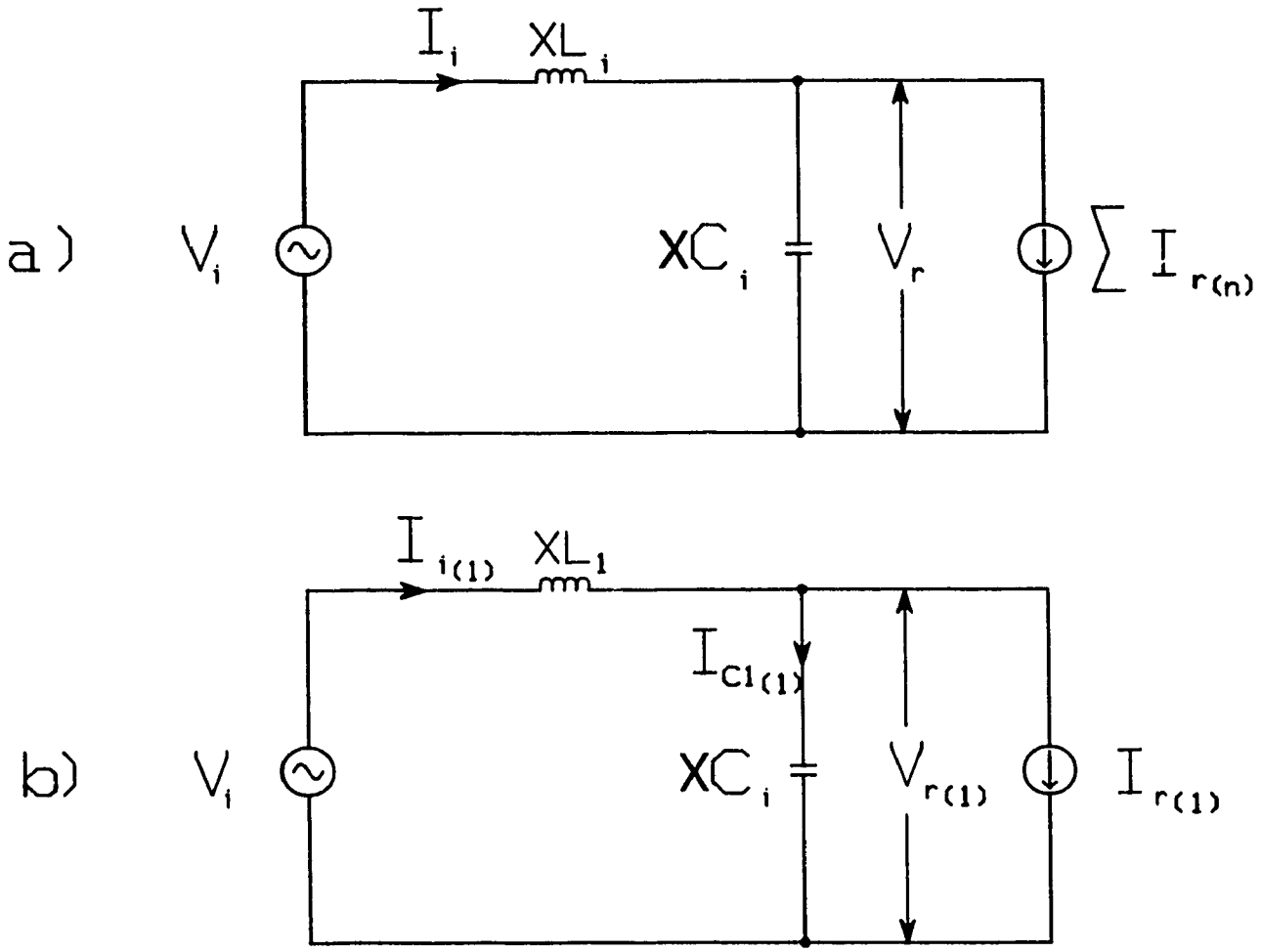

Fig. 4-1: Converter input filter.

(a) Single-phase equivalent circuit.
(b) Single phase equivalent circuit at fundamental frequency.

c)

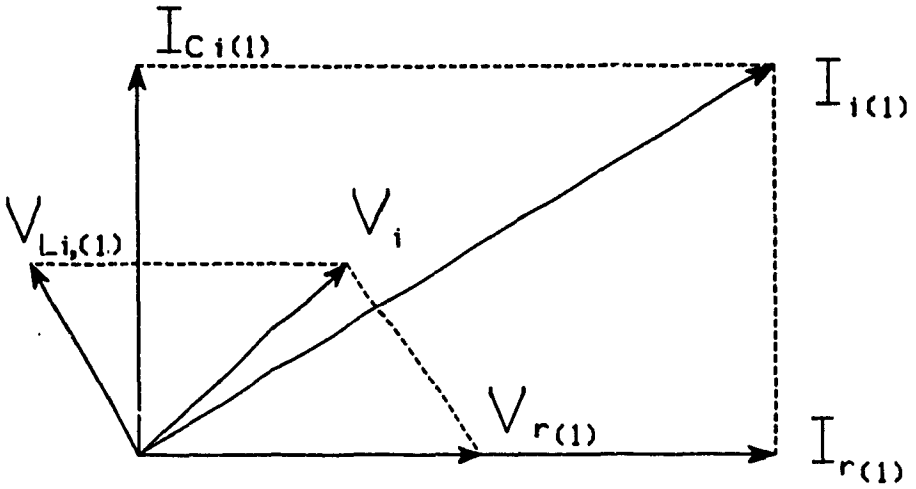

d)

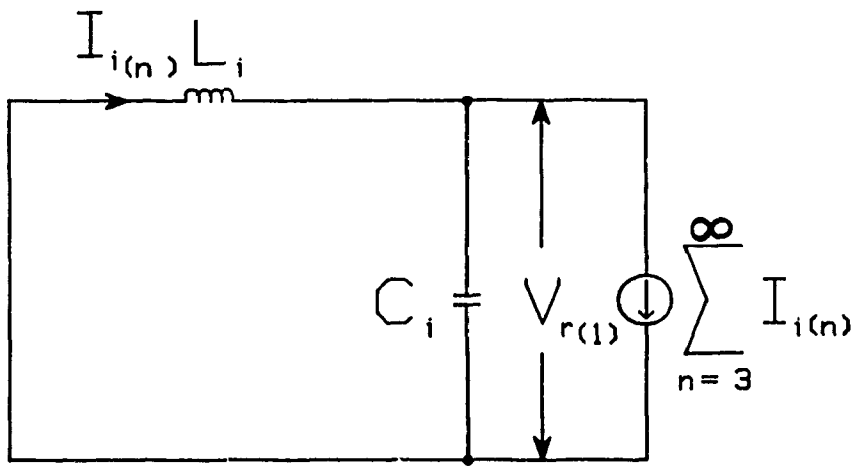

Fig. 4-1: Converter input filter.

(c) Phasor diagram at fundamental frequency.
(d) Single-phase equivalent circuit at harmonic frequencies.

the rectifier input current and the current through the filter capacitor.

$$I_{i(1)} = I_{r(1)} + I_{ci(1)} \tag{4.4}$$

where the capacitor current is found as:

$$I_{ci(1)} = - \frac{V_{r(1)}}{X_{ci}} \tag{4.5}$$

and $V_{r(1)}$ is also the fundamental rectifier input voltage.

In many situations, where a rectifier is connected to a power system supplying loads sensitive to harmonics, restrictions are applied to the 'quality' of the source current. There are no strict rules limiting the value of harmonic pollution. This level varies widely. But a common practice is to restrict the total harmonic distortion (THD) of the source current below 5% [25]. The THD is calculated as:

$$THD(\%) = [\sum_{n=1}^{\infty} (I_{i,rms(n)}/I_{i,rms(1)})^2]^{1/2} \times 100 \tag{4.6}$$

where:

$I_{i,rms(n)}$ - rms input current.

$I_{i,rms(1)}$ - rms fundamental current.

4.1.1 Input filter evaluation

Figure 4-2 shows a family of curves of THD_i vs. X_{Ci} for various values of X_{Li} and for a supply unbalance of 5%. The source current THD has been computed for three values of filter inductor in a range of 0.4 pu to 0.8 pu of filter capacitor values. It is noteworthy that these THDs are calculated for that range of converter operation where the worst harmonic pollution occurs, e.g. at maximum delay angle of 119^{o}. This is based on the fact that any combination of filter X_{Li} and X_{Ci}, that guarantees 5% distortion at the worst harmonic pollution, will also keep the distortion below 5% at other delay angles.

It can be seen from Fig. 4-2 for X_{Ci}= 0.8 pu, that X_{Li}= 0.28 pu gives THD $\simeq$ 9.5%. This is above our accepted value. Whereas X_{Li}= 0.42 gives THD = 3.5 %. This is below our accepted value of THD = 5%, and obviously the filter components are under-used. X_{Li}= 0.35 pu gives THD $\simeq$ 5.5%. Though this is slightly above our accepted value, it is not expected to cause major harmonic pollution. Therefore, this can be taken as the 'accepted value'. The likely choice for X_{Ci} is 0.8 pu.

Figure 4-3 shows the THD of the source current (filter input current) over the whole converter operation range with the above accepted filter inductor and capacitor values (X_{Li}= 0.35 pu, X_{Ci}= 0.8 pu). It is evident that the THD stays below or at 5.5% over almost the entire converter operation range. Though at the lowest converter output

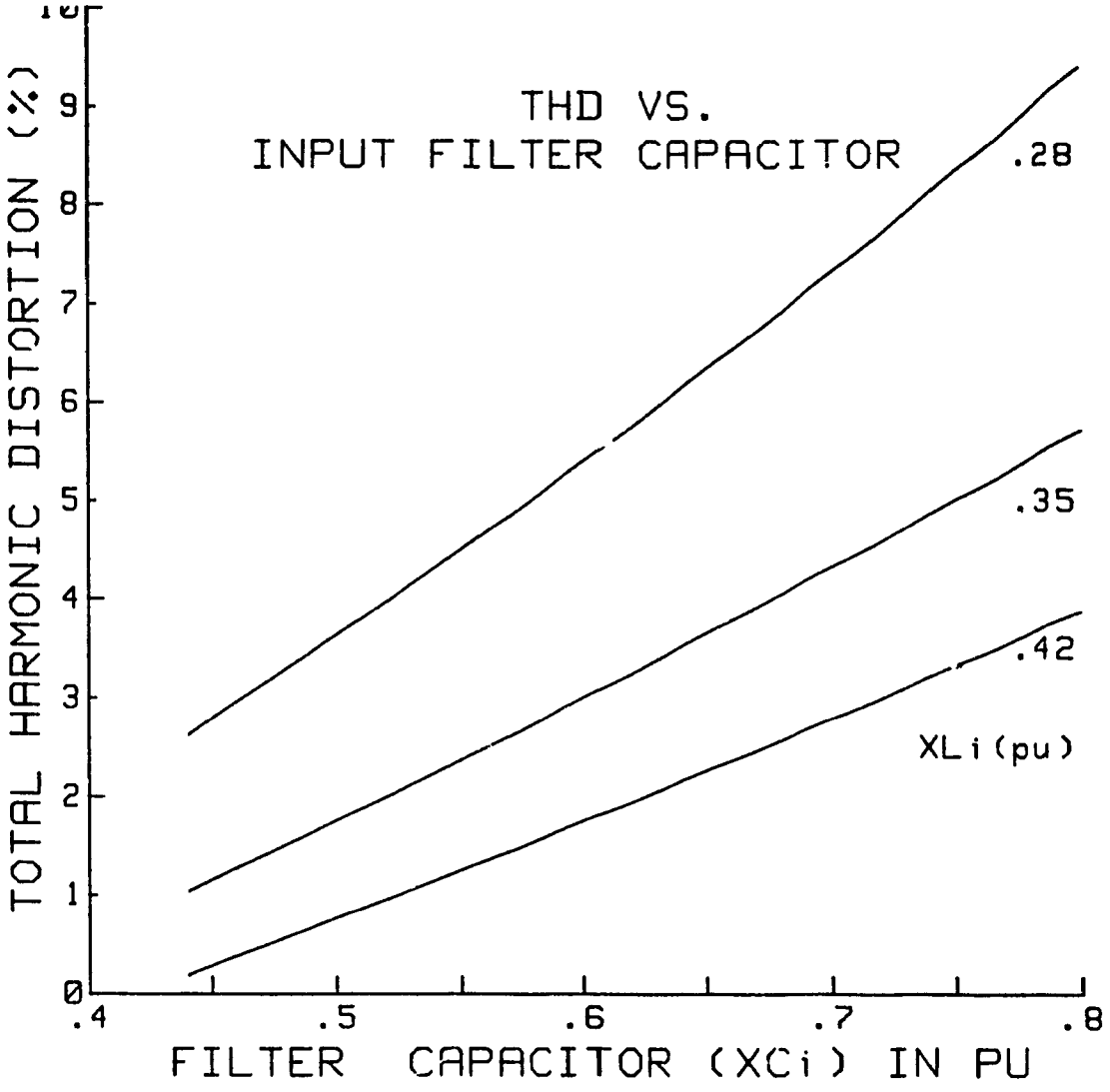

Fig. 4-2: Total harmonic distortion of filter input current vs. input filter capacitor.

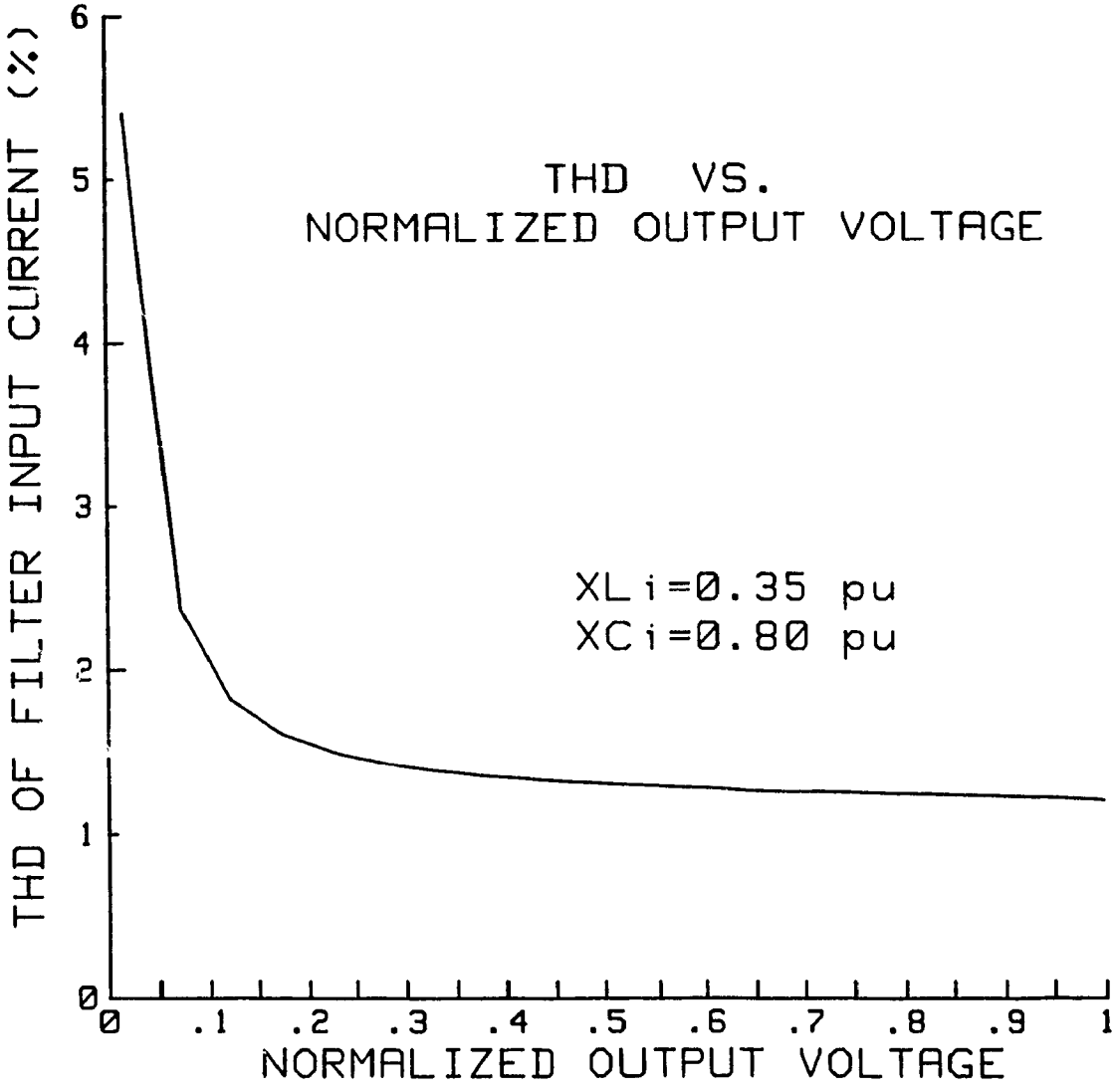

Fig. 4-3: Total harmonic distortion of filter input current vs. normalized output voltage.

region, THD exceeds 5%, In practice a converter is hardly expected to operate at that range.

4.1.2 Total kVA of input filter

The total kVA (TkVA) rating of the input filter is expressed as:

$$TkVA = \rho LkVA + CkVA$$

where:

ρ - ratio between the price of the inductor to that of the capacitor.

The kVA rating of the inductor L_i is found as:

$$LkVA = \sum_{n=1}^{\infty} n \; I_{i,rms(n)}^2 \; X_{L(i)} \tag{4.7}$$

and the kVA rating of the capacitor is;

$$CkVA = \sum_{n=1}^{\infty} \frac{n \; V_{i(n)}^2}{X_{c(i)}} \tag{4.8}$$

where:

$I_{i,rms(n)}, V_{i(n)}$ - rms value of the nth component of harmonic currents and voltages.

$V_{i(n)}$ is found as:

$$V_{i(n)} = \frac{n \; X_{Li} \; X_{ci}}{n^2 X_{Li} - X_c} \; I_{i,rms(n)}, \text{ for } n = 3,5,7,9... \tag{4.9}$$

Then the converter input voltage is calculated as:

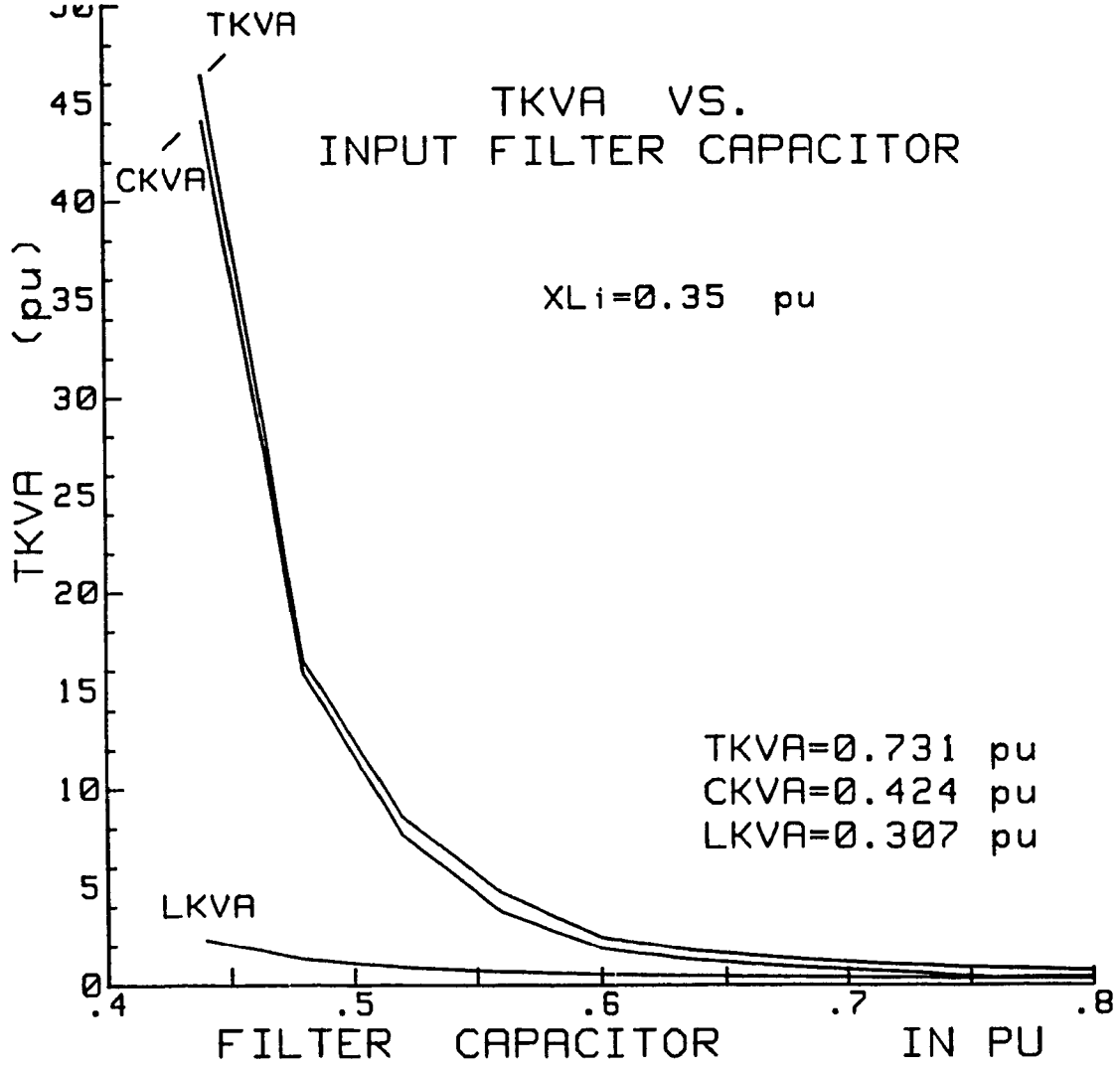

Fig. 4-4 TkVA vs. input filter capacitor.

$$V_i = \left(V_{i(1)}^2 + \sum_{n=3}^{\infty} V_{i(n)}^2 \right)^{1/2} \qquad (4.10)$$

$V_{i(1)}$- rms value of the fundamental component of $V_{i(n)}(\theta)$.

Considering all these, the total kVA rating of the input filter is found as:

$$TkVA = \sum_{n=1}^{\infty} \left(\rho \, n \, I_{i(n)}^2 X_{Li} + \frac{n \, V_{i(n)}^2}{X_{ci}} \right) \qquad (4.11)$$

The filter inductor and capacitor cost is directly proportional to the TkVA rating. Hence an 'optimal' filter may be built by minimizing the TkVA rating by assuming ρ to be known. A dependency between TkVA and X_{ci} can be found (assume, ρ = 1), and is shown in Fig. 4-4 for X_{Li}= 0.35 pu. It is evident that the value of TkVA decreases as we increase X_{ci}. At X_{ci}= 0.8 pu, TkVA has the lowest magnitude and is $\simeq$ 0.731 pu. From the economical point of view, X_{ci}= 0.8 pu is the 'optimum' value of the input filter capacitor.

4.2 Output voltage analysis

The output voltage along with its ripple contents is expressed as:

$$V_o(\theta) = V_{dc} + \sum_{n=2}^{\infty} V_{o(n)} \sin(n\theta + \psi_{o(n)}) \qquad (4.12)$$

n = 6,12,18... for balanced supply.
n = 2,4,6,8... for unbalanced supply.

where:

V_{dc}- dc component of the output voltage.

$V_{o(n)}$- amplitude of the nth component of output voltage, $v_o(\theta)$.

$\psi_{o(n)}$- Phase displacement of the nth component of $v_o(\theta)$.

For converters using delay angle (α) control technique, the average and the ripple output voltage of orders 2n (where n is an integer) are functions of the delay angles (α). It has been found from experiment that the output ripple voltage of harmonic orders 2,4,8,10, etc. which are present only when the supply is unbalanced, stays constant with the increment of delay angle (α). They are found to be functions of the degree of unbalances. Harmonics of orders 6n however increase with the increment of delay angle (α).

The average output voltage is calculated as:

$$V_{dc} = \frac{\sqrt{3}}{\pi} \left(\bar{V}_{an} + \bar{V}_{bn} + \bar{V}_{cn} \right) \cos(\alpha) \qquad (4.13)$$

Where:

$\bar{V}_{an}$, $\bar{V}_{bn}$, $\bar{V}_{cn}$ - are the line to neutral rms voltages.

α - delay angle in radian.

The output ripple voltages of harmonic orders 6n are found as:

$$V_{o(n)} = (a_n^2 + b_n^2)^{1/2} \qquad (4.14)$$

Where:

$$a_n = \frac{2}{\pi} \int_{\alpha}^{\pi+\alpha} V_{o\ (peak)} \sin(\theta)\ \cos(n\theta)\ d\theta \qquad (4.15a)$$

and $$b_n = \frac{2}{\pi} \int_{\alpha}^{\pi+\alpha} V_{o(peak)} \sin(\theta)\ \cos(n\theta)\ d\theta \qquad (4.15b)$$

4.3 Steps in Output Filter design

Figure 4-5 represents the analytical model of the output filter to be designed. A second-order filter 'sees' the converter as a voltage source. A load is connected to the filter. The load can be resistive, inductive, back emf etc.

To calculate the transfer function of the filter, it is assumed that the load is purely resistive and has a value of 1 pu. Then the transfer function can be written as :

$$H_n = \frac{X_{co}}{(X_{co} - n^2 X_{Lo}) + jn\ X_{Lo}X_{co}} = \frac{1}{(1 - n^2 X_{Lo}/X_{co}) + jn\ X_{Lo}} \qquad (4.16)$$

$$n = 2,4,6,....$$

where:

X_{co}- Filter capacitor impedance at source frequency

X_{Lo}- Filter inductor impedance at source frequency

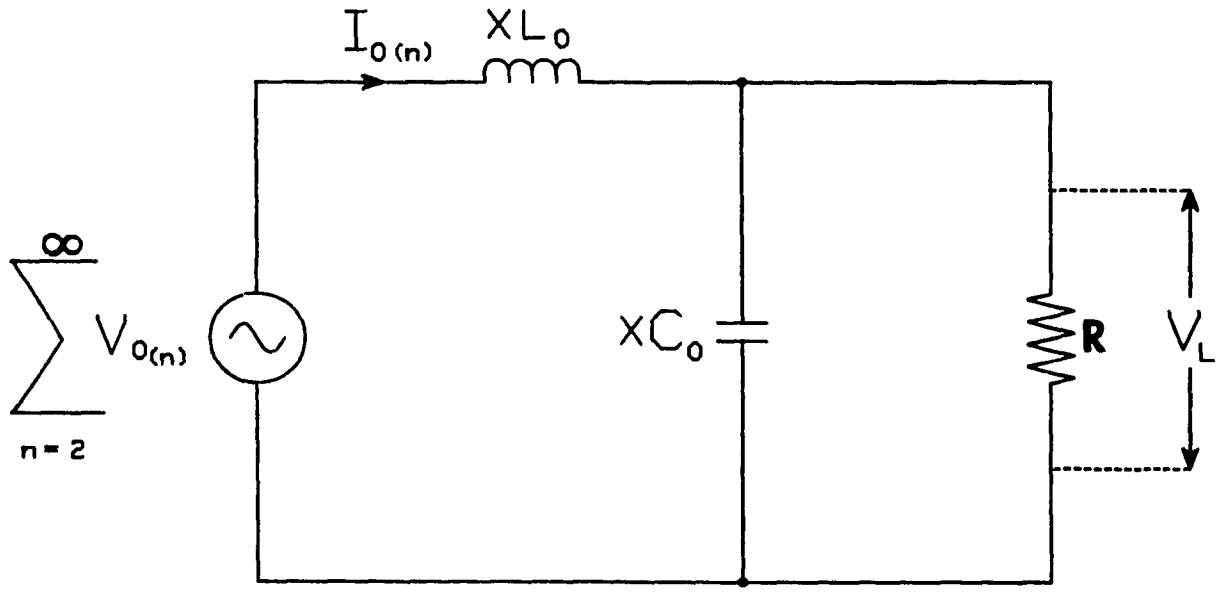

Fig. 4-5: Analytical model of the output filter.

The load voltage $v_L(\theta)$ can be represented in Fourier series as:

$$v_L(\theta) = V_{dc} + \sum_{n=2}^{\infty} V_{L(n)} \sin (n\theta + \varphi_{L(n)}) \qquad (4.17)$$

where:

$V_{L(n)}$- amplitude of the nth harmonic component of load voltage.

$\varphi_{L(n)}$- phase angle of the nth harmonic component of load voltage.

The harmonics at the converter output can be reduced by the filter, and the harmonic component of the load voltage can be written as:

$$V_{L(n)} = H_n \; V_{o(n)} \qquad (4.18)$$

where:

$V_{o(n)}$- amplitude of the nth component of the output voltage.

It is important to realize that there are no particular rules by which one can choose the optimum value of the filter capacitor (C), or the filter inductor (L). Rather, emphasis has to be placed on the conditions imposed by certain users (utilities, etc.). It is also important to consider the economical aspect of the design. As it was found before, that under unbalanced supply conditions the 2nd harmonic is the highest among all other harmonic components present in the output current. So, primary

consideration is to reduce it.

Neglecting the load current effect, a dc filter can be designed primarily by considering the ripple factor of the load voltage. The ripple factor of the load voltage is expressed as:

$$RF(V_L) = \frac{100}{V_{dc}} \left(V_L^2 - V_{dc}^2 \right)^{1/2} \qquad (4.19)$$

Where: V_L - rms load voltage.

4.3.1 Design guidelines for output filter

To design a proper filter, the following guidelines are found useful:

(a) A relatively low L/C ratio reduces the chance of 'overshoot' of the output voltage if the load is suddenly disconnected, which is quite common in practice. It also reduces the 'dip' of the output voltage, in case the load is suddenly increased.

(b) The inductor dissipates more power than the capacitor. From the efficiency point of view a low L/C ratio is desirable.

(c) If the L/C ratio is too low, the load circuit is capacitive. This will make the load current discontinuous.

(d) At the moment of switching, if the inductor is too low compared to the capacitor, a large peak output current ($i = C\frac{dv}{dt}$ and $e = L\frac{di}{dt}$) flows out of the converter.

(e) For the economic aspect, the price of an inductor is much higher than the price of a capacitor.

4.3.2 Output filter component selection

The following steps are followed to choose the 'optimum' value of filter components:

(a) The ripple factor of the load voltage ($RF(V_L)$) is plotted against X_{CO} for different values of X_{LO}.

(b) Values of X_{LO} that satisfy the predetermined ripple factor ($RF(V_L)$) of load voltage were chosen.

(c) The guidelines were taken into account.

Although there is no particular value of $RF(V_L)$, that has to be satisfied, rather it depends on the tolerance of the harmonic pollution of the load circuit. However, the

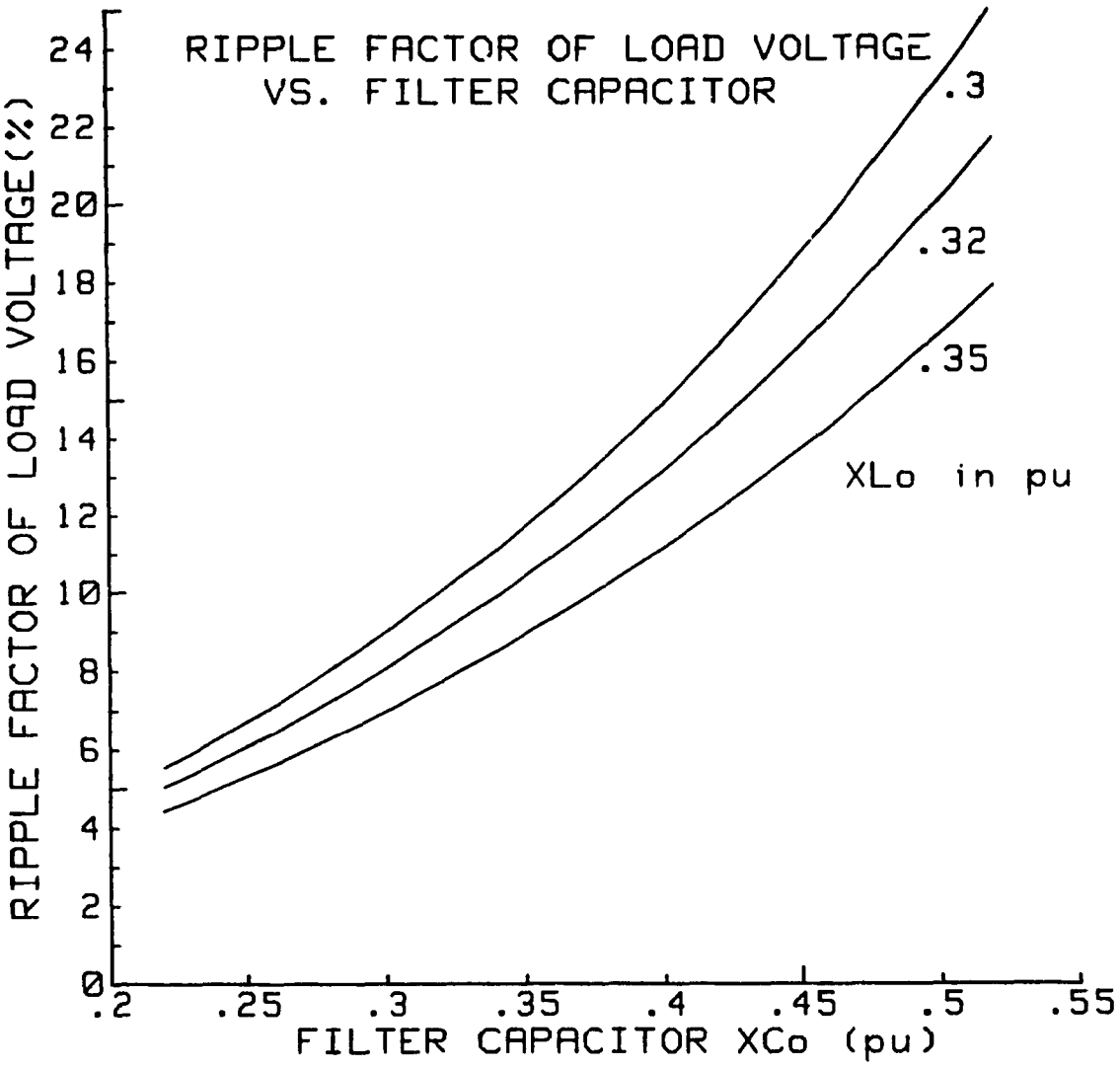

Fig. 4-6: Ripple factor of load voltage vs. output filter capacitor.

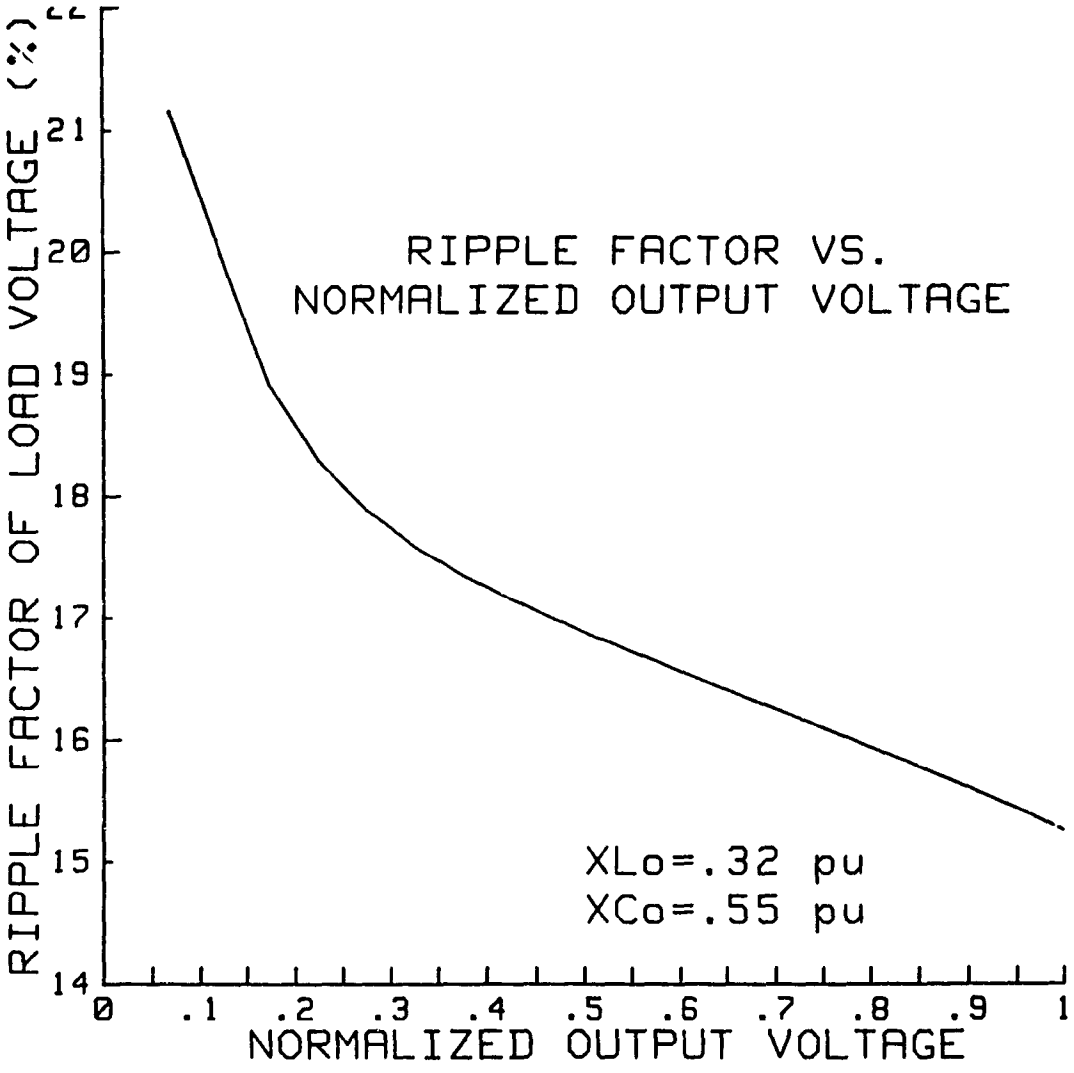

Fig. 4-7: Ripple factor of load voltage vs. normalized output voltage.

following can be considered in general:

> The ripple factor of the load voltage remains below 20% of the dc component (dc output voltage) over the entire converter operation range (0.05- 1 pu output dc voltage).

Fig. 4-6 shows the $RF(V_L)$ for various values of X_{Lo} with respect to X_{co} for a supply unbalance of 5% and a delay angle of 119^o(at $\alpha=119^o$, the worst harmonic pollution occurs). X_{Lo}= 0.3 pu gives $RF(V_L)$ above 20%. It is above our accepted value of 20%, and is thus rejected. X_{Lo}= 0.35 pu gives a $RF(V_L)$ that is under-used. X_{Lo}= 0.32 pu gives $RF(V_L)$ little higher than 20%. This is the most likely choice and the suitable X_{co} is = 0.55 pu.

Fig. 4-7 shows the $RF(V_L)$ with the output filter chosen above (X_{CO}= 0.55 pu, X_{Lo}= 0.32 pu). The $RF_{(Lv)}$stays well below the accepted level of 20% over most of the converter operation range. At the normalized output voltage above 0.05 ($\alpha>115^o$), the $RF_{(LV)}$ becomes a little bigger than 20% . This however does not cause a serious problem, since a converter is unlikely to operate at this region ($\alpha>115^o$).

The complete circuit diagram of the converter along with the input and output filters is shown in fig. 4-8.

4.4 Discussion

It is important to note that in the design procedure of the input and output filters, the chosen values of filter

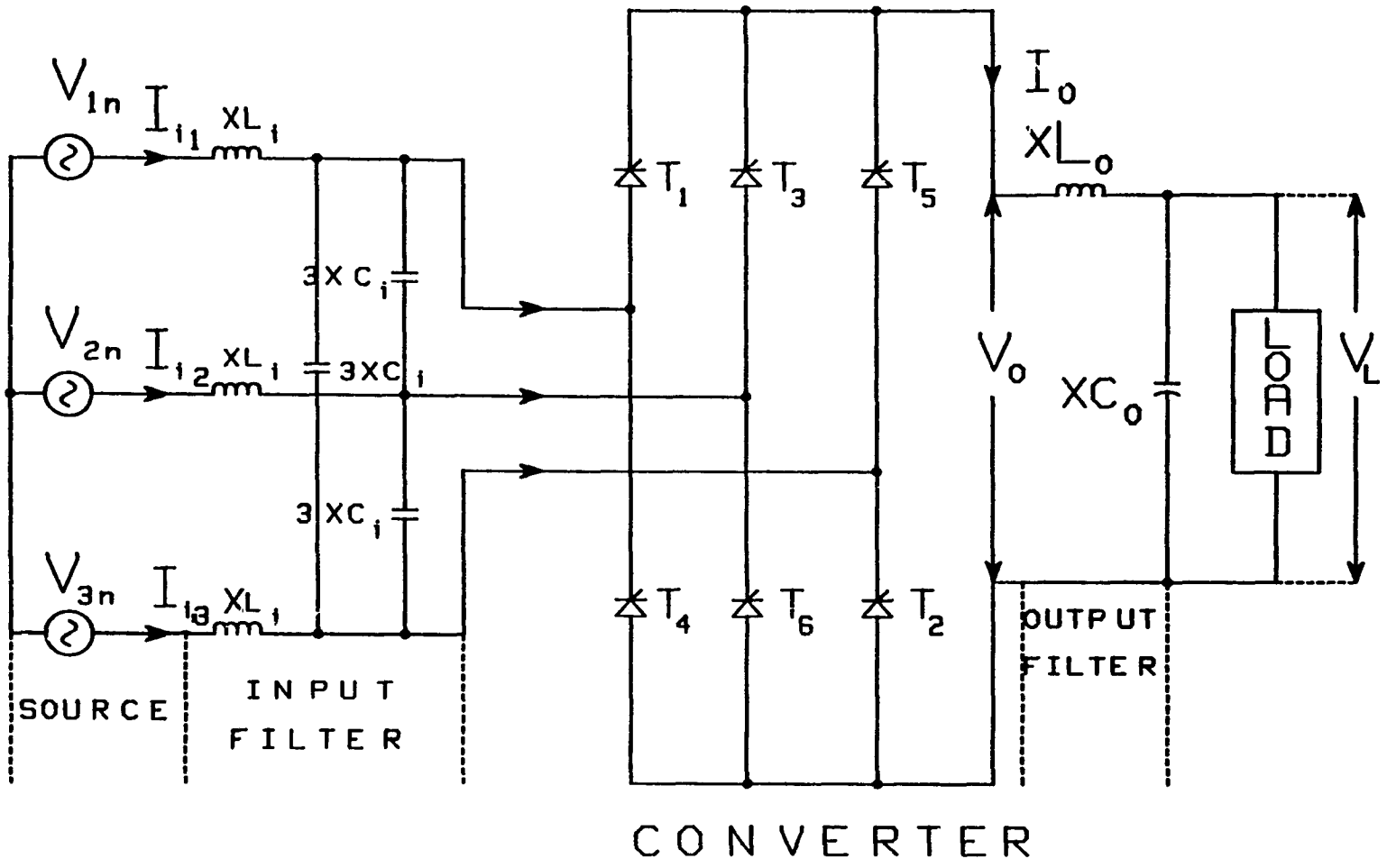

Fig. 4-8: Complete circuit diagram of the 3-phase ac-dc converter with input and output filters.

X_{LO} and X_{CO} may not represent the 'optimum' values from economical point of view. An altogether different type of filter could have been designed by introducing a trap for a particular harmonic component (i.e. one with the highest magnitude). This would lead to the reduction of X_{CO}, X_{LO}values of the main filter at the cost of an extra set of trap X_c and X_L. Further information on this topic can be obtained in [26].

4.5 Input and output current spectra with the proposed filter

A laboratory experimental 3-phase 1 kW converter setup was constructed. Unbalanced supply was provided by using 3 variable resistors for three different phases (unbalance in magnitude). The logic circuit was built to generate firing of the thyristors, and also to provide the delay angle (α).The ratio of inductor (L) and resistor (R) was chosen such that they follow the R and L of the simulated converter and hence give the same load factor. The setup has the following specifications:

(a) Rated output voltage: 200 V, dc.

(b) Input frequency: 60 Hz.

(c) Rated output current: 5 A, dc.

(d) Load resistance = 4.825 Ohms.

(e) Load inductance = 32 mH.

(f) Load factor (R/XL) = .4 pu.

Comparing this with the simulated converter, yields:

1 pu output voltage: 200 V.

1 pu output current: 5 A.

1 pu load impedance: $\frac{200\ V}{5\ A}$ = 40 Ohms.

The input parameters are determined as follows:

(a) Input line to neutral voltage (V_{an}) = ($\sqrt{2}/3$) pu x 200 V = 94.3 V.

(b) Rated rms line current ($1/\sqrt{2}$) pu x 5 A = 3.54 A.

Figures 4-9 (a), (b), (c) show the three input line currents along with their harmonic spectra for an unbalance of about 5% and a delay angle of 107^{o}. The harmonic spectra are found by using Data 6000 harmonic analyzer. This highly sensitive harmonic analyzer analyzes a given waveform and displays the magnitudes of the individual harmonics as a function of frequency. This is illustrated in the lower parts of figs. 4-9, (a), (b), (c). It is evident from these figures that they are in agreement with the predicted harmonic spectra obtained from the simulated converter in section 3.2 with a similar unbalance supply and delay angle (α). However, it is evident, a small dc component is present in the input current wave-form that is absent in the case of a simulated converter. This can be attributed to the imperfections of the sequence of firing of the thyristors by

phase 1.

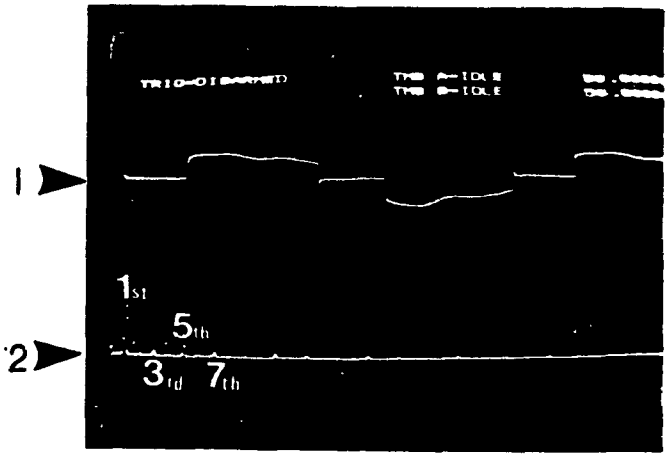

phase 2.

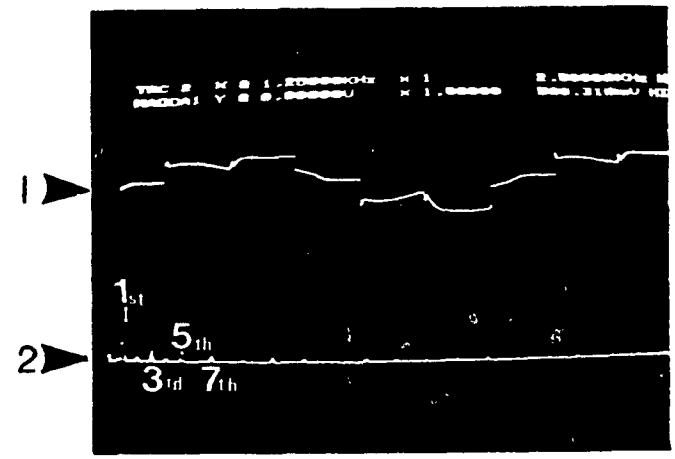

phase 3.

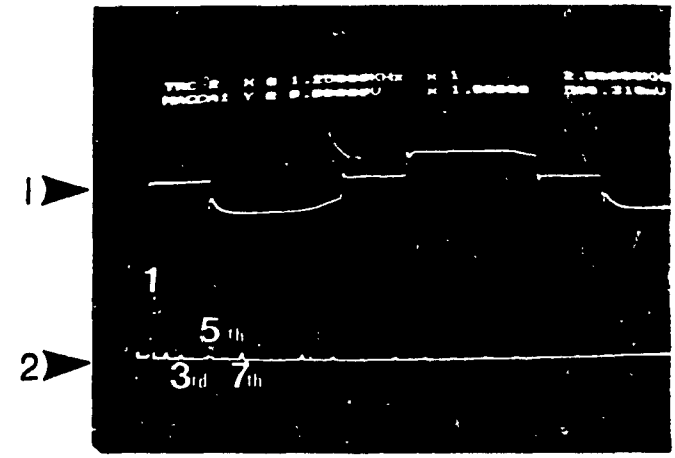

Fig. 4-9(a), (b), (c): Input line currents for phases 1, 2, and 3.

(1) Waveform.
(2) Harmonic spectrum.

the logic circuit. Any discrepancy between the positive and the negative pulse duration will eventually give rise to a situation where the net area under the current waveform in a complete period is not equal to zero. So, the constant term of the Fourier series of the input current is not equal to zero and this will give rise to the dc component.

Tables 4.1 and 4.2 show the input current harmonic spectra of the experimental converter with and without the input and output filters respectively. The harmonics are shown as a percentage of fundamental components for individual phases.

Table 4-1 Input Currents Spectra without Filter

Harmonics	Phase 1	Phase 2	phase 3
Fundamental	100 %	100 %	100 %
3rd	8.9 %	18 %	10.5 %
5th	22 %	18 %	18.6 %
7th	9.5 %	10 %	10.5 %

Table 4-2 Input Currents Spectra with Filter

Harmonics	Phase 1	Phase 2	Phase 3
Fundamental	100 %	100 %	100 %
3rd	2.4 %	1.2 %	3.16 %
5th	2.8 %	1.49 %	3.9 %
7th	2.2 %	0.87 %	2.89 %

Figs. 4-10 and 4-12 show the output current and the load voltage waveforms. Their spectra are also in close agreement with the harmonic spectra of the predicted values.

4.6 Examples with Input and Output Filters

The filters are designed with a supply frequency of 60 Hz and a load impedance of 40 Ohms.

Input harmonic filter components, with X_{Li} = 0.35 pu, and X_{Ci} = 0.8 pu :

L_i= (0.35 pu x 40)/377 = 37.13 mH.

C_i= 1/(0.8 pu x 40 x377) = 82.8 μF.

Filter kVA ratings from Fig. 4-4:

LkVA = 0.307 pu x 1kVA = 0.307 kVA

CkVA = 0.424 pu x 1kva = 0.424 kVA

TkVA = ρLkVA + CkVA = 0.731 kVA

Output filter parameters from Fig. 4-7:

L_o= (0.32 pu x 40)/377 = 33.9 mH.

C_o= 1/(0.55 pu x 40 x 377) = 120 μF.

The input and the output filters which were designed with the parameters calculated above were connected to the experimental setup, and the input line currents and the

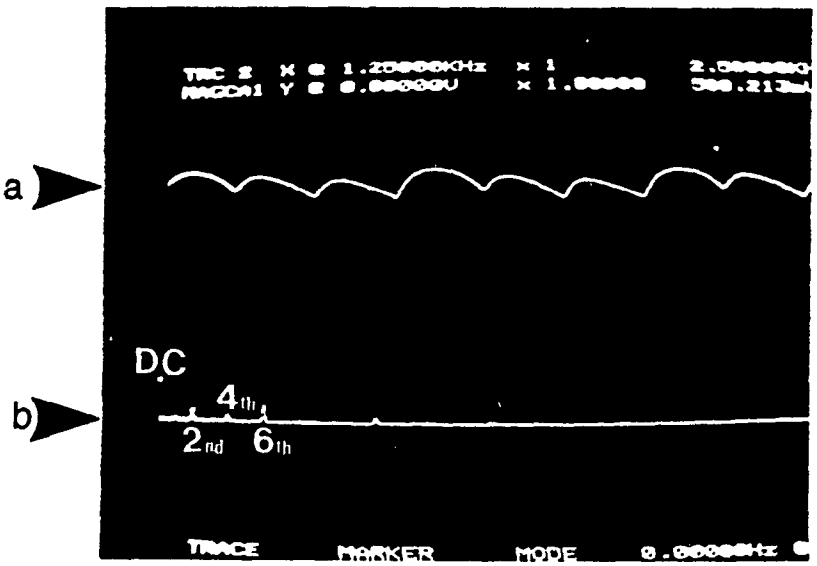

Fig. 4-10: Output current.
(a) Waveform.
(b) Harmonic spectrum.

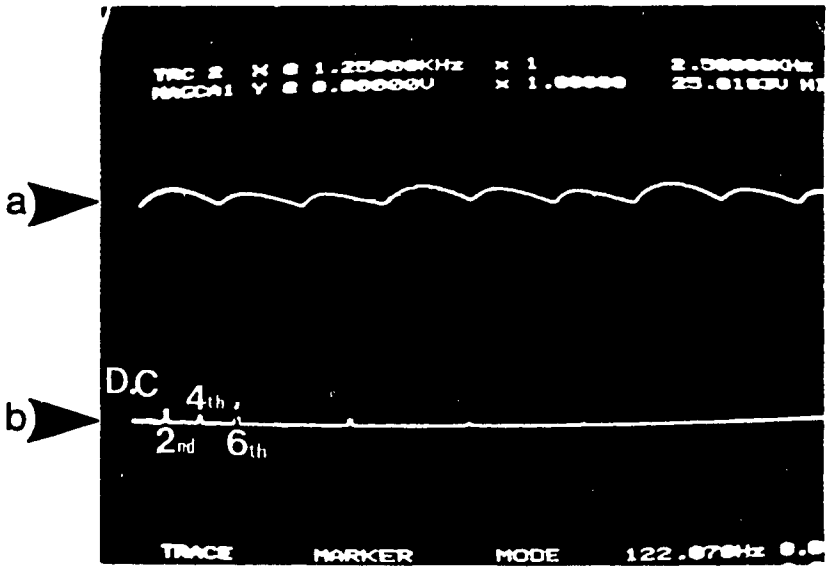

Fig. 4-11: Harmonic load voltage.
(a) Waveform.
(b) Harmonic spectrum.

output harmonic load voltage were recorded using the Data 6000 harmonic analyzer. It is evident from the harmonic spectra of the input currents of Figs. 4-12,(a), (b), and (c) that the harmonic components have been successfully suppressed. Though very small magnitudes of certain harmonics are present, but they are not expected to cause substantial problem to other users.

Fig. 4-13 shows the load voltage with the output filter connected. The harmonic contents are almost negligible and should keep the 'ripple factor' below 5%.

phase 1.

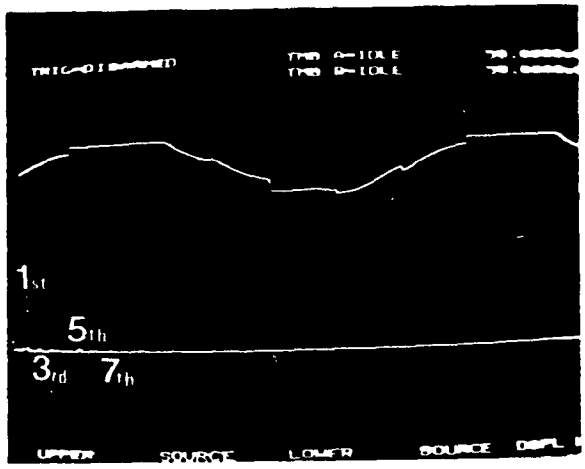

phase 2.

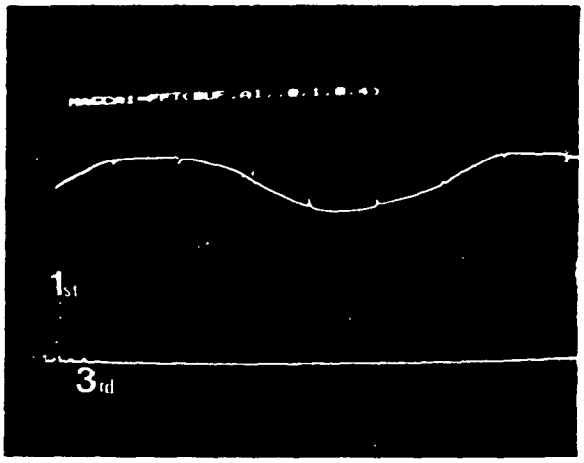

phase 3.

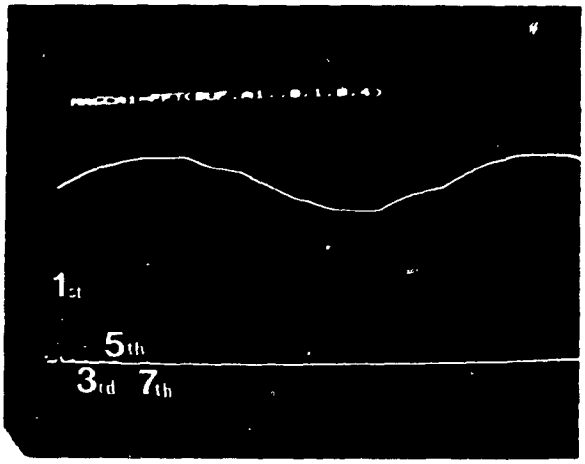

Fig. 4-12(a), (b), (c): Filter input currents for phases 1, 2, and 3.

(1) Waveform.
(2) Harmonic spectrum.

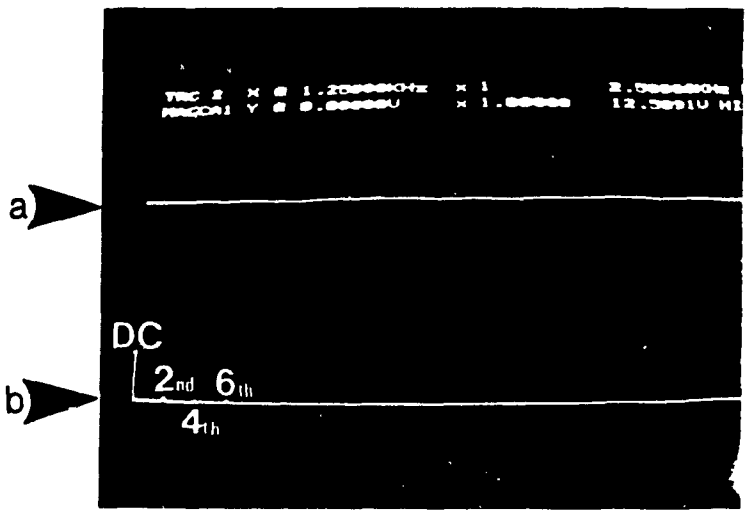

Fig. 4-13: Load voltage with filter.
(a) Waveform.
(b) Harmonic spectrum.

CHAPTER 5

CONVERTERS USING FORCED COMMUTATION

5.1 Concept Of Forced Commutation

Unlike the natural or line commutation described in the previous chapters where the thyristors (or switches) turn-off when the polarity of the supply voltage changes, forced commutation is the method of 'forcibily' turning on and off of a switch at any instant. It does not depend whether the supply voltage is positive or not, neither does it depend on the direction of current through the switches. Since we can control the firing instants, and usually they are fired very fast, the frequency of the output ripples usually are much higher than the converter input frequency. Hence harmonics are shifted to the higher orders and are easy to eliminate. However, the complexity, cost and size of the commutation circuitry did not make forced commutation attractive until recently.

Recent advancement in semiconductor technology has made forced commutation economical and attractive. Devices such as a gate turn-off thyristor (GTO), FET-gated bipolar transistor (FGT) and gate assisted turn-off thyristors (GATT) do not require commutation circuitry to turn them off. This reduces the cost and complexity, and increases

reliability.

5.2 Types of Switching Functions in Forced Commutation

There are four different switching functions that are widely used in forced commutation. They are :

1. Sinusoidal pulse width modulated (PWM) (switching function).

2. Modified sinusoidal PWM (switching function).

3. PWM (switching function) for optimum current distortion.

4. PWM (switching function) for specific harmonic elimination.

Among them, for practicality, we will analyze the modified sinusoidal PWM scheme, the PWM switching scheme for optimum input current distortion and specific harmonic elimination only.

5.3 Modified Sinusoidal PWM Scheme (MSPWM)

In order to increase the resulting fundamental component, and hence to improve the harmonic

characteristics, a modified form of sinusoidal PWM scheme (SPWM) was proposed by T. Omnishi and H. Okitsee [27]. According to this scheme, a carrier triangular wave is compared to a reference sine wave by leaving middle 60^{o} of the sine wave untouched. This is presented in Fig. 5-1(a). The gating signals of the switches are generated from the intersections between the carrier and the reference signals. The pulses in-between 60^{o} and 120^{o} are found by considering the pulses of the first and last 60^{o} intervals, as is seen in Fig. 5-1(b). The pulses for the next half cycle can very easily be found from the half-wave symmetry of the switching function.

It is evident from the figures that the width of the pulses and the amplitude of the switching function can be manipulated by varying the ratio of the amplitudes of reference and carrier signals. This ratio is known as modulation index (MI). MI is expressed as:

$$MI = \frac{A_r}{A_c} \tag{5.1}$$

where:

A_r- peak value of the reference wave.

A_c- peak value of the carrier wave.

The output voltage of the converter can be controlled by controlling the modulation index. Theoretically MI=1 will give the highest output voltage. MI is usually kept little below 1 for normal converter operation. Furthermore, to

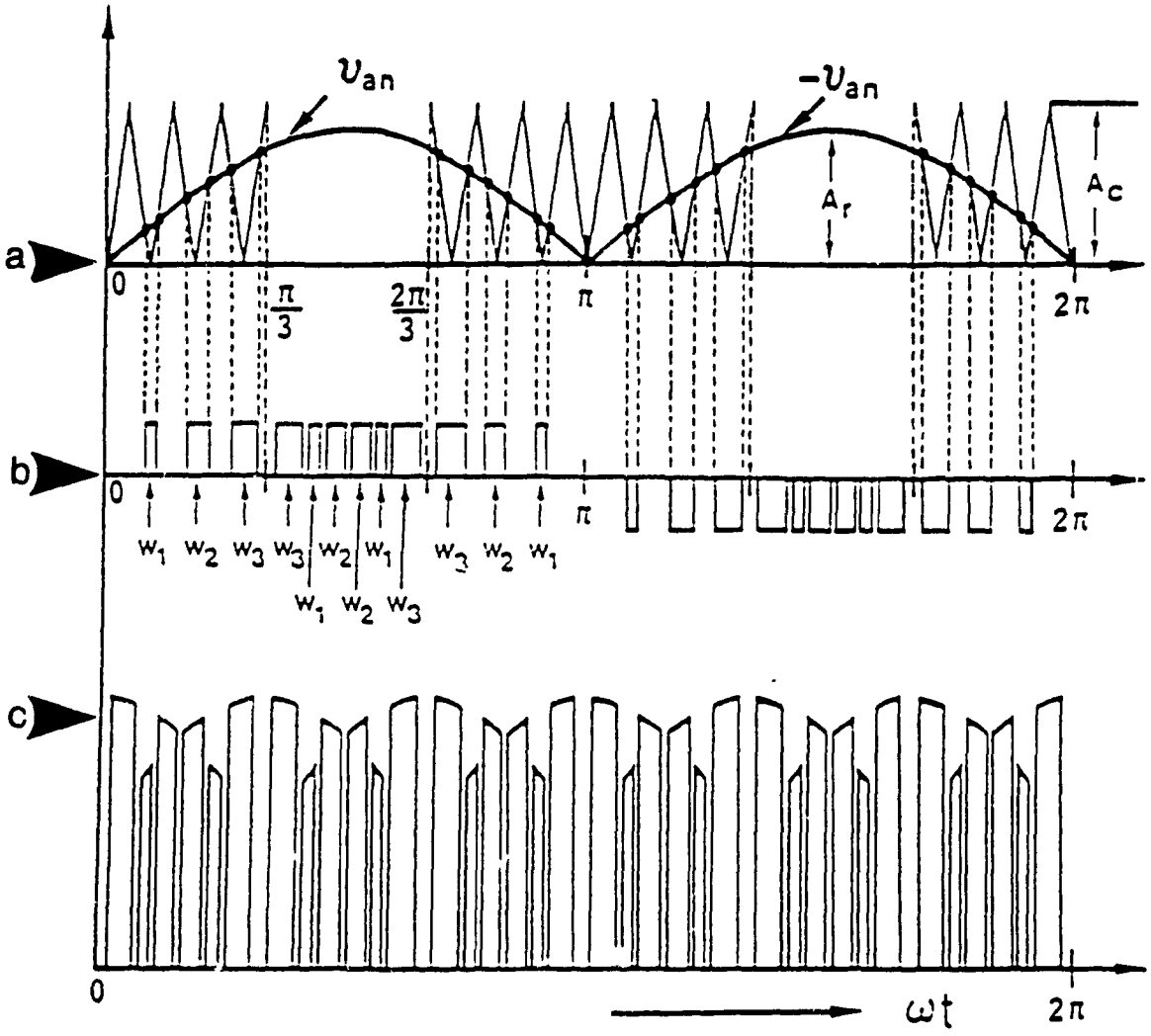

Fig. 5-1: Modified sinusoidal PWM scheme.
(a) Modulation scheme.
(b) Switching function derivation.
(c) Rectifier output voltage.

ensure normal converter operation, the following condition must also be fulfilled:

$$\frac{f_c}{f_r} = 6n + 3 \qquad (5.2)$$

$$n = 1,2,3,....$$

where;

f_c = carrier wave frequency.

f_r = reference wave frequency.

'n' is also the number of pulses in the first 60^o interval.

The switching angles (T_1, T_2, T_3, ...T_6) of the pulses W_1, W_2, W_3 can be obtained from the intersection points of the A_c and A_r (Fig. 5-1(a)). The rest of the switching angles T_7 through T_{12} can be obtained as shown in Fig. 5-2, by utilizing the quarter wave symmetry. These are as follows:

$$\begin{aligned} T_7 &= \frac{2\pi}{3} - T_6. \\ T_8 &= \frac{2\pi}{3} - T_5. \\ T_9 &= \frac{\pi}{3} + T_1. \\ T_{10} &= \frac{\pi}{3} + T_2. \\ T_{11} &= \frac{2\pi}{3} - T_4. \\ T_{12} &= \frac{2\pi}{3} - T_3. \end{aligned} \qquad (5.3)$$

The increase of number of pulses per half cycle by increasing the frequency of the carrier signal shifts the

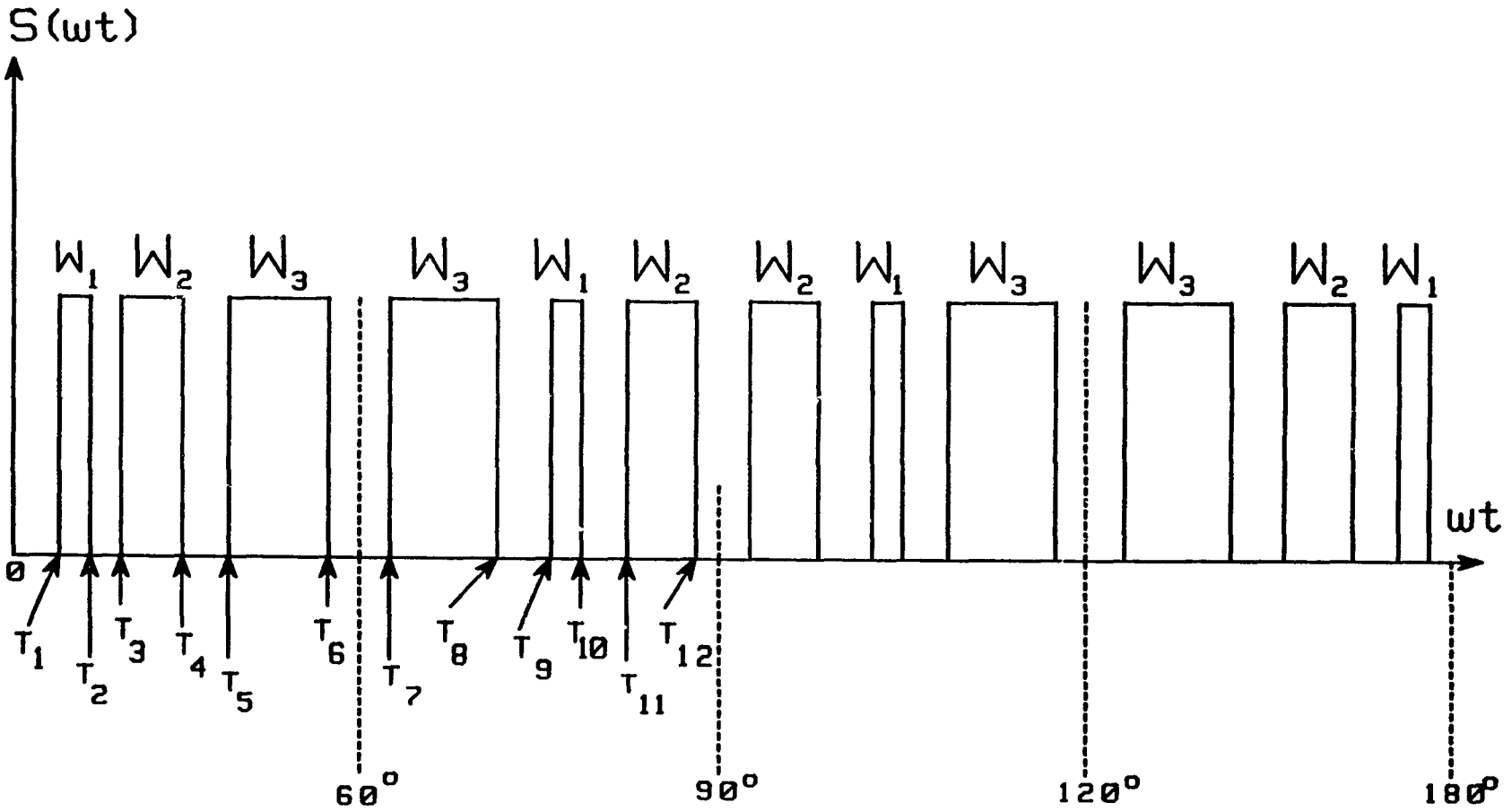

Fig. 5-2: Details of switching function derivation in MSPWM scheme.

significant harmonic components (harmonics that are above 3% of the fundamental component [29]) toward the higher order frequencies. This will eventually decrease the input line current distortion.

5.4 PWM Scheme for Optimum Current Distortion Factor (PWMOCD)

A fixed pattern PWM switching function can be found by varying the width of the pulses of Fig. 5-1 until the distortion factor of the input line current is minimum. Theoretically an infinite number of pulses would make the current least distorted. However, in practice the number of pulses is limited to reduce switching losses.

PWMOCD is shown in Fig. 5-3 having quarter wave symmetry. The number of pulses per half cycle is chosen to be 9. To guarantee continuous load current, the width of the pulse w_1 should be equal to the distance between T_9 and T_8, width of W_2 should be equal to the distance between T_7 and T_6 and so on. Under this condition, the distortion factor is related to the switching angles as :

$$DF = f\ (T_1, T_2, T_3, T_4, ..Tn) \qquad (5.4)$$

switching angles T_1 through T_n can be found for optimum distortion factor by solving the above equation. This is done by assuming the output current of the converter to be ripple-free, thus the input line current becomes identical

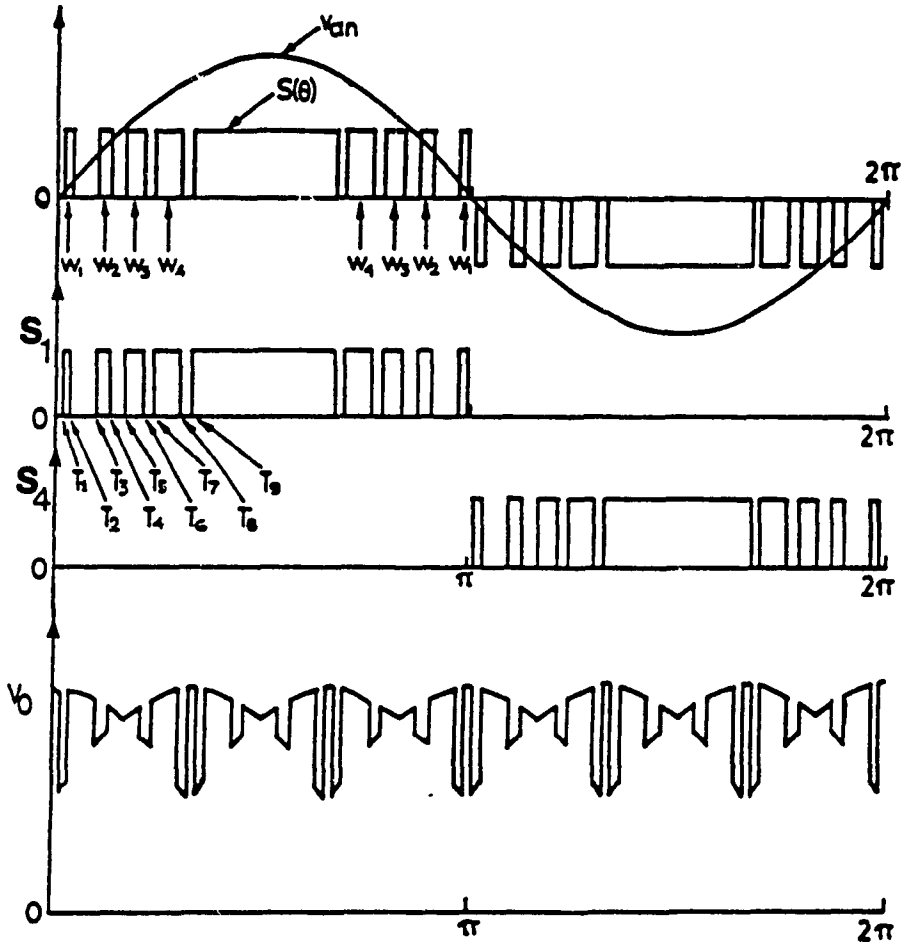

Fig. 5-3: PWM switching scheme for optimum current distortion.

to the switching function. Distortion factor (DF) decreases with the increase of pulse number. Setting the number of pulses per half cycle, and assuming a switching function with quarter wave symmetry, the switching function becomes:

$$S(\theta) = \sum_{n=1}^{\infty} H_n \sin (n\theta + \psi_n) \qquad (5.5)$$

where:
$$H_n = \frac{4}{\pi} \int_0^{\pi/2} (S(\theta)\ n\theta)\ d\theta$$

H_n can also be expressed as :

$$H_n = \frac{4}{\pi n} [\cos (nT1) - \cos(nT_2) + \cos(nT_3) + \ldots\ldots + \cos(nT_n)] \qquad (5.6)$$

where: T_n - nth switching angle (in radian).

It can be seen from Eqn. (5.5) that the harmonic component of the switching function becomes the function of the switching angles ($T_1, T_2, T_3, \ldots$ Tn). Hence, the harmonic components of a switching function with 7 pulses per half cycle are :

$$H_1 = \frac{4}{\pi} [\cos(T_1) - \cos(T_2) + \cos(T_3) - \cos(T_4) + \cos(T_5) - \cos(T_6) + \cos(T_7)] \quad (5.7)$$

$$\vdots$$

$$H_7 = \frac{4}{7\pi} [\cos(7T_1) - \cos(7T_2) + \cos(7T_3) - \cos(7T_4) + \cos(7T_5) - \cos(7T_6) + \cos(7T_7)] \quad (5.8)$$

and so on.

Knowing the values of $H_1, H_2, \ldots H_n$, its distortion factor can be evaluated by using:

$$DF = \frac{[\sum_{n=2}^{\infty} (H_n/n^2)^2]^{1/2}}{H_1} \times 100 \quad (5.9)$$

A computer program has been written to find the minimum DF. Using this program, the optimum DF is calculated for all possible combinations of switching angles. Hence by knowing the optimum DF, switching angles are derived for minimum DF.

5.5 PWM Scheme for Specific Harmonic Elimination (PWMSHE)

To derive the switching function for specific harmonic elimination, the output current is considered continuous and ripple free. The switching function can eliminate '(number of pulses - 1)/2' number of harmonic components. This generates a system of equations.

$$H_n = \frac{4}{\pi} \int_0^{\pi/2} S(\theta) \sin(n\theta)\, d\theta = 0 \qquad (5.10)$$

where : n - order of harmonic component to be eliminated (n assume different values depending on the number of pulses/half cycle).

If we have a switching function of 5 pulses/half cycle, we can eliminate 2 harmonic components. Hence, Eqn.(5.7) can be written as:

$$H_5 = \frac{4}{\pi} \sum_0^{\pi/2} S(\theta)\ \mathrm{Sin}(5\theta)\ d(\theta) = 0 \qquad (5.11)$$

and

$$H_7 = \frac{4}{\pi} \sum_0^{\pi/2} S(\theta)\ \mathrm{Sin}(7\theta)\ d(\theta) = 0 \qquad (5.12)$$

Substituting the values of θ in Eqn (5.8), we have :

$$H_5 = \frac{4}{5\pi} [\cos(5T_1) - \cos(5T_2) + \cos(5T_3) - \cos(5T_4) + \cos(5T_5)] = 0 \qquad (5.13)$$

and

$$H_7 = \frac{4}{7\pi} [\cos(7T_1) - \cos(7T_2) + \cos(7T_3) - \cos(7T_4) + \cos(7T_5)] = 0 \qquad (5.14)$$

Newton's method was used to solve the above equations. The solution gives the switching angles of the switching functions to eliminate 5th and 7th input harmonic current

components.

5.6 Performance Parameters with Forced Commutation

To find the performance parameters of the MSPWM scheme, a 3-Phase converter has been simulated using 3 different transfer functions, and is tested under both balance and unbalanced supply voltage conditions. The converter output voltage is controlled by controlling the modulation index. In this scheme, the switching function does not require any phase shift to control the output voltage. This gives the advantage of zero phase shift between the supply voltage and the fundamental component of input line current. Hence the fundamental or the displacement PF stays at unity value throughout the whole converter operation range. 8 pulses per half cycle has been chosen to find the converter input PF, and HF of input line current. The choice of 8 is arbitrary.

To find the performance parameters of PWMOCD and PWMSHE schemes, the input power factor (PF) of the converter, and the harmonic factor (HF) of the input line current have been evaluated to find out the converter performance and the 'quality' of the input current. These parameters have been found by providing both balanced and unbalanced supply to the simulated converter. The converters have been simulated using the transfer function approach as described in chapter 1 and 2. Under unbalanced supply, three transfer functions have been calculated for three different phases separately.

The necessity of calculating three different transfer functions has been outlined in chapter 2. The detail procedures of the calculation of the output dc and ripple voltages, output current, and harmonic input currents have been described in Appendix A.

7 pulses per half cycle has been chosen for PWMSHE scheme to eliminate specific harmonics of the converter input current. Pulses beyond 7/half cycle to eliminate 5, 7, 11, 13 harmonics was not used.

For PWMOCD scheme however, we are free to choose the number of pulses. The chosen number of pulses/half cycle for PWMOCD equals 9.

The following tables show the switching angles (T_1, T_2,...T_n) for both PWMOCD and PWMSHE schemes:

Table: 5.1 PWM with specific harmonic elimination scheme

T_1	2.24^o
T_2	5.60^o
T_3	21.26^o
T_4	30.00^o
T_5	38.74^o
T_6	54.40^o
T_7	57.76^o
T_8	90.00^o

Table: 5.2 PWM with optimum current distortion scheme

T_1	2.00^o
T_2	4.60^o
T_3	17.40^o
T_4	22.30^o
T_5	30.00^o
T_6	37.70^o
T_7	42.60^o
T_8	55.40^o
T_9	58.00^o
T_{10}	90.00^o

5.6.1 Input power factor of the converter

To calculate the input power factor of the converter, Eqn. (3.10) of chapter 3, section 3.5.1 is used under both balanced and unbalanced supply conditions. This holds true for all MSPWM, PWMOCD and PWMSHE schemes.

It is evident from the input PF characteristics of MSPWM scheme of Fig.(5-4) that the supply unbalance does not have a significant effect. This has been tested from 5% to 20% supply unbalances and is found to be practically unchanged. This can be attributed to the fact that no phase shifting is used to vary the converter output voltage. The unbalance supply affects converter performance by phase shifting the switching function.

Another important difference of the PF characteristics of the MSPWM scheme is that at a relatively lower converter

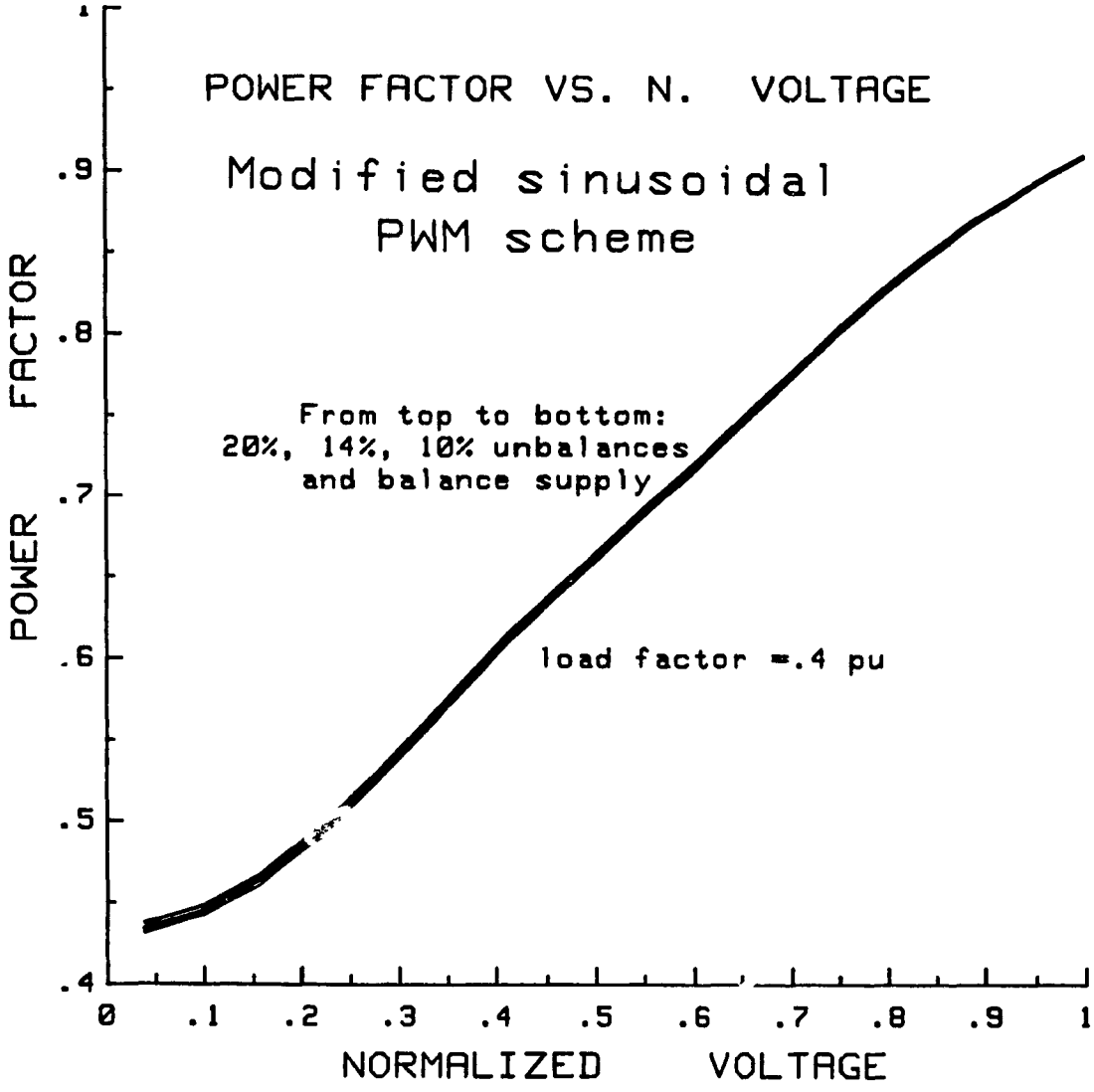

Fig. 5-4: Input power factor using modified sinusoidal PWM scheme.

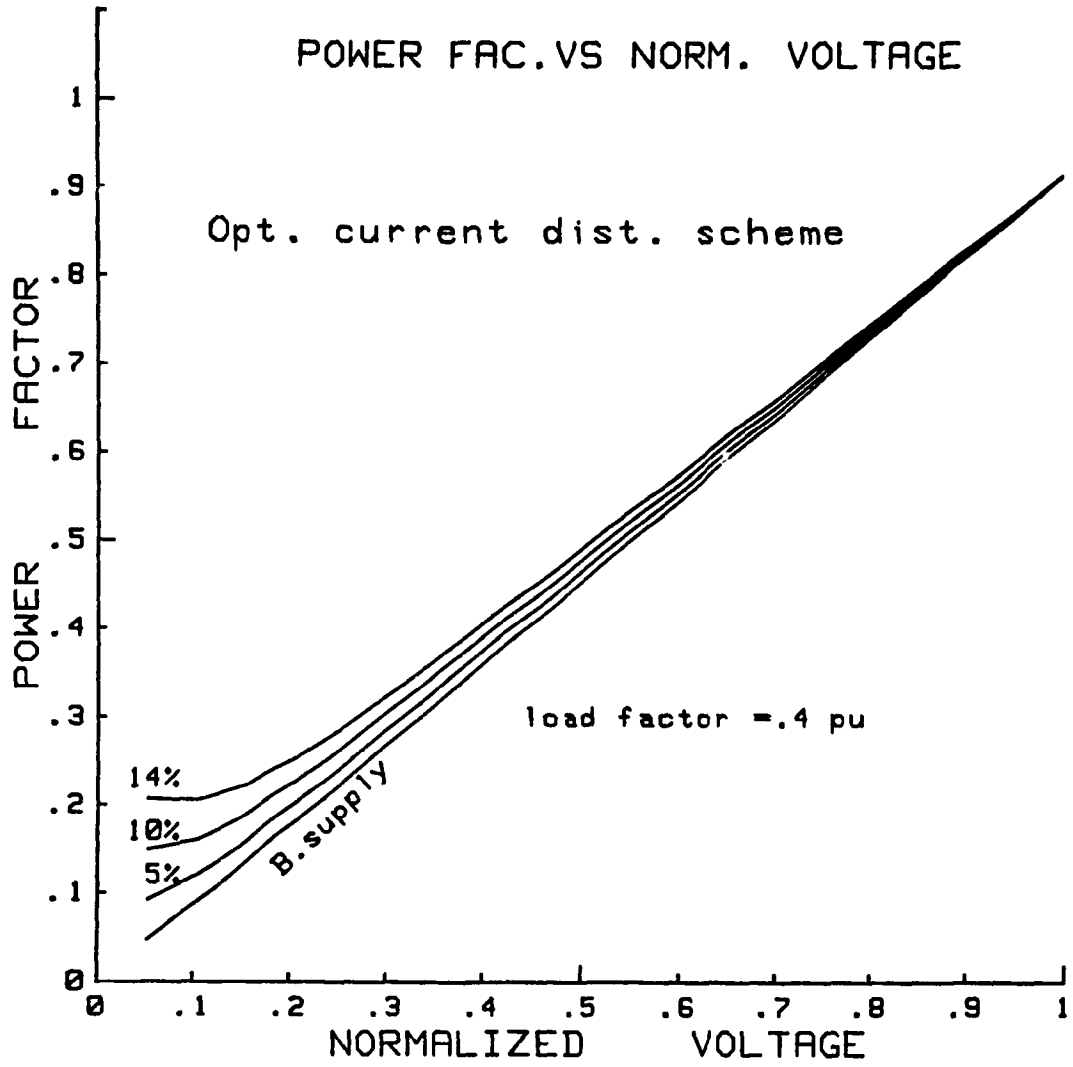

Fig. 5-5: Input power factor using PWMOCD scheme.

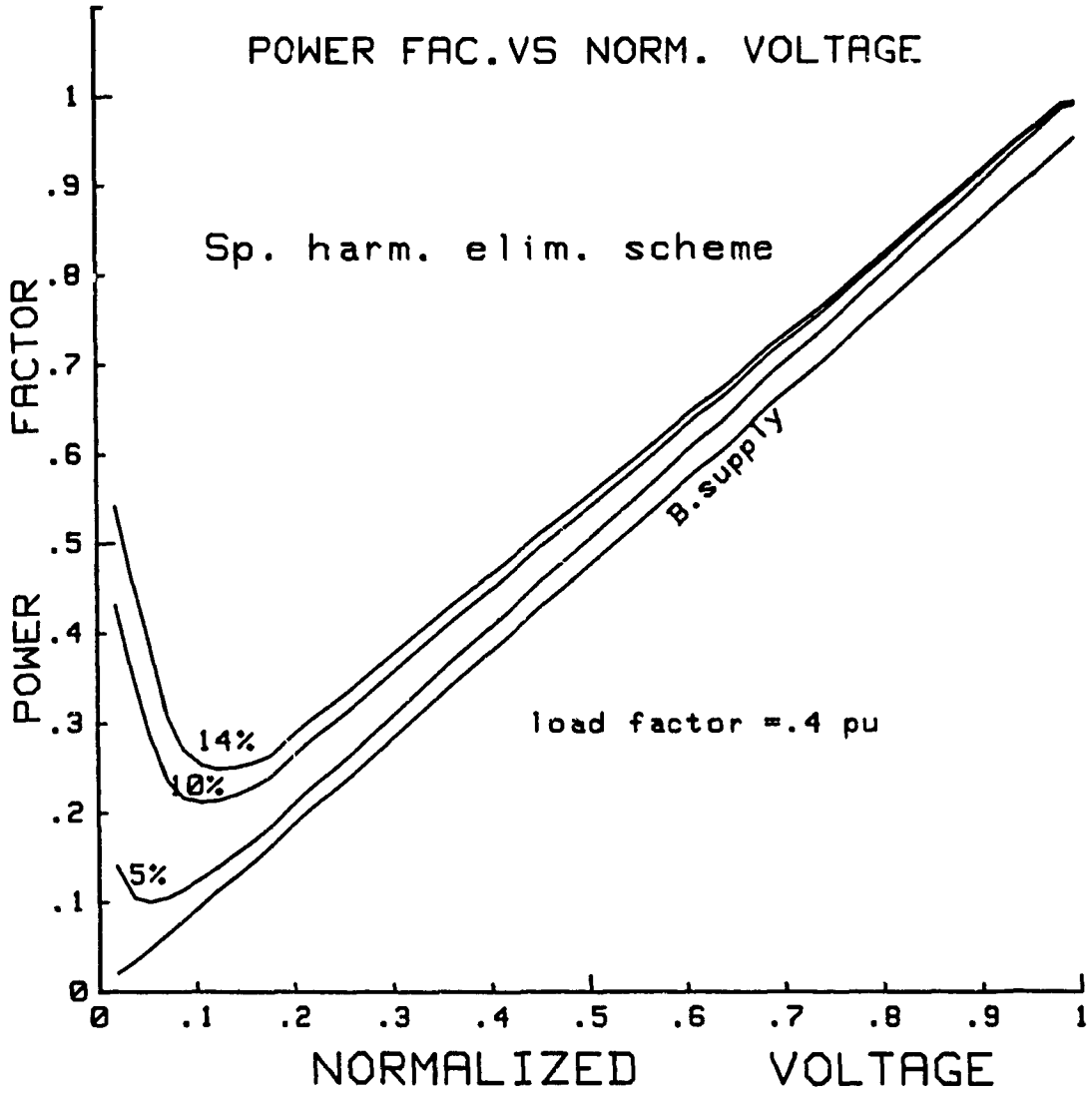

Fig. 5-6: Input power factor using PWMSHE scheme.

output voltage region, the PF holds a relatively high value.

The PF for the PWMOCD scheme shows that with a balanced supply, the PF decreases uniformly and linearly along with the decrement of converter output voltage. As the supply becomes unbalanced, PF still decreases uniformly. But at the very low converter output region it loses its uniformity, and does not decrease appreciably.

The PF of the PWMSHE scheme under balanced supply shows approximately the same characteristics as it does in PWMOCD scheme. However, under unbalanced supply, and at a very low converter output region ($\alpha>110^{o}$), PF apparently increases. This little gain of PF has to be weighed against the sharp increase in HF at that particular region. The explanation of this PF increase has been given in section 3.5.1.

5.6.2 Harmonic Factor of the input line current

The HF of the input line currents for MSPWM, PWMOCD and PWMSHE schemes have been calculated using Eqn. (2.30) of chapter 2, section (2.5.2).

The HF for MSPWM scheme is shown in Fig.(5-7). It is evident from the Fig. that the supply voltage unbalances donot change HF. However,at the very low output region of the converter, the HFs are different under different supply unbalances.

For both PWMOCD and PWMSHE schemes, and at balanced supply, HF stays constant throughout the whole converter

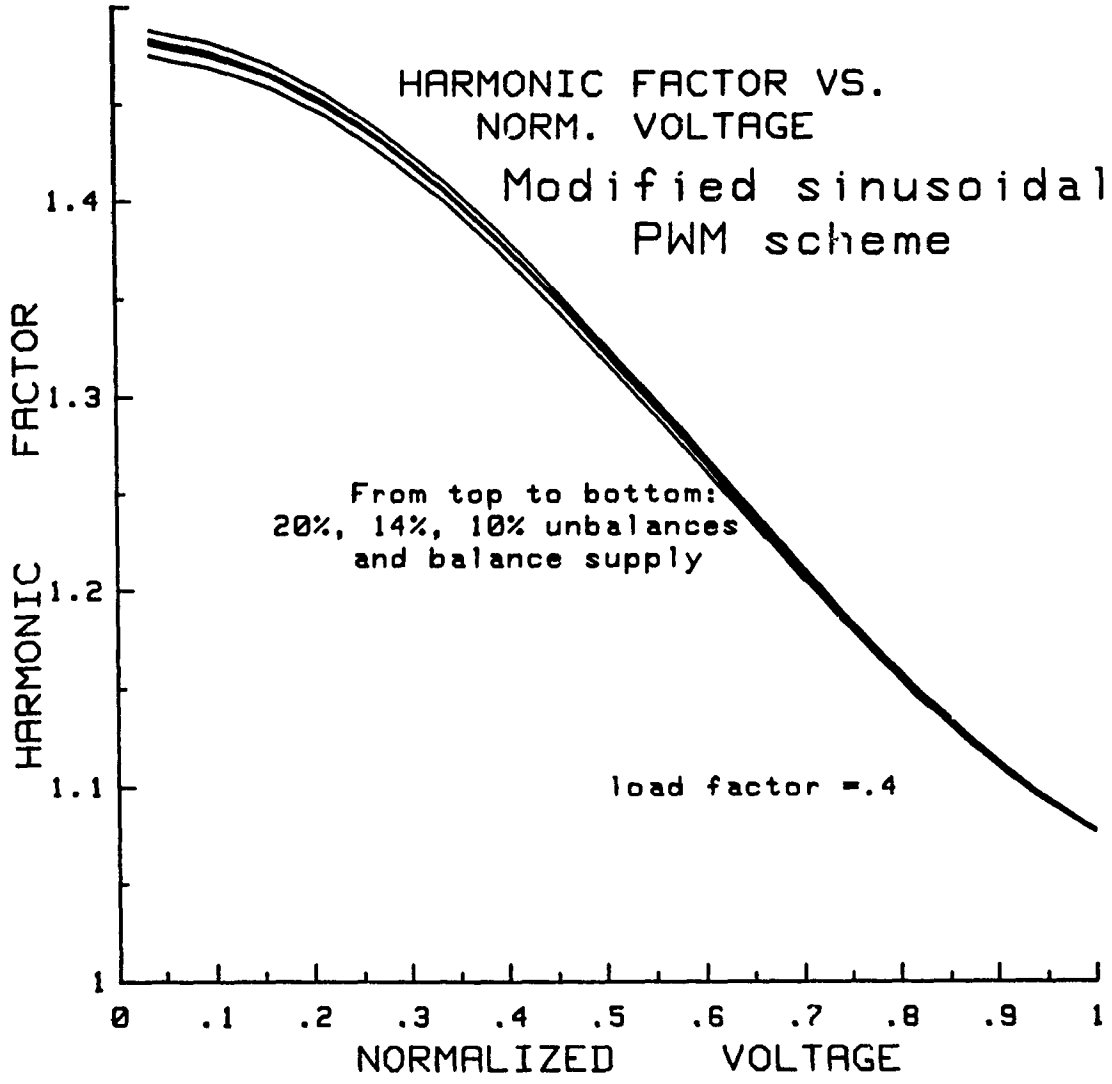

Fig. 5-7: Harmonic factor of input current using modified sinusoidal PWM scheme.

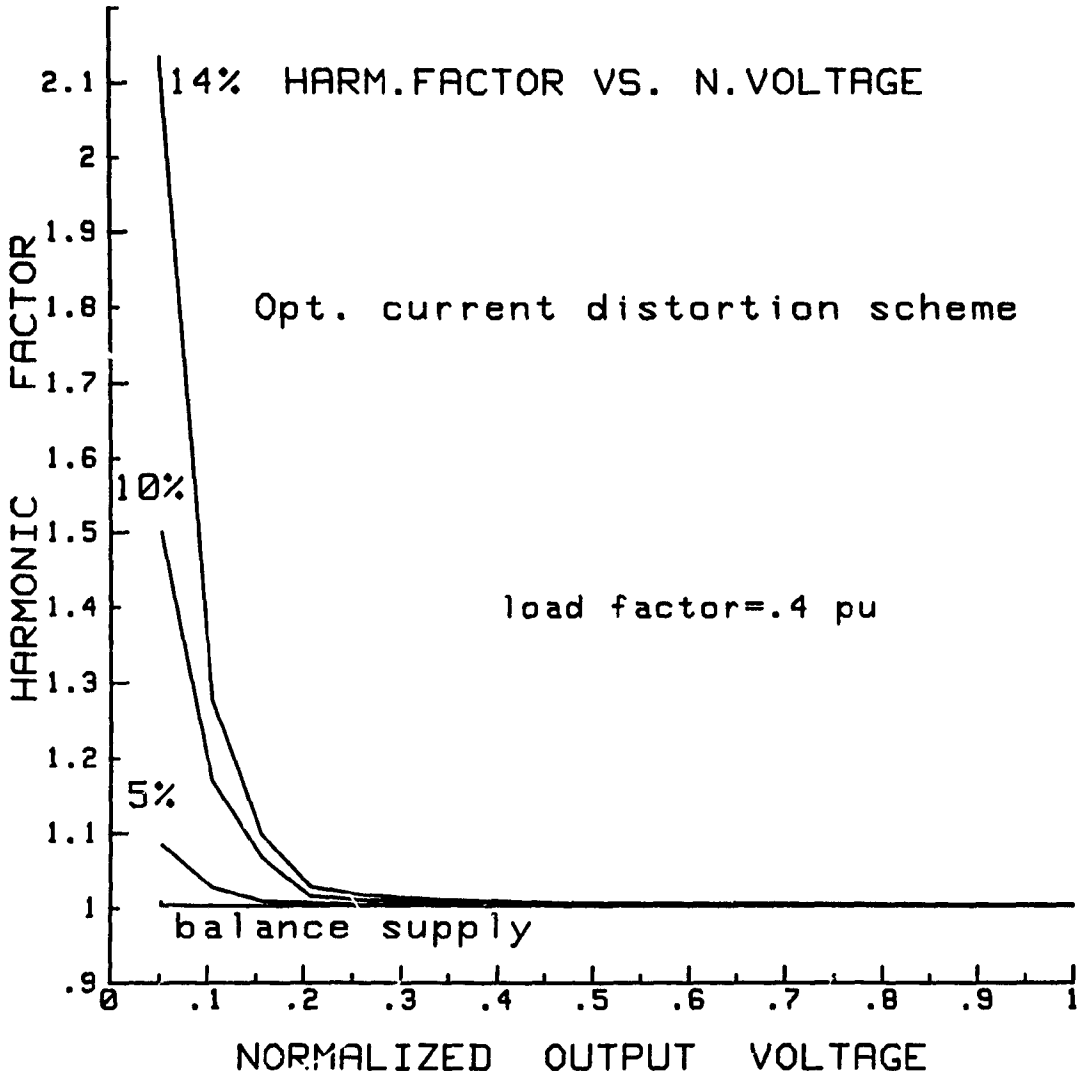

Fig. 5-8: Harmonic factor of input current using PWMOCD scheme.

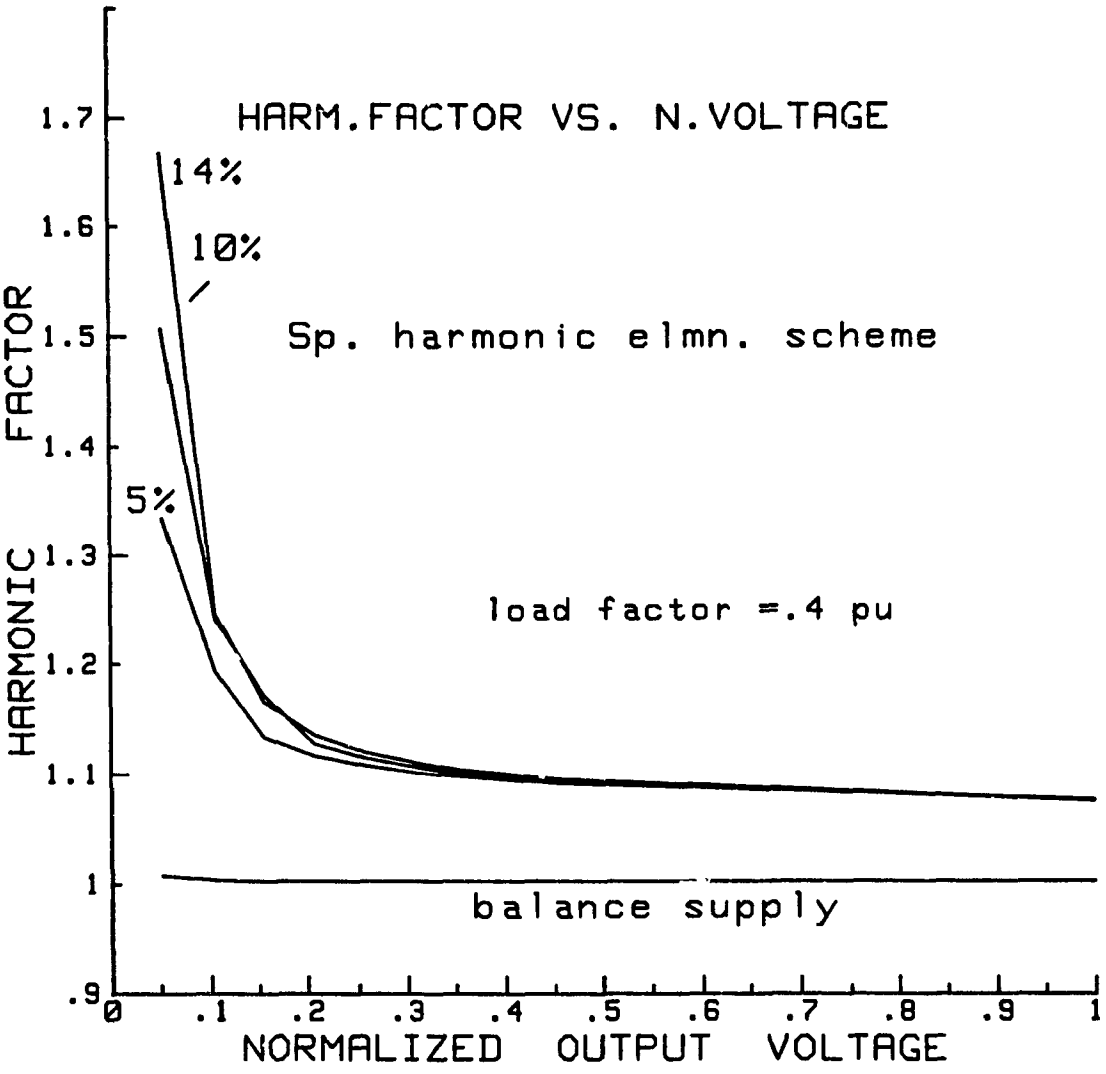

Fig. 5-9: Harmonic factor of input current using PWMSHE scheme.

operation range. In most of the higher converter output region, and at unbalanced supply condition, HF increases slightly along with the decrement of the converter output voltage. But the HF takes a sharp jump at the very low converter output region. It can generally be said that higher the unbalance, the higher the magnitude of the HF at this region. The PWMSHE scheme however has a somewhat smaller value than the PWMOCD scheme.

CHAPTER 6

SUMMARY, CONCLUSIONS AND SUGGESTIONS

6.1 Summary and Conclusions

In this thesis, three-phase ac-dc converters using four different control schemes have been investigated in detail. Problems associated with them have been analyzed and solutions have been suggested to overcome these problems. Computer programs have been developed to simulate converters using the 4 control schemes. Finally, an experimental circuit has been built in the laboratory in order to verify the simulated results. Emphasis has been placed on converters using phase angle control for the following four reasons:

(1) In converters using forced commutation, the input current harmonics are of a high order, hence their magnitudes are comparatively small and can be filtered easily.

(2) The effect of unbalance is not significant in converters using forced commutation, especially in the MSPWM scheme.

(3) A great deal of work has been done previously on converters using forced commutation under balanced supply conditions. This existent work details the input current spectra, describes converter input and output current filter design [36], and discusses associated problems. Further work in this field is redundant.

(4) For high power applications, converters using delay-angle control are more practical. Such converters are the object of a great deal of interest to industry.

The novelty of this work lies in the use of three different transfer functions to simulate the converters, the design of the input and the output filters under unbalanced supply, and the effect of the load factor and the fixed dc voltage (E_c) on the converter performance parameters. The use of different transfer functions gives a more accurate profile of the harmonic spectra. This is essential to design proper input and output filters. The unusual increase of the input PF in the lower converter output region has also been investigated and explained in Chapter 2. New expressions which calculate the Converter input PF been derived, and they clearly show that under unbalanced supply, the 'true PF' of the converter is found by including the three different input currents.

A computer-aided design (CAD)procedure has been utilized in order to evaluate the input and output filters in Chapter 3. Numerous combinations of filter inductors and capacitors have been tested to meet the specified criteria. During this selection process, care has been taken to keep the price of the filter low. Finally, the filters designed have been tested to meet the accepted values of RF and THD throughout the entire converter operating range.

In chapter 4, the harmonic spectrum found from the experimental setup confirmed the accuracy of the simulated converter. The 'effectivenesses' of the filters are quite evident from the harmonic spectra of the input currents and load voltages obtained through the use of the Data precision DATA 6000 harmonic analyzer.

For low power applications, when there is a possibility of an unbalanced supply voltage, the MSPWM converter scheme is a practical choice. It is virtually unaffected by supply unbalance and maintains a relatively high PF. Use of gate turn-off thyristors (GTOs) eliminate the bulky commutation circuitry and increase in the current and voltage ratings of switching devices. This technique allows forced commutated converters to be used more in relatively higher power applications.

It is acknowledged that in all the previous simulation work, the ac mains feeding the converter was considered a perfect distortion-less sinusoidal waveform. This may be true for large utilities but in many situations power is

generated by small local diesel plants having fewer restrictions on the quality of the power they supply. Moreover a low quality mains voltage will in turn degrade converter performance and may lead to system instability caused by filter resonance. In addition, a non-ideal supply will give rise to dc components and may lead to transformer core saturation.

6.2 Suggestions for Future Work

Due to the switching nature of the power converters, harmonics are generated and injected into the power system. In practical systems, line inductances are always present and they are different in each line. These inductances will cause voltage drops between the supply bus and converter input port.

Unbalances are caused by the magnetic shunt of the transformer core. These unbalances can cause harmonics, which in turn will cause more unbalances. To include the non-linearity of a transformer, it is necessary to derive the harmonic model of the transformer.

In addition to the input/output filters, there are other elements which could cause problems of resonance. Their study is an idealized investigation of the harmonic characteristics under typical simulated conditions. The unbalances presented in table 3-1 are only typical conditions. There could be different combinations of supply

unbalances which would give the same degrees of unbalances. However, the consideration of all these combined will lead to a very complex problem. However, such a complexity is beyond the scope of this work.

System instability due to resonance caused by filter L-C elements may be a substantial problem for proper harmonic assessment. Further work is necessary to study this problem in depth. Initially, converters using only a single reactor input filter, (e.g. synchronous reactors) [30,31] might be studied. In the case of a microprocessor based controller, all the equations derived in this work are still applicable if the delay angle (α) is replaced by the angle α_m (m = 1, 2, 3, ...6), where $\alpha_m = \alpha + \frac{\pi m}{6}$.

No matter what direction subsequent research takes, the treatment of converter generated harmonics in this thesis has been generalized in order to serve as a foundation for future work, and to accommodate a number of idealized approaches.

There are seven ideal avenues which might see further development:

(1) This work can be extended to study the effect of harmonics on the supply transformer and any input current dc component. However, the non-linear nature of the switches are not included in this work. Therefore, once the input current harmonics are characterized, it is of practical importance

to do some harmonic measurement from the secondary side to the primary side. This would require harmonic modeling of the transformer, and would also involve the calculation of the switching functions of the converter on-line bus to minimize or optimize certain performance criteria.

(2) Emphasis can be placed on finding a adaptive switching scheme that eliminates the effects of unbalances by automatically adjusting the width of the switching functions.

(3) The delays associated with the turning 'on' and 'off' of the switching devices slightly change the results of simulation used in this thesis. Further work may be done to analyze the switching losses.

(4) Inductances present in the line will change the converter performance due to commutation.

(5) Dynamic loads such as dc machines with time varying inductances will change the load current harmonic spectrum.

(6) The switches are considered ideal. Practical switches will have impedances to current flow. The impedances of the switches can be taken into

account.

(7) This thesis assumes that the supply voltages are pure sinusoidal waveforms, but in practice voltages could be non-sinusoidal. The effect of the non-sinusoidal supply could also be investigated.

Essentially these research opportunities would analyze further complications in the already unbalanced system under steady state conditions. Another dimension could be added to the research, however, by studying the entire unbalance problem under transient conditions.

REFERENCES AND BIBLIOGRAPHIES

[1] P. D. Ziogas and P. Photiadis, 'An exact input current analysis of ideal static PWM inverters', IEEE Transactions on Industry Applications, vol. IA-119, No. 2, March/April 1983, pp.281-295.

[2] M. H. Rashid and Ali I. Maswood, 'Effects of unbalances on Power factor and harmonics of 3-Phase AC-DC converter', International conference of Hungarian Electrotechnical association, Budapest Oct. 1984, pp. 315-324.

[3] M. H. Rashid and Ali I. Maswood, Analysis of 3-Phase Ac-Dc converters under unbalanced supply conditions', IEEE Industry applications society conference record, 1984, pp. 315-324.

[4] M. H. Rashid and Ali I. Maswood, 'Harmonics generated by Ac-Dc converters into the Power supply', Midwest symposium on circuits and systems Louisville, Kentucky, Aug. 1985, pp. 337-340.340.

[5] M. H. Rashid and Ali I. Maswood, 'A novel method of harmonic assessment generated by 3-Phase AC-DC converters under unbalanced supply conditions', IAS

annual meeting of the IEEE in Denver, Oct. 1986, pp. 679-684.

[6] M. H. Rashid and Ali I. Maswood, 'Problems of harmonics in shunt compensation ', paper presented at the first symposium on Electrical power systems in fast developing countries, sponsored by IEEE region 8, Riyadh, March 1987, 361-364.

[7] M. H. Rashid and Ali I. Maswood, 'Analysis of 3-Phase AC-DC converters under unbalanced supply conditions' , an extended and modified version of the previous publication (#3), published in the Transactions of the Industry Applications Society (IAS) of the IEEE, VOL. 24, NO. 3, May/June 1988, pp. 449-455.

[8] M. H. Rashid and Ali I. Maswood, 'A novel method of harmonic assessment generated by 3-Phase AC-DC converters under unbalanced supply conditions' , an extended and modified version of the previous publication (#5) published in the Transactions of the Industry Applications Society (IAS) of the IEEE, VOL. 24, NO. 4, July/August 1988, pp. 590-597.

[9] M. H. Rashid and Ali I. Maswood, 'Harmonics of phase controlled Rectifiers at different load Power factors', to be presented at the Middle East Power System Conference, MEPCON - 89, Cairo - Assiut, Egypt, January

9 - 13, 1989.

[10] John Reeve and P. C. S. Krishnaya 'Unusual current harmonics arising from High-voltage DC transmission' IEEE Transactions on Power Apparatus and Systems, vol. PAS-87, No.3 March 1968, pp. 883-892.

[11] John Reeve, John A. Baron, and P.C.S. Krisshnayya, 'A general approach to harmonic current generation by HVDC converters', IEEE Transactions on Power Apparatus and Systems, vol. PAS-88, No.7, July 1969, pp. 989-996.

[12] T. Subbarao, J. Reeve, 'Harmonics caused by imbalanced transformer impedances and imperfect twelve-pulse operation in HVDC conversion', IEEE transaction on power apparatus and systems, vol. Pas-95, no. 5, september/october 1976. pp. 1732-1735.

[13] Arun G. Phadke and James H. Harlow, 'Generation of abnormal harmonics in High Voltage AC-DC power systems', IEEE transactions on power apparatus and systems, vol. PAS-87, No. 3, March 1968.

[14] J. D. Anisworth, 'Harmonic instability between controlled static converters and ac networks', IEE Proceedings, Vol. 114, July, 1967. pp. 949-957.

[15] R. Yacamini, and W. J. Smith, 'Negative sequence impedance of converters', proceeding IEE, vol. 128, pt.

B, No. 3, May 1981, pp.161-166.

[16] R. W. Lye, 'Power Converter Handbook, theory design and application', Canadian General electric company Ltd. 1979.

[17] R. Yacamini and J. C. de Oliveira, 'Harmonics produced by direct current converter transformers', IEE proceeding, vol. 125, No. 9, September 1978, pp. 157-166.

[18] R. Yacamini, 'Power system converter harmonics', International conference on harmonics in Power systems, UMIST, Manchester, England, September 1981, pp. 111-123.

[19] J. Arrillaga, D. A. Bradley, P. S. Bodger, 'Power System Harmonics', A Wiley Interscience Publications, John Wiley and Sons, 1981.

[20] John R. Linders, 'Electric wave distortions: their hidden costs and containment', IEEE Transactions on Industry Applications, vol. IA-15, No. 5, Sept./Oct. 1979, pp.453-457.

[21] N. A. Choudhury, 'Analysis of switching schemes for 3-Phase AC-DC converter', Master's Thesis, Concordia University, Montreal, 1984.

[22] B. R. Pelly, 'Thyristor phase-controlled converters and cycloconverters', A Wiley Interscience Publications, 1971.

[23] B. D. Bedford and R. G. Hoft, 'Principles of inverter circuits', A Wiley Interscience Publication, New-York, 1964.

[24] 'Power system harmonics: an overview', IEEE Transactions on Power Apparatus and Systems, vol. Pas-102, No.8, August 1983, pp. 2455-2459.

[25] E. Kamm, 'Design guide for electromagnetic interference (EMI) reduction in power supplies', MIL-HDBK-241B, USA naval electronic systems command.

[26] P. D. Ziogas, 'Optimum filter design for a single phase solid state UPS system', Master's Thesis, Toronto University, 1975.

[27] T. Ohnishi and H. Okitsu, 'A novel PWM technique for three-phase inverter/converter', IPEC Conference Record 1983, pp.384-395.

[28] M. H. Rashid and Ali I. Maswood, 'Analysis and performances of forced commutated 3-phase AC-DC converters under unbalanced supply conditions', paper presented at the International conference on Harmonics

'Characterization of programmed-waveform pulse width modulation', IEEE Transaction on Industry Applications, vol. IA-16, No.5, pp. 707-715, Sept./Oct., 1980.

[36] Young goo Kang, 'Analysis and design of optimum three-phase PWM rectifiers and rectifier-inverter frequency changes', Ph.D Thesis, Concordia University, 1985.

[37] M. H. Rashid, 'Power Electronics-circuits, devices and applications", Prentice Hall Inc. 1988.

[38] P. C. Sen, 'Thyristor DC drives', John Wiley and sons, 1981.

[39] S. B. Dewan and A. Straughen, 'Power semiconductor circuits', John Wiley and Sons, 1975.

[40] NEMA publication no.MG1-1972. National electrical manufacturers association, 155 East, 44th st. New york N.Y.

APPENDIX A

Transfer Function and Converter Performance parameter derivations

The transfer function of a converter can be written in Fourier series as:

$$S(\theta) = \sum_{n=1}^{\infty} H_n \sin (n\theta + \psi_n) \quad (1)$$

where ψ_n is the phase of the nth harmonic component of the switching function.

The transfer functions with respect to the input port of the converter can be expressed as $[S_1(\theta)-S_4(\theta)]$, $[S_3(\theta)-S_6(\theta)]$, and $[S_5(\theta)-S_2(\theta)]$. $S_1(\theta)$, $S_2(\theta).....S_6(\theta)$ are the corresponding gating functions. If the supply line to neutral voltages are:

$$v_1 = E_1 \sin (\theta-\phi_1) \quad (2)$$

$$v_2 = E_2 \sin (\theta-\phi_2) \quad (3)$$

$$v_3 = E_3 \sin (\theta-\phi_3) \quad (4)$$

A.1 Output Voltage

The output voltage expression is:

$$v_o(\theta) = \{v_i(\theta)\}\{S(\theta)\} = \{S_1(\theta) - S_4(\theta)\}E_1\sin(\theta - \phi_1) + \{S_3(\theta) - S_6(\theta)\}E_2\sin(\theta - \phi_2) + \{S_5(\theta) - S_2(\theta)\} E_3 \sin(\theta - \phi_3) \quad (5)$$

where:

ϕ_1, ϕ_2, and ϕ_3 are the phase angles of the respective phases.

Eqn. (5) can be written as:

$$v_o(\theta) = F_1 + F_2 + F_3 \quad (6)$$

where $F_1(\theta)$, $F_2(\theta)$, and $F_3(\theta)$ are given by:

$$F_1(\theta) = E_1 \sin(\theta-\phi_1) \sum_{n=1}^{\infty} H_n \sin(n\theta-n\alpha-n\phi_1) \quad (7)$$

$$F_2(\theta) = E_2 \sin(\theta-\phi_2) \sum_{n=1}^{\infty} H_n \sin(n\theta-n\alpha-n\phi_2) \quad (8)$$

$$F_3(\theta) = E_3 \sin(\theta-\phi_3) \sum_{n=1}^{\infty} H_n \sin(n\theta-n\alpha-n\phi_3) \quad (9)$$

After trigonometrical transformations, the above three equations can be written as:

$$F_1(\theta) = \sum_{n=1}^{\infty} \frac{E_1 H_n}{2} [\cos\{(n-1)\theta-(n-1)\phi_1-n\alpha\}$$

$$-\cos\{(n+1)\theta-(n+1)\phi_1-n\alpha\}] \quad (10)$$

Similarly,

$$F_2(\theta) = \sum_{n=1}^{\infty} \frac{E_2 H_n}{2} [\cos\{(n-1)\theta-(n-1)\phi_2-n\alpha\}$$

$$-\cos\{(n+1)\theta-(n+1)\phi_2-n\alpha\}] \quad (11)$$

and

$$F_3(\theta) = \sum_{n=1}^{\infty} \frac{E_3 H_n}{2} [\cos\{(n-1)\theta-(n-1)\phi_3-n\alpha\}$$

$$-\cos\{(n+1)\theta-(n+1)\phi_3-n\alpha\}] \quad (12)$$

The output dc voltage can be obtained from Eqn. (5) for n = 1,

$$V_{dc} = 1/2\ (E_1 + E_2 + E_3)\ H_1 \cos(\alpha) \quad (13)$$

Substituting n = 1,2,3,4.... in Eqn.s (10), (11), and (12), the corresponding output voltage harmonic components can be calculated as:

1st harmonic component = 0

2nd harmonic component is:

$$v_{o_2} = \frac{E_1 H_3}{2} \cos\ (2\theta - 2\phi_1 - 3\alpha) - \frac{E_1 H_1}{2} \cos\ (2\theta - 2\phi_1 - \alpha)$$

$$+ \frac{E_2 H_3}{2} \cos\ (2\theta - 2\phi_2 - 3\alpha) - \frac{E_2 H_1}{2} \cos\ (2\theta - 2\phi_2 - \alpha)$$

$$+\frac{E_3H_3}{2}\cos(2\theta - 2\phi_3 - 3\alpha) - \frac{E_3H_1}{2}\cos(2\theta - 2\phi_3 - \alpha) \tag{14}$$

kth harmonic component is ;

$$v_{0_k} = \frac{E_1H_{K+1}}{2}\cos\{k\theta - k\phi_1 - (k+1)\alpha\} \frac{E_1H_{k-1}}{2}\cos\{k\theta - k\phi_1 - (k-1)\alpha\}$$

$$+\frac{E_2H_{k+1}}{2}\cos\{k\theta - k\phi_2 - (k+1)\alpha\} \frac{E_2H_{k-1}}{2}\cos\{k\theta - k\phi_2 - (k-1)\alpha\}$$

$$+\frac{E_3H_{k+1}}{2}\cos\{k\theta - k\phi_3 - (k+1)\alpha\} \frac{E_3H_{k-1}}{2}\cos\{k\theta - k\phi_3 - (k-1)\alpha\} \tag{15}$$

A.2 Output Current

For kth component of output voltage, the load impedance can be expressed as:

$$Z_k \angle \sigma_k = \{R^2 + (2k\pi fl)^2\}^{1/2} \angle \tan^{-1}\left(\frac{2kf\pi L}{R}\right) \tag{16}$$

and the average output current,

$$I_{dc} = \frac{V_{dc}}{R} - \frac{E_e}{R} \tag{17}$$

where: E_e is the dc voltage of the load circuit, e.g., battery or back emf of dc machines.

A.3 Input Line Current

Considering the converter to be loss-less, the

instantaneous input power to the converter = instantaneous output power from the converter. Thus:

$$\{v_i(\theta)\}\ \{\ i_1(\theta)\} = \{v_0(\theta)\}\ \{\ i_0(\theta)\ \} \qquad (18)$$

From Eqn.(5),

$$\{\ v_i(\theta)\}\ \{\ i\ (\theta)\ \} = \{\ v_i(\theta)\ \}\ \{\ S\ (\theta)\ \}\ \{\ i_\theta(\theta)\ \} \qquad (19)$$

$$i_i\ (\theta) = \{\ S\ (\theta)\ \}\ \{\ i_0\ (\theta) \qquad (20)$$

Rewriting Eqn. (20) in terms of Fourier series and substituting values of $i_0(\theta)$, the instantaneous input line current can be expressed as:

$$i_i\ (\theta) = \{\ \sum_{k=1}^{\infty} H_k \sin\ (k\theta + \psi_k)\ \}\ (I_{dc} + \sum_{n=1}^{\infty} I_n \sin(n\theta + \beta n)$$

$$= I_{dc} \sum_{k=1}^{\infty} H_k \sin(k\theta + \psi_k) + \{ \sum_{k=1}^{\infty} \sum_{n=1}^{\infty} \frac{H_k I_n}{2}$$

$$[\cos\{(n-k)\theta+\beta_n-\psi_k\} - \cos\{(n+k)\ \theta + \beta_n + \psi_k\}] \qquad (21)$$

Where: I_n is the rms value of the nth component of output current. Analyzing Eqn. (21), it can be seen that the first term gives us mth harmonic component for k = m. The second term gives mth harmonic components when :

$$n - k = m \quad \text{i.e.,} \quad n = m+k \tag{22}$$

$$n + k = m \quad \text{i.e.,} \quad n = m-k \tag{23}$$

$$n - k = -m \quad \text{i.e.,} \quad k = n+m \tag{24}$$

Taking into account the above three conditions, the expressions for mth harmonic component of the input line current can be written as:

$$i_{i,m}(\theta) = I_{dc} H_k \sin(k_\theta + \psi_k) + \sum_{n=1}^{\infty} \frac{H_k I_{m+k}}{2} \cos(m\theta + \beta_{m+k} - \psi_k) - \sum_{k=1}^{m-1} \frac{H_k I_{m-k}}{2} \cos(m\theta + \beta_{m-k} + \psi_k) \sum_{n=1}^{\infty} \frac{H_{n+m} I_n}{2} \cos(-m\theta + \beta_n - \psi_{n+m}) \tag{25}$$

The third term of Eqn. (25) gives second and higher order harmonic components.

APPENDIX B

Some Useful Descriptions and Definitions

B.1 Switching Functions

Any power conversion scheme whether it is a rectifier or an inverter, and whether it is a voltage or current source, the scheme can be modeled as a 'black box' whose transfer characteristics are analytically described by the Fourier series expansion of its proper set of switching functions [32], [33]. By ignoring the specific circuit topology, a general model can be achieved to find relationships between the input and output port variables of the conversion scheme [35]. This model is conceptually represented in Fig. 1-1.

According to the model, the input and output port variables are related as follows:

Current Source

$$V_{ac}(\omega t) = V_1(\omega t) \tag{1}$$

$$I_1(\omega t) = S(\omega t) \times E \tag{2}$$

$$V_2(\omega t) = S(\omega t) \times V_{ac}(\omega t) \tag{3}$$

$$E = I_2(0) \tag{4}$$

Voltage Source

$$V_{ac} = I_1(\omega t) \tag{5}$$

$$I_2(\omega t) = S(\omega t) \times I_1(\omega t) \quad (6)$$

$$V_1(\omega t) = S(\omega t) \times E \quad (7)$$

$$E = V_2\ (0) \quad (8)$$

The function $S(\omega t)$ sometimes written as $S(\theta)$ describing the switching operations of the switches S_1 through S_4 is called switching function, and is mathematically expressed as:

$$S(\omega t) = \frac{V_2(\omega t)}{V_1(\omega t)} \quad (9)$$

Depending on which pair of switches is closed or open altogether, the switching functions can assume values of 1, -1, and 0. Hence, switching functions can be used to synthesize a particular waveform. Knowing the converter input voltage $V_{ac}(\omega t)$, and multiplying it by the switching function $S(\omega t)$. Synthesizing the common switching function (or transfer function), individual switching functions for switches S_1 and S_2 can also be found. For example, the upper switch S_1 in Fig. B-1 gives the positive pulse and the lower switch S_2 gives the negative pulse of a transfer function.

B.2 Fourier Series

B.2.1 Even function

A function $y = f(t)$ is said to be even [34], if;

$$f(-t) = f(t) \quad (10)$$

The graph of such a function is symmetrical with respect to y axis. The function $\cos(\omega t)$ is even.

The Fourier series of an even function f(t) having period T contains only Cosine terms, i.e.

$$f(t) = a_o + \sum_{n=1}^{\infty} a_n \cos\left(\frac{2\pi n}{T} t\right) \tag{11}$$

D.2.2 Odd function

A function is said to be odd, if;

$$f(-t) = -f(t) \tag{12}$$

The graph of such a function is not symmetric with respect to y-axis. The function Sin(ωt) is an odd function.

The Fourier series of an odd function f(t) having period T contains sine terms only, i.e.

$$f(t) = \sum_{n=1}^{\infty} b_n \sin\left(\frac{2\pi n}{T} t\right) \tag{13}$$

B.3 Per-unit (pu) system

The per-unit system is a means to express numbers for ease in comparing them. The per-unit value is a ratio, expressed as:

$$\text{Per-unit} = \frac{\text{number}}{\text{Base number}} \tag{14}$$

B.4 Percent

By definition percent is found as:

$$\text{Percent} = \frac{\text{number}}{\text{Base number}} \times 100 \qquad (15)$$

As evident the percent of a value can be obtained from per-unit value by multiplying the per-unit value by 100. For example, a transformer that has an impedance of 0.08 per-unit has an impedance of eight percent.